Steam pipe bridge in a geothermal power plant. Pipe flows are everywhere, often occurring in groups or networks. They are designed using the principles outlined in this chapter. *(Courtesy of Dr. E. R. Degginger/Color-Pic Inc.)*

Chapter 6
Viscous Flow in Ducts

Motivation. This chapter is completely devoted to an important practical fluids engineering problem: flow in ducts with various velocities, various fluids, and various duct shapes. Piping systems are encountered in almost every engineering design and thus have been studied extensively. There is a small amount of theory plus a large amount of experimentation.

The basic piping problem is this: Given the pipe geometry and its added components (such as fittings, valves, bends, and diffusers) plus the desired flow rate and fluid properties, what pressure drop is needed to drive the flow? Of course, it may be stated in alternate form: Given the pressure drop available from a pump, what flow rate will ensue? The correlations discussed in this chapter are adequate to solve most such piping problems.

6.1 Reynolds-Number Regimes

Now that we have derived and studied the basic flow equations in Chap. 4, you would think that we could just whip off myriad beautiful solutions illustrating the full range of fluid behavior, of course expressing all these educational results in dimensionless form, using our new tool from Chap. 5, dimensional analysis.

The fact of the matter is that no general analysis of fluid motion yet exists. There are several dozen known particular solutions, there are some rather specific digital-computer solutions, and there are a great many experimental data. There is a lot of theory available if we neglect such important effects as viscosity and compressibility (Chap. 8), but there is no general theory and there may never be. The reason is that a profound and vexing change in fluid behavior occurs at moderate Reynolds numbers. The flow ceases being smooth and steady (*laminar*) and becomes fluctuating and agitated (*turbulent*). The changeover is called *transition* to turbulence. In Fig. 5.3*a* we saw that transition on the cylinder and sphere occurred at about $\mathrm{Re} = 3 \times 10^5$, where the sharp drop in the drag coefficient appeared. Transition depends upon many effects, e.g., wall roughness (Fig. 5.3*b*) or fluctuations in the inlet stream, but the primary parameter is the Reynolds number. There are a great many data on transition but only a small amount of theory [1 to 3].

Turbulence can be detected from a measurement by a small, sensitive instrument such as a hot-wire anemometer (Fig. 6.29*e*) or a piezoelectric pressure transducer. The

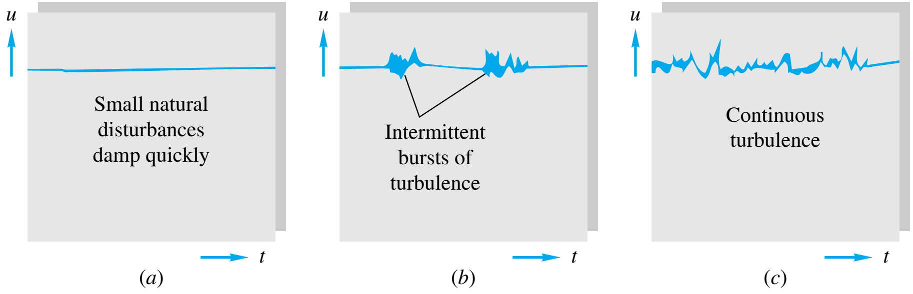

Fig. 6.1 The three regimes of viscous flow: (*a*) laminar flow at low Re; (*b*) transition at intermediate Re; (*c*) turbulent flow at high Re.

flow will appear steady on average but will reveal rapid, random fluctuations if turbulence is present, as sketched in Fig. 6.1. If the flow is laminar, there may be occasional natural disturbances which damp out quickly (Fig. 6.1*a*). If transition is occurring, there will be sharp bursts of turbulent fluctuation (Fig. 6.1*b*) as the increasing Reynolds number causes a breakdown or instability of laminar motion. At sufficiently large Re, the flow will fluctuate continually (Fig. 6.1*c*) and is termed *fully turbulent*. The fluctuations, typically ranging from 1 to 20 percent of the average velocity, are not strictly periodic but are random and encompass a continuous range, or spectrum, of frequencies. In a typical wind-tunnel flow at high Re, the turbulent frequency ranges from 1 to 10,000 Hz, and the wavelength ranges from about 0.01 to 400 cm.

EXAMPLE 6.1

The accepted transition Reynolds number for flow in a circular pipe is $\mathrm{Re}_{d,\mathrm{crit}} \approx 2300$. For flow through a 5-cm-diameter pipe, at what velocity will this occur at 20°C for (*a*) airflow and (*b*) water flow?

Solution

Almost all pipe-flow formulas are based on the *average* velocity $V = Q/A$, not centerline or any other point velocity. Thus transition is specified at $\rho Vd/\mu \approx 2300$. With d known, we introduce the appropriate fluid properties at 20°C from Tables A.3 and A.4:

(*a*) Air: $$\frac{\rho Vd}{\mu} = \frac{(1.205\ \mathrm{kg/m^3})V(0.05\ \mathrm{m})}{1.80\ \mathrm{E\text{-}5\ kg/(m \cdot s)}} = 2300 \qquad \text{or} \qquad V \approx 0.7\ \frac{\mathrm{m}}{\mathrm{s}}$$

(*b*) Water: $$\frac{\rho Vd}{\mu} = \frac{(998\ \mathrm{kg/m^3})V(0.05\ \mathrm{m})}{0.001\ \mathrm{kg/(m \cdot s)}} = 2300 \qquad \text{or} \qquad V = 0.046\ \frac{\mathrm{m}}{\mathrm{s}}$$

These are very low velocities, so most engineering air and water pipe flows are turbulent, not laminar. We might expect laminar duct flow with more viscous fluids such as lubricating oils or glycerin.

In free surface flows, turbulence can be observed directly. Figure 6.2 shows liquid flow issuing from the open end of a tube. The low-Reynolds-number jet (Fig. 6.2*a*) is smooth and laminar, with the fast center motion and slower wall flow forming different trajectories joined by a liquid sheet. The higher-Reynolds-number turbulent flow (Fig. 6.2*b*) is unsteady and irregular but, when averaged over time, is steady and predictable.

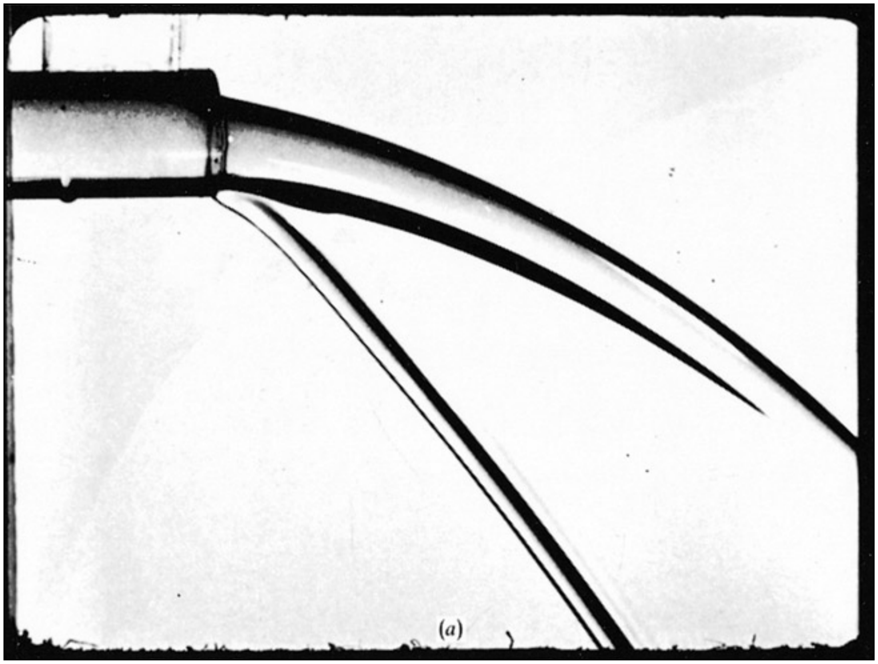

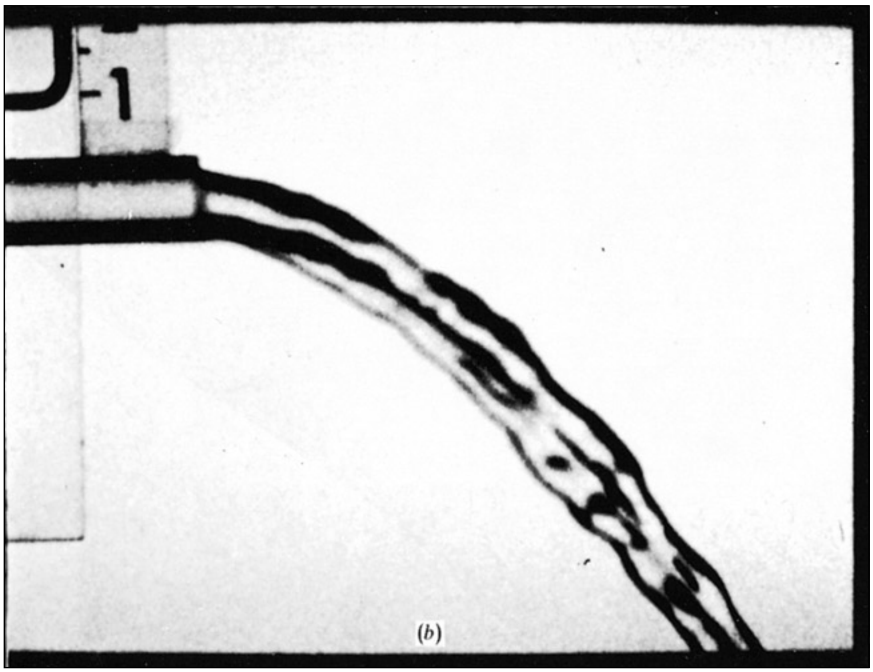

Fig. 6.2 Flow issuing at constant speed from a pipe: (*a*) high-viscosity, low-Reynolds-number, laminar flow; (*b*) low-viscosity, high-Reynolds-number, turbulent flow. *[From* Illustrated Experiments in Fluid Mechanics *(The NCFMF Book of Film Notes), National Committee for Fluid Mechanics Films, Education Development Center, Inc., copyright 1972.]*

How did turbulence form inside the pipe? The laminar parabolic flow profile, which is similar to Eq. (4.143), became unstable and, at $\mathrm{Re}_d \approx 2300$, began to form "slugs" or "puffs" of intense turbulence. A puff has a fast-moving front and a slow-moving rear

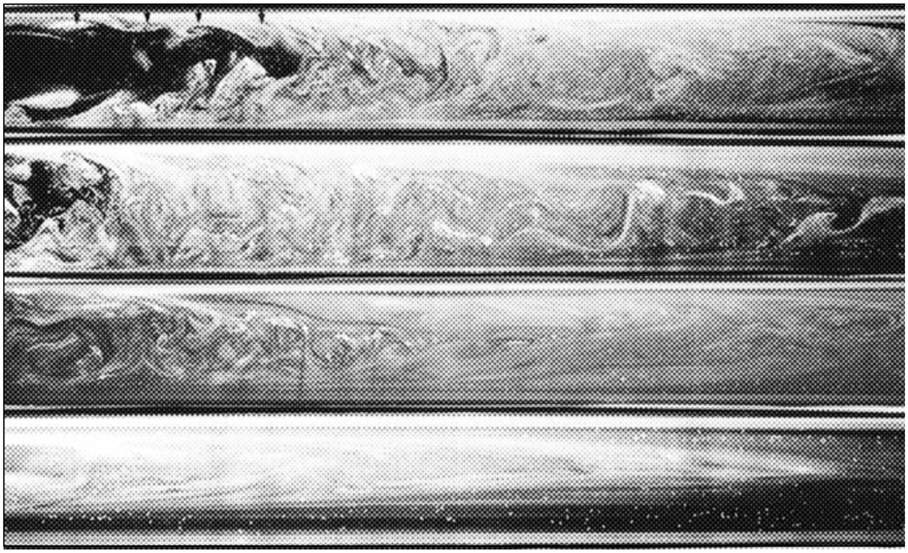

Fig. 6.3 Formation of a turbulent puff in pipe flow: (*a*) and (*b*) near the entrance; (*c*) somewhat downstream; (*d*) far downstream. *(From Ref. 45, courtesy of P. R. Bandyopadhyay.)*

and may be visualized by experimenting with glass tube flow. Figure 6.3 shows a puff as photographed by Bandyopadhyay [45]. Near the entrance (Fig. 6.3*a* and *b*) there is an irregular laminar-turbulent interface, and vortex roll-up is visible. Further downstream (Fig. 6.3*c*) the puff becomes fully turbulent and very active, with helical motions visible. Far downstream (Fig. 6.3*d*), the puff is cone-shaped and less active, with a fuzzy ill-defined interface, sometimes called the "relaminarization" region.

A complete description of the statistical aspects of turbulence is given in Ref. 1, while theory and data on transition effects are given in Refs. 2 and 3. At this introductory level we merely point out that the primary parameter affecting transition is the Reynolds number. If Re $= UL/\nu$, where U is the average stream velocity and L is the "width," or transverse thickness, of the shear layer, the following approximate ranges occur:

$0 < \text{Re} < 1$: highly viscous laminar "creeping" motion
$1 < \text{Re} < 100$: laminar, strong Reynolds-number dependence
$100 < \text{Re} < 10^3$: laminar, boundary-layer theory useful
$10^3 < \text{Re} < 10^4$: transition to turbulence
$10^4 < \text{Re} < 10^6$: turbulent, moderate Reynolds-number dependence
$10^6 < \text{Re} < \infty$: turbulent, slight Reynolds-number dependence

These are representative ranges which vary somewhat with flow geometry, surface roughness, and the level of fluctuations in the inlet stream. The great majority of our analyses are concerned with laminar flow or with turbulent flow, and one should not normally design a flow operation in the transition region.

Historical Outline

Since turbulent flow is more prevalent than laminar flow, experimenters have observed turbulence for centuries without being aware of the details. Before 1930 flow instruments were too insensitive to record rapid fluctuations, and workers simply reported mean values of velocity, pressure, force, etc. But turbulence can change the mean values dramatically, e.g., the sharp drop in drag coefficient in Fig. 5.3. A German engineer named G. H. L. Hagen first reported in 1839 that there might be *two* regimes of viscous flow. He measured water flow in long brass pipes and deduced a pressure-drop law

$$\Delta p = (\text{const}) \frac{LQ}{R^4} + \text{entrance effect} \tag{6.1}$$

This is exactly our laminar-flow scaling law from Example 5.4, but Hagen did not realize that the constant was proportional to the fluid viscosity.

The formula broke down as Hagen increased Q beyond a certain limit, i.e., past the critical Reynolds number, and he stated in his paper that there must be a second mode of flow characterized by "strong movements of water for which Δp varies as the second power of the discharge. . . ." He admitted that he could not clarify the reasons for the change.

A typical example of Hagen's data is shown in Fig. 6.4. The pressure drop varies linearly with $V = Q/A$ up to about 1.1 ft/s, where there is a sharp change. Above about $V = 2.2$ ft/s the pressure drop is nearly quadratic with V. The actual power $\Delta p \propto V^{1.75}$ seems impossible on dimensional grounds but is easily explained when the dimensionless pipe-flow data (Fig. 5.10) are displayed.

In 1883 Osborne Reynolds, a British engineering professor, showed that the change depended upon the parameter $\rho V d/\mu$, now named in his honor. By introducing a dye

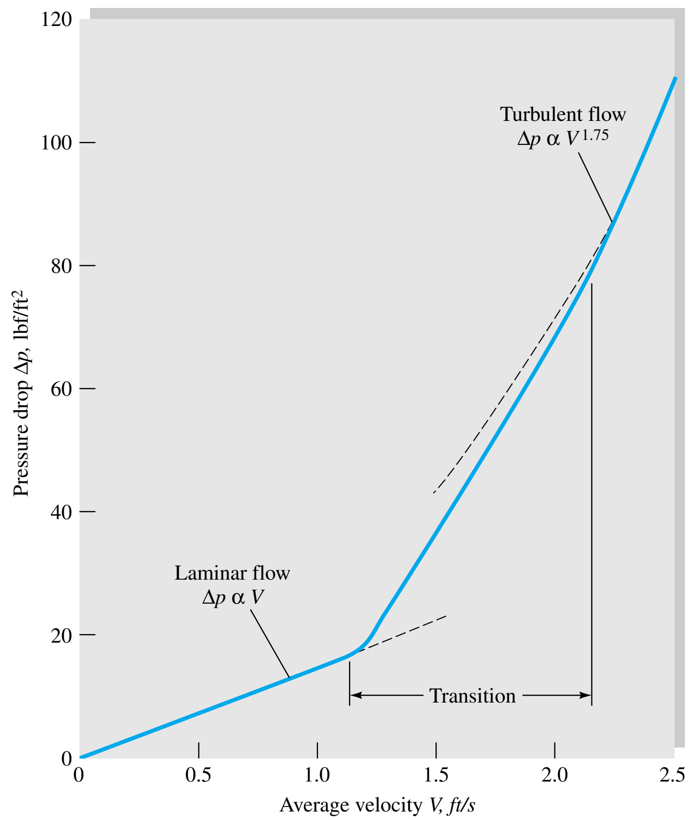

Fig. 6.4 Experimental evidence of transition for water flow in a $\frac{1}{4}$-in smooth pipe 10 ft long.

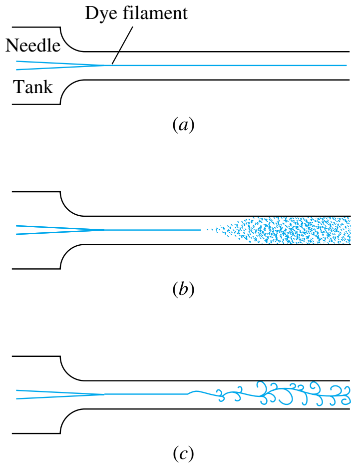

Fig. 6.5 Reynolds' sketches of pipe-flow transition: (*a*) low-speed, laminar flow; (*b*) high-speed, turbulent flow; (*c*) spark photograph of condition (*b*). *(From Ref. 4.)*

streak into a pipe flow, Reynolds could observe transition and turbulence. His sketches of the flow behavior are shown in Fig. 6.5.

If we examine Hagen's data and compute the Reynolds number at $V = 1.1$ ft/s, we obtain $\text{Re}_d = 2100$. The flow became fully turbulent, $V = 2.2$ ft/s, at $\text{Re}_d = 4200$. The accepted design value for pipe-flow transition is now taken to be

$$\text{Re}_{d,\text{crit}} \approx 2300 \tag{6.2}$$

This is accurate for commercial pipes (Fig. 6.13), although with special care in providing a rounded entrance, smooth walls, and a steady inlet stream, $\text{Re}_{d,\text{crit}}$ can be delayed until much higher values.

Transition also occurs in external flows around bodies such as the sphere and cylinder in Fig. 5.3. Ludwig Prandtl, a German engineering professor, showed in 1914 that the thin boundary layer surrounding the body was undergoing transition from laminar to turbulent flow. Thereafter the force coefficient of a body was acknowledged to be a function of the Reynolds number [Eq. (5.2)].

There are now extensive theories and experiments of laminar-flow instability which explain why a flow changes to turbulence. Reference 5 is an advanced textbook on this subject.

Laminar-flow theory is now well developed, and many solutions are known [2, 3], but there are no analyses which can simulate the fine-scale random fluctuations of turbulent flow.[1] Therefore existing turbulent-flow theory is semiempirical, based upon dimensional analysis and physical reasoning; it is concerned with the mean flow properties only and the mean of the fluctuations, not their rapid variations. The turbulent-flow "theory" presented here in Chaps. 6 and 7 is unbelievably crude yet surprisingly effective. We shall attempt a rational approach which places turbulent-flow analysis on a firm physical basis.

6.2 Internal versus External Viscous Flows

Both laminar and turbulent flow may be either internal, i.e., "bounded" by walls, or external and unbounded. This chapter treats internal flows, and Chap. 7 studies external flows.

An internal flow is constrained by the bounding walls, and the viscous effects will grow and meet and permeate the entire flow. Figure 6.6 shows an internal flow in a long duct. There is an *entrance region* where a nearly inviscid upstream flow converges and enters the tube. Viscous boundary layers grow downstream, retarding the axial flow $u(r, x)$ at the wall and thereby accelerating the center-core flow to maintain the incompressible continuity requirement

$$Q = \int u \, dA = \text{const} \tag{6.3}$$

At a finite distance from the entrance, the boundary layers merge and the inviscid core disappears. The tube flow is then entirely viscous, and the axial velocity adjusts slightly further until at $x = L_e$ it no longer changes with x and is said to be *fully developed,* $u \approx u(r)$ only. Downstream of $x = L_e$ the velocity profile is constant, the wall

[1]Reference 32 is a computer model of large-scale turbulent fluctuations.

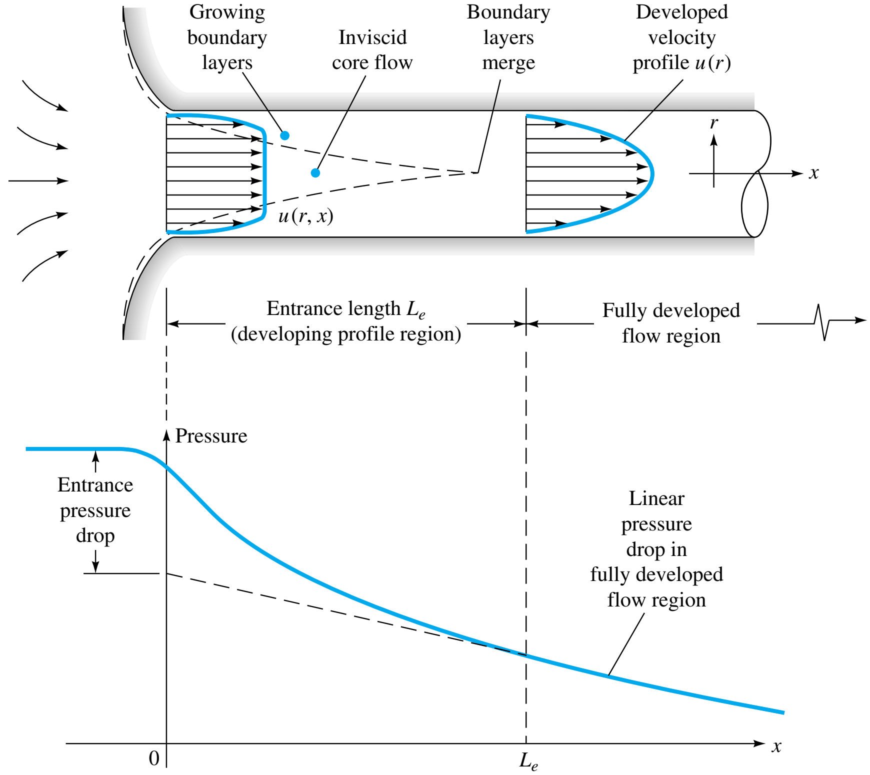

Fig. 6.6 Developing velocity profiles and pressure changes in the entrance of a duct flow.

shear is constant, and the pressure drops linearly with x, for either laminar or turbulent flow. All these details are shown in Fig. 6.6.

Dimensional analysis shows that the Reynolds number is the only parameter affecting entrance length. If

$$L_e = f(d, V, \rho, \mu) \qquad V = \frac{Q}{A}$$

then
$$\frac{L_e}{d} = g\left(\frac{\rho V d}{\mu}\right) = g(\text{Re}) \tag{6.4}$$

For laminar flow [2, 3], the accepted correlation is

$$\frac{L_e}{d} \approx 0.06\ \text{Re} \qquad \text{laminar} \tag{6.5}$$

The maximum laminar entrance length, at $\text{Re}_{d,\text{crit}} = 2300$, is $L_e = 138d$, which is the longest development length possible.

In turbulent flow the boundary layers grow faster, and L_e is relatively shorter, according to the approximation for smooth walls

$$\frac{L_e}{d} \approx 4.4\ \text{Re}_d^{1/6} \qquad \text{turbulent} \tag{6.6}$$

Some computed turbulent entrance lengths are thus

Re_d	4000	10^4	10^5	10^6	10^7	10^8
L_e/d	18	20	30	44	65	95

Now 44 diameters may seem "long," but typical pipe-flow applications involve an L/d value of 1000 or more, in which case the entrance effect may be neglected and a simple analysis made for fully developed flow (Sec. 6.4). This is possible for both laminar and turbulent flows, including rough walls and noncircular cross sections.

EXAMPLE 6.2

A $\frac{1}{2}$-in-diameter water pipe is 60 ft long and delivers water at 5 gal/min at 20°C. What fraction of this pipe is taken up by the entrance region?

Solution

Convert

$$Q = (5 \text{ gal/min}) \frac{0.00223 \text{ ft}^3/\text{s}}{1 \text{ gal/min}} = 0.0111 \text{ ft}^3/\text{s}$$

The average velocity is

$$V = \frac{Q}{A} = \frac{0.0111 \text{ ft}^3/\text{s}}{(\pi/4)[(\frac{1}{2}/12) \text{ ft}]^2} = 8.17 \text{ ft/s}$$

From Table 1.4 read for water $\nu = 1.01 \times 10^{-6}$ m^2/s $= 1.09 \times 10^{-5}$ ft^2/s. Then the pipe Reynolds number is

$$Re_d = \frac{Vd}{\nu} = \frac{(8.17 \text{ ft/s})[(\frac{1}{2}/12) \text{ ft}]}{1.09 \times 10^{-5} \text{ ft}^2/\text{s}} = 31{,}300$$

This is greater than 4000; hence the flow is fully turbulent, and Eq. (6.6) applies for entrance length

$$\frac{L_e}{d} \approx 4.4\, Re_d^{1/6} = (4.4)(31{,}300)^{1/6} = 25$$

The actual pipe has $L/d = (60 \text{ ft})/[(\frac{1}{2}/12) \text{ ft}] = 1440$. Hence the entrance region takes up the fraction

$$\frac{L_e}{L} = \frac{25}{1440} = 0.017 = 1.7\% \qquad \textit{Ans.}$$

This is a very small percentage, so that we can reasonably treat this pipe flow as essentially fully developed.

Shortness can be a virtue in duct flow if one wishes to maintain the inviscid core. For example, a "long" wind tunnel would be ridiculous, since the viscous core would invalidate the purpose of simulating free-flight conditions. A typical laboratory low-speed wind-tunnel test section is 1 m in diameter and 5 m long, with $V = 30$ m/s. If we take $\nu_{air} = 1.51 \times 10^{-5}$ m^2/s from Table 1.4, then $Re_d = 1.99 \times 10^6$ and, from Eq. (6.6), $L_e/d \approx 49$. The test section has $L/d = 5$, which is much shorter than the development length. At the end of the section the wall boundary layers are only 10 cm thick, leaving 80 cm of inviscid core suitable for model testing.

An external flow has no restraining walls and is free to expand no matter how thick the viscous layers on the immersed body may become. Thus, far from the body the flow is nearly inviscid, and our analytical technique, treated in Chap. 7, is to patch an inviscid-flow solution onto a viscous boundary-layer solution computed for the wall region. There is no external equivalent of fully developed internal flow.

6.3 Semiempirical Turbulent Shear Correlations

Throughout this chapter we assume constant density and viscosity and no thermal interaction, so that only the continuity and momentum equations are to be solved for velocity and pressure

$$\text{Continuity:} \qquad \frac{\partial u}{\partial x} + \frac{\partial \upsilon}{\partial y} + \frac{\partial w}{\partial z} = 0$$

$$\text{Momentum:} \qquad \rho \frac{d\mathbf{V}}{dt} = -\nabla p + \rho \mathbf{g} + \mu \nabla^2 \mathbf{V} \tag{6.7}$$

subject to no slip at the walls and known inlet and exit conditions. (We shall save our free-surface solutions for Chap. 10.)

Both laminar and turbulent flows satisfy Eqs. (6.7). For laminar flow, where there are no random fluctuations, we go right to the attack and solve them for a variety of geometries [2, 3], leaving many more, of course, for the problems.

Reynolds' Time-Averaging Concept

For turbulent flow, because of the fluctuations, every velocity and pressure term in Eqs. (6.7) is a rapidly varying random function of time and space. At present our mathematics cannot handle such instantaneous fluctuating variables. No single pair of random functions $\mathbf{V}(x, y, z, t)$ and $p(x, y, z, t)$ is known to be a solution to Eqs. (6.7). Moreover, our attention as engineers is toward the average or *mean* values of velocity, pressure, shear stress, etc., in a high-Reynolds-number (turbulent) flow. This approach led Osborne Reynolds in 1895 to rewrite Eqs. (6.7) in terms of mean or time-averaged turbulent variables.

The time mean $\overline{u}$ of a turbulent function $u(x, y, z, t)$ is defined by

$$\overline{u} = \frac{1}{T}\int_0^T u \, dt \tag{6.8}$$

where T is an averaging period taken to be longer than any significant period of the fluctuations themselves. The mean values of turbulent velocity and pressure are illustrated in Fig. 6.7. For turbulent gas and water flows, an averaging period $T \approx 5$ s is usually quite adequate.

The *fluctuation* u' is defined as the deviation of u from its average value

$$u' = u - \overline{u} \tag{6.9}$$

also shown in Fig. 6.7. It follows by definition that a fluctuation has zero mean value

$$\overline{u'} = \frac{1}{T}\int_0^T (u - \overline{u}) \, dt = \overline{u} - \overline{u} = 0 \tag{6.10}$$

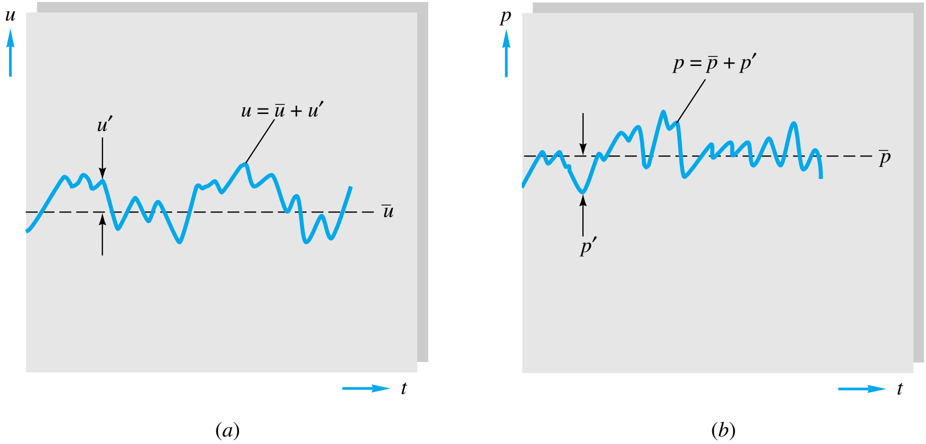

Fig. 6.7 Definition of mean and fluctuating turbulent variables: (*a*) velocity; (*b*) pressure.

However, the mean square of a fluctuation is not zero and is a measure of the *intensity* of the turbulence

$$\overline{u'^2} = \frac{1}{T}\int_0^T u'^2\,dt \neq 0 \tag{6.11}$$

Nor in general are the mean fluctuation products such as $\overline{u'v'}$ and $\overline{u'p'}$ zero in a typical turbulent flow.

Reynolds' idea was to split each property into mean plus fluctuating variables

$$u = \overline{u} + u' \quad v = \overline{v} + v' \quad w = \overline{w} + w' \quad p = \overline{p} + p' \tag{6.12}$$

Substitute these into Eqs. (6.7), and take the time mean of each equation. The continuity relation reduces to

$$\frac{\partial \overline{u}}{\partial x} + \frac{\partial \overline{v}}{\partial y} + \frac{\partial \overline{w}}{\partial z} = 0 \tag{6.13}$$

which is no different from a laminar continuity relation.

However, each component of the momentum equation (6.7*b*), after time averaging, will contain mean values plus three mean products, or *correlations,* of fluctuating velocities. The most important of these is the momentum relation in the mainstream, or *x*, direction, which takes the form

$$\begin{aligned}\rho\,\frac{d\overline{u}}{dt} = -\frac{\partial \overline{p}}{\partial x} + \rho g_x + \frac{\partial}{\partial x}\left(\mu\frac{\partial \overline{u}}{\partial x} - \rho\overline{u'^2}\right) \\ + \frac{\partial}{\partial y}\left(\mu\frac{\partial \overline{u}}{\partial y} - \rho\overline{u'v'}\right) + \frac{\partial}{\partial z}\left(\mu\frac{\partial \overline{u}}{\partial z} - \rho\overline{u'w'}\right)\end{aligned} \tag{6.14}$$

The three correlation terms $-\rho\overline{u'^2}$, $-\rho\overline{u'v'}$, and $-\rho\overline{u'w'}$ are called *turbulent stresses* because they have the same dimensions and occur right alongside the newtonian (laminar) stress terms $\mu(\partial\overline{u}/\partial x)$, etc. Actually, they are convective acceleration terms (which is why the density appears), not stresses, but they have the mathematical effect of stress and are so termed almost universally in the literature.

The turbulent stresses are unknown a priori and must be related by experiment to

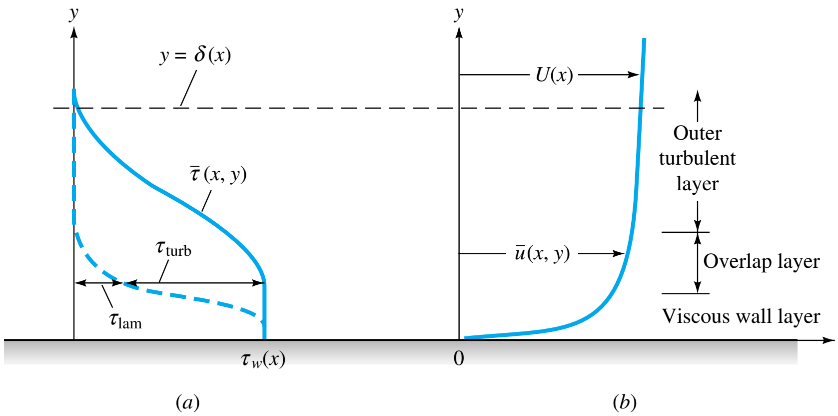

Fig. 6.8 Typical velocity and shear distributions in turbulent flow near a wall: (*a*) shear; (*b*) velocity.

geometry and flow conditions, as detailed in Refs. 1 to 3. Fortunately, in duct and boundary-layer flow, the stress $-\rho\overline{u'v'}$ associated with direction y normal to the wall is dominant, and we can approximate with excellent accuracy a simpler streamwise momentum equation

$$\rho\frac{d\bar{u}}{dt} \approx -\frac{\partial\bar{p}}{\partial x} + \rho g_x + \frac{\partial\tau}{\partial y} \tag{6.15}$$

where
$$\tau = \mu\frac{\partial\bar{u}}{\partial y} - \rho\overline{u'v'} = \tau_{lam} + \tau_{turb} \tag{6.16}$$

Figure 6.8 shows the distribution of τ_{lam} and τ_{turb} from typical measurements across a turbulent-shear layer near a wall. Laminar shear is dominant near the wall (the *wall layer*), and turbulent shear dominates in the *outer layer*. There is an intermediate region, called the *overlap layer,* where both laminar and turbulent shear are important. These three regions are labeled in Fig. 6.8.

In the outer layer τ_{turb} is two or three orders of magnitude greater than τ_{lam}, and vice versa in the wall layer. These experimental facts enable us to use a crude but very effective model for the velocity distribution $\bar{u}(y)$ across a turbulent wall layer.

The Logarithmic-Overlap Law

We have seen in Fig. 6.8 that there are three regions in turbulent flow near a wall:

1. Wall layer: Viscous shear dominates.
2. Outer layer: Turbulent shear dominates.
3. Overlap layer: Both types of shear are important.

From now on let us agree to drop the overbar from velocity $\bar{u}$. Let τ_w be the wall shear stress, and let δ and U represent the thickness and velocity at the edge of the outer layer, $y = \delta$.

For the wall layer, Prandtl deduced in 1930 that u must be independent of the shear-layer thickness

$$u = f(\mu, \tau_w, \rho, y) \tag{6.17}$$

By dimensional analysis, this is equivalent to

$$u^+ = \frac{u}{u^*} = F\left(\frac{yu^*}{\nu}\right) \qquad u^* = \left(\frac{\tau_w}{\rho}\right)^{1/2} \tag{6.18}$$

Equation (6.18) is called the *law of the wall,* and the quantity u^* is termed the *friction velocity* because it has dimensions $\{LT^{-1}\}$, although it is not actually a flow velocity.

Subsequently, Kármán in 1933 deduced that u in the outer layer is independent of molecular viscosity, but its deviation from the stream velocity U must depend on the layer thickness δ and the other properties

$$(U - u)_{\text{outer}} = g(\delta, \tau_w, \rho, y) \tag{6.19}$$

Again, by dimensional analysis we rewrite this as

$$\frac{U - u}{u^*} = G\left(\frac{y}{\delta}\right) \tag{6.20}$$

where u^* has the same meaning as in Eq. (6.18). Equation (6.20) is called the *velocity-defect law* for the outer layer.

Both the wall law (6.18) and the defect law (6.20) are found to be accurate for a wide variety of experimental turbulent duct and boundary-layer flows [1 to 3]. They are different in form, yet they must overlap smoothly in the intermediate layer. In 1937 C. B. Millikan showed that this can be true only if the overlap-layer velocity varies logarithmically with y:

$$\frac{u}{u^*} = \frac{1}{\kappa} \ln \frac{yu^*}{\nu} + B \qquad \text{overlap layer} \tag{6.21}$$

Over the full range of turbulent smooth wall flows, the dimensionless constants κ and B are found to have the approximate values $\kappa \approx 0.41$ and $B \approx 5.0$. Equation (6.21) is called the *logarithmic-overlap layer*.

Thus by dimensional reasoning and physical insight we infer that a plot of u versus $\ln y$ in a turbulent-shear layer will show a curved wall region, a curved outer region, and a straight-line logarithmic overlap. Figure 6.9 shows that this is exactly the case. The four outer-law profiles shown all merge smoothly with the logarithmic-overlap law but have different magnitudes because they vary in external pressure gradient. The wall law is unique and follows the linear viscous relation

$$u^+ = \frac{u}{u^*} = \frac{yu^*}{\nu} = y^+ \tag{6.22}$$

from the wall to about $y^+ = 5$, thereafter curving over to merge with the logarithmic law at about $y^+ = 30$.

Believe it or not, Fig. 6.9, which is nothing more than a shrewd correlation of velocity profiles, is the basis for most existing "theory" of turbulent-shear flows. Notice that we have not solved any equations at all but have merely expressed the streamwise velocity in a neat form.

There is serendipity in Fig. 6.9: The logarithmic law (6.21), instead of just being a short overlapping link, actually approximates nearly the entire velocity profile, except for the outer law when the pressure is increasing strongly downstream (as in a diffuser). The inner-wall law typically extends over less than 2 percent of the profile and can be neglected. Thus we can use Eq. (6.21) as an excellent approximation to solve

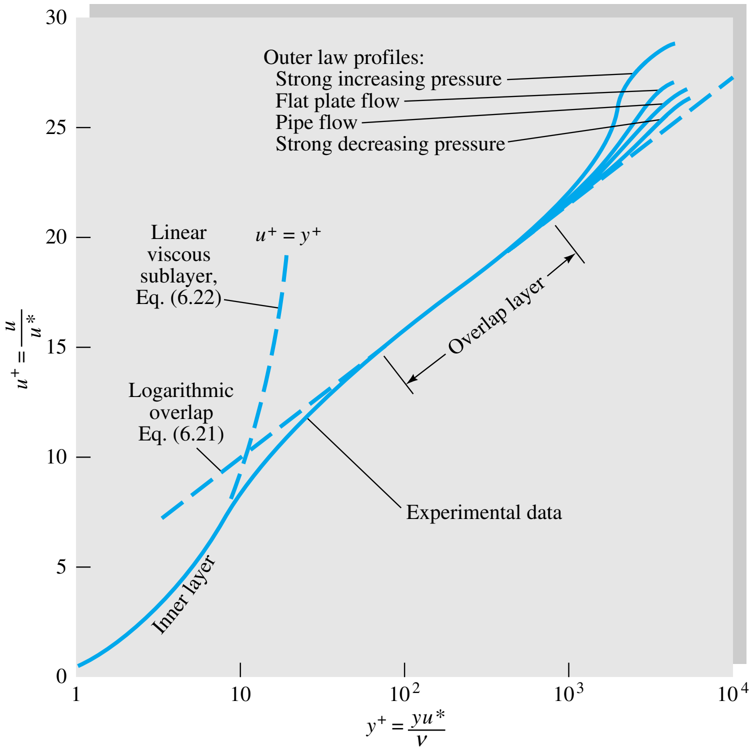

Fig. 6.9 Experimental verification of the inner-, outer-, and overlap-layer laws relating velocity profiles in turbulent wall flow.

nearly every turbulent-flow problem presented in this and the next chapter. Many additional applications are given in Refs. 2 and 3.

EXAMPLE 6.3

Air at 20°C flows through a 14-cm-diameter tube under fully developed conditions. The centerline velocity is $u_0 = 5$ m/s. Estimate from Fig. 6.9 (*a*) the friction velocity u^*, (*b*) the wall shear stress τ_w, and (*c*) the average velocity $V = Q/A$.

Solution

Part (a)

For pipe flow Fig. 6.9 shows that the logarithmic law, Eq. (6.21), is accurate all the way to the center of the tube. From Fig. E6.3 $y = R - r$ should go from the wall to the centerline as shown. At the center $u = u_0$, $y = R$, and Eq. (6.21) becomes

$$\frac{u_0}{u^*} = \frac{1}{0.41} \ln \frac{Ru^*}{\nu} + 5.0 \qquad (1)$$

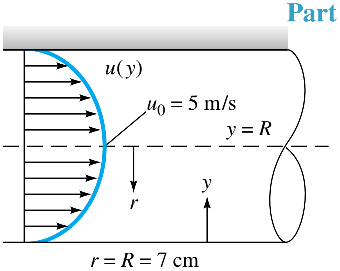

E6.3

Since we know that $u_0 = 5$ m/s and $R = 0.07$ m, u^* is the only unknown in Eq. (1). Find the solution by trial and error or by EES

$$u^* = 0.228 \text{ m/s} = 22.8 \text{ cm/s} \qquad \textit{Ans. (a)}$$

where we have taken $\nu = 1.51 \times 10^{-5}$ m²/s for air from Table 1.4.

Part (b) Assuming a pressure of 1 atm, we have $\rho = p/(RT) = 1.205\ \text{kg/m}^3$. Since by definition $u^* = (\tau_w/\rho)^{1/2}$, we compute

$$\tau_w = \rho u^{*2} = (1.205\ \text{kg/m}^3)(0.228\ \text{m/s})^2 = 0.062\ \text{kg/(m}\cdot\text{s}^2) = 0.062\ \text{Pa} \qquad \textit{Ans. (b)}$$

This is a very small shear stress, but it will cause a large pressure drop in a long pipe (170 Pa for every 100 m of pipe).

Part (c) The average velocity V is found by integrating the logarithmic-law velocity distribution

$$V = \frac{Q}{A} = \frac{1}{\pi R^2}\int_0^R u\, 2\pi r\, dr \tag{2}$$

Introducing $u = u^*[(1/\kappa)\ln(yu^*/\nu) + B]$ from Eq. (6.21) and noting that $y = R - r$, we can carry out the integration of Eq. (2), which is rather laborious. The final result is

$$V = 0.835u_0 = 4.17\ \text{m/s} \qquad \textit{Ans. (c)}$$

We shall not bother showing the integration here because it is all worked out and a very neat formula is given in Eqs. (6.49) and (6.59).

Notice that we started from almost nothing (the pipe diameter and the centerline velocity) and found the answers without solving the differential equations of continuity and momentum. We just used the logarithmic law, Eq. (6.21), which makes the differential equations unnecessary for pipe flow. This is a powerful technique, but you should remember that all we are doing is using an experimental velocity correlation to approximate the actual solution to the problem.

We should check the Reynolds number to ensure turbulent flow

$$\text{Re}_d = \frac{Vd}{\nu} = \frac{(4.17\ \text{m/s})(0.14\ \text{m})}{1.51 \times 10^{-5}\ \text{m}^2/\text{s}} = 38{,}700$$

Since this is greater than 4000, the flow is definitely turbulent.

6.4 Flow in a Circular Pipe

As our first example of a specific viscous-flow analysis, we take the classic problem of flow in a full pipe, driven by pressure or gravity or both. Figure 6.10 shows the geometry of the pipe of radius R. The x-axis is taken in the flow direction and is inclined to the horizontal at an angle ϕ.

Before proceeding with a solution to the equations of motion, we can learn a lot by making a control-volume analysis of the flow between sections 1 and 2 in Fig. 6.10. The continuity relation, Eq. (3.23), reduces to

$$Q_1 = Q_2 = \text{const}$$

or

$$V_1 = \frac{Q_1}{A_1} = V_2 = \frac{Q_2}{A_2} \tag{6.23}$$

since the pipe is of constant area. The steady-flow energy equation (3.71) reduces to

$$\frac{p_1}{\rho} + \frac{1}{2}\alpha_1 V_1^2 + gz_1 = \frac{p_2}{\rho} + \frac{1}{2}\alpha_2 V_2^2 + gz_2 + gh_f \tag{6.24}$$

since there are no shaft-work or heat-transfer effects. Now assume that the flow is fully

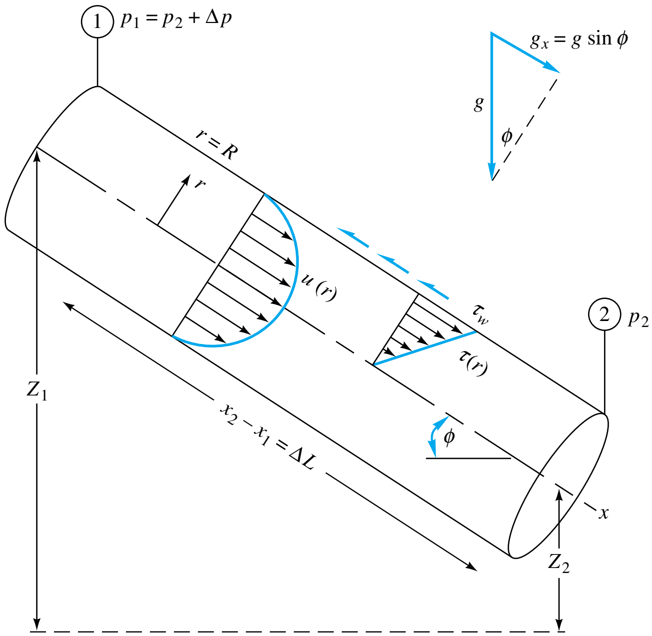

Fig. 6.10 Control volume of steady, fully developed flow between two sections in an inclined pipe.

developed (Fig. 6.6), and correct later for entrance effects. Then the kinetic-energy correction factor $\alpha_1 = \alpha_2$, and since $V_1 = V_2$ from (6.23), Eq. (6.24) now reduces to a simple expression for the friction-head loss h_f

$$h_f = \left(z_1 + \frac{p_1}{\rho g}\right) - \left(z_2 + \frac{p_2}{\rho g}\right) = \Delta\left(z + \frac{p}{\rho g}\right) = \Delta z + \frac{\Delta p}{\rho g} \tag{6.25}$$

The pipe-head loss equals the change in the sum of pressure and gravity head, i.e., the change in height of the hydraulic grade line (HGL). Since the velocity head is constant through the pipe, h_f also equals the height change of the energy grade line (EGL). Recall that the EGL decreases downstream in a flow with losses unless it passes through an energy source, e.g., as a pump or heat exchanger.

Finally apply the momentum relation (3.40) to the control volume in Fig. 6.10, accounting for applied forces due to pressure, gravity, and shear

$$\Delta p\ \pi R^2 + \rho g(\pi R^2)\ \Delta L \sin \phi - \tau_w(2\pi R)\ \Delta L = \dot{m}(V_2 - V_1) = 0 \tag{6.26}$$

This equation relates h_f to the wall shear stress

$$\Delta z + \frac{\Delta p}{\rho g} = h_f = \frac{2\tau_w}{\rho g}\frac{\Delta L}{R} \tag{6.27}$$

where we have substituted $\Delta z = \Delta L \sin \phi$ from Fig. 6.10.

So far we have not assumed either laminar or turbulent flow. If we can correlate τ_w with flow conditions, we have solved the problem of head loss in pipe flow. Functionally, we can assume that

$$\tau_w = F(\rho, V, \mu, d, \epsilon) \tag{6.28}$$

where ϵ is the wall-roughness height. Then dimensional analysis tells us that

$$\frac{8\tau_w}{\rho V^2} = f = F\left(\text{Re}_d, \frac{\epsilon}{d}\right) \tag{6.29}$$

The dimensionless parameter f is called the *Darcy friction factor,* after Henry Darcy (1803–1858), a French engineer whose pipe-flow experiments in 1857 first established the effect of roughness on pipe resistance.

Combining Eqs. (6.27) and (6.29), we obtain the desired expression for finding pipe-head loss

$$h_f = f\frac{L}{d}\frac{V^2}{2g} \tag{6.30}$$

This is the *Darcy-Weisbach equation,* valid for duct flows of any cross section and for laminar and turbulent flow. It was proposed by Julius Weisbach, a German professor who in 1850 published the first modern textbook on hydrodynamics.

Our only remaining problem is to find the form of the function F in Eq. (6.29) and plot it in the Moody chart of Fig. 6.13.

Equations of Motion

For either laminar or turbulent flow, the continuity equation in cylindrical coordinates is given by (App. D)

$$\frac{1}{r}\frac{\partial}{\partial r}(r\upsilon_r) + \frac{1}{r}\frac{\partial}{\partial \theta}(\upsilon_\theta) + \frac{\partial u}{\partial x} = 0 \tag{6.31}$$

We assume that there is no swirl or circumferential variation, $\upsilon_\theta = \partial/\partial\theta = 0$, and fully developed flow: $u = u(r)$ only. Then Eq. (6.31) reduces to

$$\frac{1}{r}\frac{\partial}{\partial r}(r\upsilon_r) = 0$$

or

$$r\upsilon_r = \text{const} \tag{6.32}$$

But at the wall, $r = R$, $\upsilon_r = 0$ (no slip); therefore (6.32) implies that $\upsilon_r = 0$ everywhere. Thus in fully developed flow there is only one velocity component, $u = u(r)$.

The momentum differential equation in cylindrical coordinates now reduces to

$$\rho u\frac{\partial u}{\partial x} = -\frac{dp}{dx} + \rho g_x + \frac{1}{r}\frac{\partial}{\partial r}(r\tau) \tag{6.33}$$

where τ can represent either laminar or turbulent shear. But the left-hand side vanishes because $u = u(r)$ only. Rearrange, noting from Fig. 6.10 that $g_x = g \sin\phi$:

$$\frac{1}{r}\frac{\partial}{\partial r}(r\tau) = \frac{d}{dx}(p - \rho g x \sin\phi) = \frac{d}{dx}(p + \rho g z) \tag{6.34}$$

Since the left-hand side varies only with r and the right-hand side varies only with x, it follows that both sides must be equal to the same constant.[2] Therefore we can integrate Eq. (6.34) to find the shear distribution across the pipe, utilizing the fact that $\tau = 0$ at $r = 0$

$$\tau = \frac{1}{2}r\frac{d}{dx}(p + \rho g z) = (\text{const})(r) \tag{6.35}$$

[2]Ask your instructor to explain this to you if necessary.

Thus the shear varies linearly from the centerline to the wall, for either laminar or turbulent flow. This is also shown in Fig. 6.10. At $r = R$, we have the wall shear

$$\tau_w = \frac{1}{2} R \frac{\Delta p + \rho g \, \Delta z}{\Delta L} \tag{6.36}$$

which is identical with our momentum relation (6.27). We can now complete our study of pipe flow by applying either laminar or turbulent assumptions to fill out Eq. (6.35).

Laminar-Flow Solution

Note in Eq. (6.35) that the HGL slope $d(p + \rho gz)/dx$ is *negative* because both pressure and height drop with x. For laminar flow, $\tau = \mu \, du/dr$, which we substitute in Eq. (6.35)

$$\mu \frac{du}{dr} = \frac{1}{2} rK \qquad K = \frac{d}{dx}(p + \rho gz) \tag{6.37}$$

Integrate once

$$u = \frac{1}{4} r^2 \frac{K}{\mu} + C_1 \tag{6.38}$$

The constant C_1 is evaluated from the no-slip condition at the wall: $u = 0$ at $r = R$

$$0 = \frac{1}{4} R^2 \frac{K}{\mu} + C_1 \tag{6.39}$$

or $C_1 = -\frac{1}{4} R^2 K/\mu$. Introduce into Eq. (6.38) to obtain the exact solution for laminar fully developed pipe flow

$$u = \frac{1}{4\mu} \left[-\frac{d}{dx}(p + \rho gz) \right] (R^2 - r^2) \tag{6.40}$$

The laminar-flow profile is thus a paraboloid falling to zero at the wall and reaching a maximum at the axis

$$u_{\max} = \frac{R^2}{4\mu} \left[-\frac{d}{dx}(p + \rho gz) \right] \tag{6.41}$$

It resembles the sketch of $u(r)$ given in Fig. 6.10.

The laminar distribution (6.40) is called *Hagen-Poiseuille flow* to commemorate the experimental work of G. Hagen in 1839 and J. L. Poiseuille in 1940, both of whom established the pressure-drop law, Eq. (6.1). The first theoretical derivation of Eq. (6.40) was given independently by E. Hagenbach and by F. Neumann around 1859.

Other pipe-flow results follow immediately from Eq. (6.40). The volume flow is

$$Q = \int_0^R u \, dA = \int_0^R u_{\max} \left(1 - \frac{r^2}{R^2} \right) 2\pi r \, dr$$

$$= \frac{1}{2} u_{\max} \pi R^2 = \frac{\pi R^4}{8\mu} \left[-\frac{d}{dx}(p + \rho gz) \right] \tag{6.42}$$

Thus the average velocity in laminar flow is one-half the maximum velocity

$$V = \frac{Q}{A} = \frac{Q}{\pi R^2} = \frac{1}{2}u_{\max} \tag{6.43}$$

For a horizontal tube ($\Delta z = 0$), Eq. (6.42) is of the form predicted by Hagen's experiment, Eq. (6.1):

$$\Delta p = \frac{8\mu LQ}{\pi R^4} \tag{6.44}$$

The wall shear is computed from the wall velocity gradient

$$\tau_w = \left|\mu \frac{du}{dr}\right|_{r=R} = \frac{2\mu u_{\max}}{R} = \frac{1}{2}R\left|\frac{d}{dx}(p + \rho g z)\right| \tag{6.45}$$

This gives an exact theory for laminar Darcy friction factor

$$f = \frac{8\tau_w}{\rho V^2} = \frac{8(8\mu V/d)}{\rho V^2} = \frac{64\mu}{\rho V d}$$

or

$$f_{\text{lam}} = \frac{64}{\text{Re}_d} \tag{6.46}$$

This is plotted later in the Moody chart (Fig. 6.13). The fact that f drops off with increasing Re_d should not mislead us into thinking that shear decreases with velocity: Eq. (6.45) clearly shows that τ_w is proportional to $u_{\max}$; it is interesting to note that τ_w is independent of density because the fluid acceleration is zero.

The laminar head loss follows from Eq. (6.30)

$$h_{f,\text{lam}} = \frac{64\mu}{\rho V d}\frac{L}{d}\frac{V^2}{2g} = \frac{32\mu L V}{\rho g d^2} = \frac{128\mu L Q}{\pi \rho g d^4} \tag{6.47}$$

We see that laminar head loss is proportional to V.

EXAMPLE 6.4

An oil with $\rho = 900\ \text{kg/m}^3$ and $\nu = 0.0002\ \text{m}^2/\text{s}$ flows upward through an inclined pipe as shown in Fig. E6.4. The pressure and elevation are known at sections 1 and 2, 10 m apart. Assuming

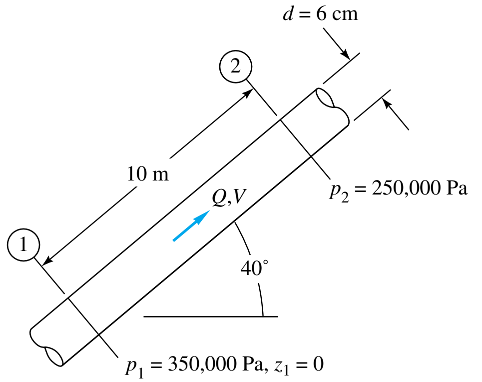

E6.4

steady laminar flow, (*a*) verify that the flow is up, (*b*) compute h_f between 1 and 2, and compute (*c*) Q, (*d*) V, and (*e*) Re_d. Is the flow really laminar?

Solution

Part (a) For later use, calculate

$$\mu = \rho\nu = (900 \text{ kg/m}^3)(0.0002 \text{ m}^2\text{/s}) = 0.18 \text{ kg/(m} \cdot \text{s)}$$

$$z_2 = \Delta L \sin 40° = (10 \text{ m})(0.643) = 6.43 \text{ m}$$

The flow goes in the direction of falling HGL; therefore compute the hydraulic grade-line height at each section

$$\text{HGL}_1 = z_1 + \frac{p_1}{\rho g} = 0 + \frac{350{,}000}{900(9.807)} = 39.65 \text{ m}$$

$$\text{HGL}_2 = z_2 + \frac{p_2}{\rho g} = 6.43 + \frac{250{,}000}{900(9.807)} = 34.75 \text{ m}$$

The HGL is lower at section 2; hence the flow is from 1 to 2 as assumed. *Ans. (a)*

Part (b) The head loss is the change in HGL:

$$h_f = \text{HGL}_1 - \text{HGL}_2 = 39.65 \text{ m} - 34.75 \text{ m} = 4.9 \text{ m} \qquad \textit{Ans. (b)}$$

Half the length of the pipe is quite a large head loss.

Part (c) We can compute Q from the various laminar-flow formulas, notably Eq. (6.47)

$$Q = \frac{\pi\rho g d^4 h_f}{128\mu L} = \frac{\pi(900)(9.807)(0.06)^4(4.9)}{128(0.18)(10)} = 0.0076 \text{ m}^3\text{/s} \qquad \textit{Ans. (c)}$$

Part (d) Divide Q by the pipe area to get the average velocity

$$V = \frac{Q}{\pi R^2} = \frac{0.0076}{\pi(0.03)^2} = 2.7 \text{ m/s} \qquad \textit{Ans. (d)}$$

Part (e) With V known, the Reynolds number is

$$\text{Re}_d = \frac{Vd}{\nu} = \frac{2.7(0.06)}{0.0002} = 810 \qquad \textit{Ans. (e)}$$

This is well below the transition value $\text{Re}_d = 2300$, and so we are fairly certain the flow is laminar.

Notice that by sticking entirely to consistent SI units (meters, seconds, kilograms, newtons) for all variables we avoid the need for any conversion factors in the calculations.

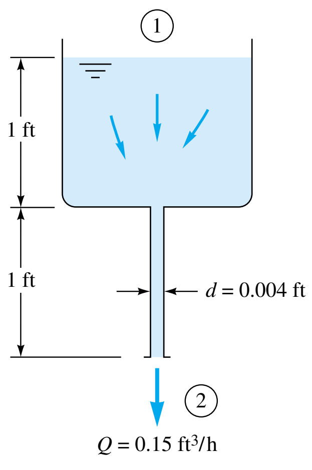

E6.5

EXAMPLE 6.5

A liquid of specific weight $\rho g = 58 \text{ lb/ft}^3$ flows by gravity through a 1-ft tank and a 1-ft capillary tube at a rate of $0.15 \text{ ft}^3\text{/h}$, as shown in Fig. E6.5. Sections 1 and 2 are at atmospheric pressure. Neglecting entrance effects, compute the viscosity of the liquid.

Solution

Apply the steady-flow energy equation (6.24), including the correction factor α:

$$\frac{p_1}{\rho g} + \frac{\alpha_1 V_1^2}{2g} + z_1 = \frac{p_2}{\rho g} + \frac{\alpha_2 V_2^2}{2g} + z_2 + h_f$$

The average exit velocity V_2 can be found from the volume flow and the pipe size:

$$V_2 = \frac{Q}{A_2} = \frac{Q}{\pi R^2} = \frac{(0.15/3600)\ \text{ft}^3/\text{s}}{\pi(0.002\ \text{ft})^2} \approx 3.32\ \text{ft/s}$$

Meanwhile $p_1 = p_2 = p_a$, and $V_1 \approx 0$ in the large tank. Therefore, approximately,

$$h_f \approx z_1 - z_2 - \alpha_2 \frac{V_2^2}{2g} = 2.0\ \text{ft} - 2.0\frac{(3.32\ \text{ft/s})^2}{2(32.2\ \text{ft/s}^2)} \approx 1.66\ \text{ft}$$

where we have introduced $\alpha_2 = 2.0$ for laminar pipe flow from Eq. (3.72). Note that h_f includes the entire 2-ft drop through the system and not just the 1-ft pipe length.

With the head loss known, the viscosity follows from our laminar-flow formula (6.47):

$$h_f = 1.66\ \text{ft} = \frac{32\mu LV}{\rho g d^2} = \frac{32\mu(1.0\ \text{ft})(3.32\ \text{ft/s})}{(58\ \text{lbf/ft}^3)(0.004\ \text{ft})^2} = 114{,}500\ \mu$$

or

$$\mu = \frac{1.66}{114{,}500} = 1.45\ \text{E-5 slug/(ft} \cdot \text{s)} \qquad \textit{Ans.}$$

Note that L in this formula is the *pipe* length of 1 ft. Finally, check the Reynolds number:

$$\text{Re}_d = \frac{\rho V d}{\mu} = \frac{(58/32.2\ \text{slug/ft}^3)(3.32\ \text{ft/s})(0.004\ \text{ft})}{1.45\ \text{E-5 slug/(ft} \cdot \text{s)}} = 1650 \qquad \text{laminar}$$

Since this is less than 2300, we conclude that the flow is indeed laminar. Actually, for this head loss, there is a *second* (turbulent) solution, as we shall see in Example 6.8.

Turbulent-Flow Solution

For turbulent pipe flow we need not solve a differential equation but instead proceed with the logarithmic law, as in Example 6.3. Assume that Eq. (6.21) correlates the local mean velocity $u(r)$ all the way across the pipe

$$\frac{u(r)}{u^*} \approx \frac{1}{\kappa} \ln \frac{(R-r)u^*}{\nu} + B \tag{6.48}$$

where we have replaced y by $R - r$. Compute the average velocity from this profile

$$\begin{aligned} V = \frac{Q}{A} &= \frac{1}{\pi R^2} \int_0^R u^* \left[\frac{1}{\kappa} \ln \frac{(R-r)u^*}{\nu} + B\right] 2\pi r\, dr \\ &= \frac{1}{2} u^* \left(\frac{2}{\kappa} \ln \frac{Ru^*}{\nu} + 2B - \frac{3}{\kappa}\right) \end{aligned} \tag{6.49}$$

Introducing $\kappa = 0.41$ and $B = 5.0$, we obtain, numerically,

$$\frac{V}{u^*} \approx 2.44 \ln \frac{Ru^*}{\nu} + 1.34 \tag{6.50}$$

This looks only marginally interesting until we realize that V/u^* is directly related to the Darcy friction factor

$$\frac{V}{u^*} = \left(\frac{\rho V^2}{\tau_w}\right)^{1/2} = \left(\frac{8}{f}\right)^{1/2} \tag{6.51}$$

Moreover, the argument of the logarithm in (6.50) is equivalent to

$$\frac{Ru^*}{\nu} = \frac{\frac{1}{2}Vd}{\nu}\frac{u^*}{V} = \frac{1}{2}\mathrm{Re}_d\left(\frac{f}{8}\right)^{1/2} \tag{6.52}$$

Introducing (6.52) and (6.51) into Eq. (6.50), changing to a base-10 logarithm, and rearranging, we obtain

$$\frac{1}{f^{1/2}} \approx 1.99 \log\,(\mathrm{Re}_d f^{1/2}) - 1.02 \tag{6.53}$$

In other words, by simply computing the mean velocity from the logarithmic-law correlation, we obtain a relation between the friction factor and Reynolds number for turbulent pipe flow. Prandtl derived Eq. (6.53) in 1935 and then adjusted the constants slightly to fit friction data better

$$\frac{1}{f^{1/2}} = 2.0 \log\,(\mathrm{Re}_d f^{1/2}) - 0.8 \tag{6.54}$$

This is the accepted formula for a smooth-walled pipe. Some numerical values may be listed as follows:

Re_d	4000	10^4	10^5	10^6	10^7	10^8
f	0.0399	0.0309	0.0180	0.0116	0.0081	0.0059

Thus f drops by only a factor of 5 over a 10,000-fold increase in Reynolds number. Equation (6.54) is cumbersome to solve if Re_d is known and f is wanted. There are many alternate approximations in the literature from which f can be computed explicitly from Re_d

$$f = \begin{cases} 0.316\,\mathrm{Re}_d^{-1/4} & 4000 < \mathrm{Re}_d < 10^5 \qquad \text{H. Blasius (1911)} \\ \left(1.8 \log \dfrac{\mathrm{Re}_d}{6.9}\right)^{-2} & \qquad\qquad \text{Ref. 9} \end{cases} \tag{6.55}$$

Blasius, a student of Prandtl, presented his formula in the first correlation ever made of pipe friction versus Reynolds number. Although his formula has a limited range, it illustrates what was happening to Hagen's 1839 pressure-drop data. For a horizontal pipe, from Eq. (6.55),

$$h_f = \frac{\Delta p}{\rho g} = f\frac{L}{d}\frac{V^2}{2g} \approx 0.316\left(\frac{\mu}{\rho V d}\right)^{1/4}\frac{L}{d}\frac{V^2}{2g}$$

or

$$\Delta p \approx 0.158\, L\rho^{3/4}\mu^{1/4}d^{-5/4}V^{7/4} \tag{6.56}$$

at low turbulent Reynolds numbers. This explains why Hagen's data for pressure drop begin to increase as the 1.75 power of the velocity, in Fig. 6.4. Note that Δp varies only slightly with viscosity, which is characteristic of turbulent flow. Introducing $Q = \frac{1}{4}\pi d^2 V$ into Eq. (6.56), we obtain the alternate form

$$\Delta p \approx 0.241 L\rho^{3/4}\mu^{1/4}d^{-4.75}Q^{1.75} \tag{6.57}$$

For a given flow rate Q, the turbulent pressure drop decreases with diameter even more sharply than the laminar formula (6.47). Thus the quickest way to reduce required pumping pressure is to increase the pipe size, although, of course, the larger pipe is more expensive. Doubling the pipe size decreases Δp by a factor of about 27 for a given Q. Compare Eq. (6.56) with Example 5.7 and Fig. 5.10.

The maximum velocity in turbulent pipe flow is given by Eq. (6.48), evaluated at $r = 0$

$$\frac{u_{max}}{u^*} \approx \frac{1}{\kappa} \ln \frac{Ru^*}{\nu} + B \tag{6.58}$$

Combining this with Eq. (6.49), we obtain the formula relating mean velocity to maximum velocity

$$\frac{V}{u_{max}} \approx (1 + 1.33\sqrt{f})^{-1} \tag{6.59}$$

Some numerical values are

Re_d	4000	10^4	10^5	10^6	10^7	10^8
V/u_{max}	0.790	0.811	0.849	0.875	0.893	0.907

The ratio varies with the Reynolds number and is much larger than the value of 0.5 predicted for all laminar pipe flow in Eq. (6.43). Thus a turbulent velocity profile, as shown in Fig. 6.11, is very flat in the center and drops off sharply to zero at the wall.

Effect of Rough Walls

It was not known until experiments in 1800 by Coulomb [6] that surface roughness has an effect on friction resistance. It turns out that the effect is negligible for laminar pipe flow, and all the laminar formulas derived in this section are valid for rough walls also. But turbulent flow is strongly affected by roughness. In Fig. 6.9 the linear viscous sublayer only extends out to $y^+ = yu^*/\nu = 5$. Thus, compared with the diameter, the sublayer thickness y_s is only

$$\frac{y_s}{d} = \frac{5\nu/u^*}{d} = \frac{14.1}{Re_d f^{1/2}} \tag{6.60}$$

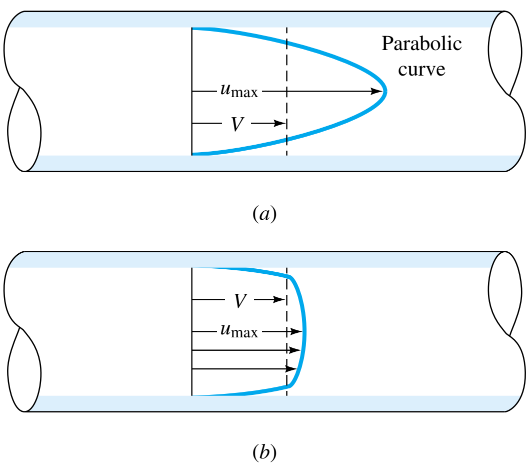

Fig. 6.11 Comparison of laminar and turbulent pipe-flow velocity profiles for the same volume flow: (*a*) laminar flow; (*b*) turbulent flow.

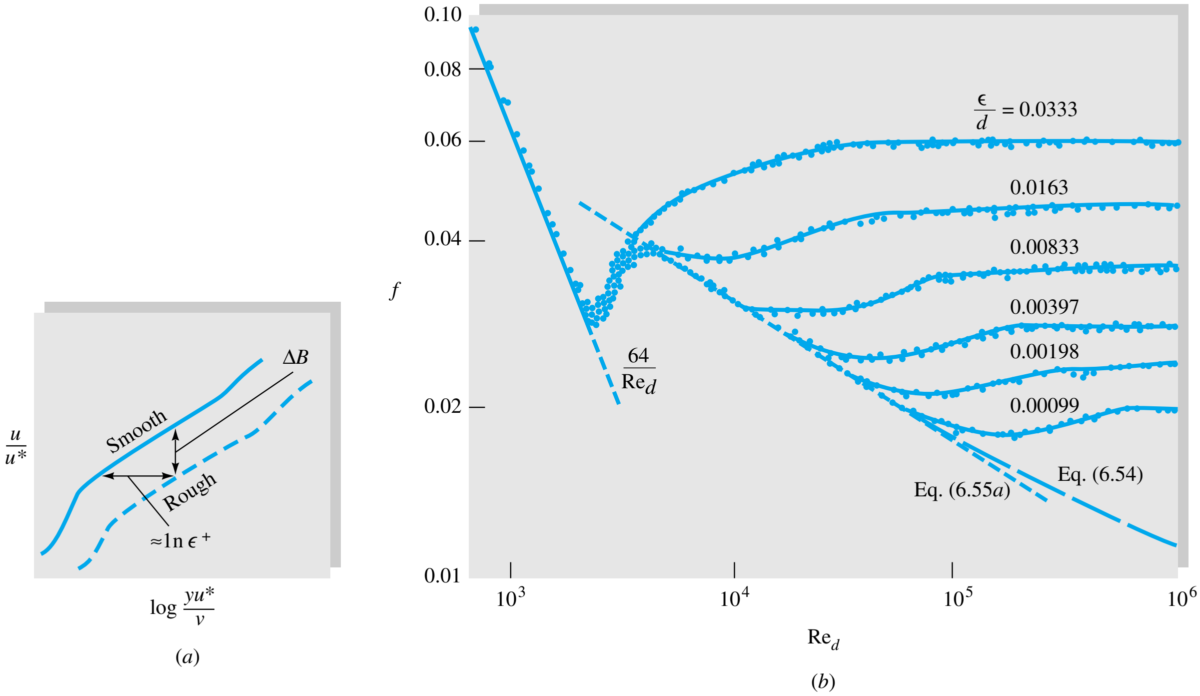

Fig. 6.12 Effect of wall roughness on turbulent pipe flow. (*a*) The logarithmic overlap-velocity profile shifts down and to the right; (*b*) experiments with sand-grain roughness by Nikuradse [7] show a systematic increase of the turbulent friction factor with the roughness ratio.

For example, at $\text{Re}_d = 10^5$, $f = 0.0180$, and $y_s/d = 0.001$, a wall roughness of about $0.001d$ will break up the sublayer and profoundly change the wall law in Fig. 6.9.

Measurements of $u(y)$ in turbulent rough-wall flow by Prandtl's student Nikuradse [7] show, as in Fig. 6.12*a*, that a roughness height ϵ will force the logarithm-law profile outward on the abscissa by an amount approximately equal to ln ϵ^+, where $\epsilon^+ = \epsilon u^*/\nu$. The slope of the logarithm law remains the same, $1/\kappa$, but the shift outward causes the constant B to be less by an amount $\Delta B \approx (1/\kappa) \ln \epsilon^+$.

Nikuradse [7] simulated roughness by gluing uniform sand grains onto the inner walls of the pipes. He then measured the pressure drops and flow rates and correlated friction factor versus Reynolds number in Fig. 6.12*b*. We see that laminar friction is unaffected, but turbulent friction, after an *onset* point, increases monotonically with the roughness ratio ϵ/d. For any given ϵ/d, the friction factor becomes constant *(fully rough)* at high Reynolds numbers. These points of change are certain values of $\epsilon^+ = \epsilon u^*/\nu$:

$\dfrac{\epsilon u^*}{\nu} < 5$: *hydraulically smooth* walls, no effect of roughness on friction

$5 \le \dfrac{\epsilon u^*}{\nu} \le 70$: *transitional* roughness, moderate Reynolds-number effect

$\dfrac{\epsilon u^*}{\nu} > 70$: *fully rough* flow, sublayer totally broken up and friction independent of Reynolds number

For fully rough flow, $\epsilon^+ > 70$, the log-law downshift ΔB in Fig. 6.12*a* is

$$\Delta B \approx \frac{1}{\kappa} \ln \epsilon^+ - 3.5 \tag{6.61}$$

and the logarithm law modified for roughness becomes

$$u^+ = \frac{1}{\kappa}\ln y^+ + B - \Delta B = \frac{1}{\kappa}\ln\frac{y}{\epsilon} + 8.5 \tag{6.62}$$

The viscosity vanishes, and hence fully rough flow is independent of the Reynolds number. If we integrate Eq. (6.62) to obtain the average velocity in the pipe, we obtain

$$\frac{V}{u^*} = 2.44\ln\frac{d}{\epsilon} + 3.2$$

or

$$\frac{1}{f^{1/2}} = -2.0\log\frac{\epsilon/d}{3.7} \qquad \text{fully rough flow} \tag{6.63}$$

There is no Reynolds-number effect; hence the head loss varies exactly as the square of the velocity in this case. Some numerical values of friction factor may be listed:

ϵ/d	0.00001	0.0001	0.001	0.01	0.05
f	0.00806	0.0120	0.0196	0.0379	0.0716

The friction factor increases by 9 times as the roughness increases by a factor of 5000. In the transitional-roughness region, sand grains behave somewhat differently from commercially rough pipes, so Fig. 6.12*b* has now been replaced by the Moody chart.

The Moody Chart

In 1939 to cover the transitionally rough range, Colebrook [9] combined the smooth-wall [Eq. (6.54)] and fully rough [Eq. (6.63)] relations into a clever interpolation formula

$$\frac{1}{f^{1/2}} = -2.0\log\left(\frac{\epsilon/d}{3.7} + \frac{2.51}{\mathrm{Re}_d f^{1/2}}\right) \tag{6.64}$$

This is the accepted design formula for turbulent friction. It was plotted in 1944 by Moody [8] into what is now called the *Moody chart* for pipe friction (Fig. 6.13). The Moody chart is probably the most famous and useful figure in fluid mechanics. It is accurate to $\pm$ 15 percent for design calculations over the full range shown in Fig. 6.13. It can be used for circular and noncircular (Sec. 6.6) pipe flows and for open-channel flows (Chap. 10). The data can even be adapted as an approximation to boundary-layer flows (Chap. 7).

Equation (6.64) is cumbersome to evaluate for f if Re_d is known, although it easily yields to the EES Equation Solver. An alternate explicit formula given by Haaland [33] as

$$\frac{1}{f^{1/2}} \approx -1.8\log\left[\frac{6.9}{\mathrm{Re}_d} + \left(\frac{\epsilon/d}{3.7}\right)^{1.11}\right] \tag{6.64a}$$

varies less than 2 percent from Eq. (6.64).

The shaded area in the Moody chart indicates the range where transition from laminar to turbulent flow occurs. There are no reliable friction factors in this range, $2000 < \mathrm{Re}_d < 4000$. Notice that the roughness curves are nearly horizontal in the fully rough regime to the right of the dashed line.

From tests with commercial pipes, recommended values for average pipe roughness are listed in Table 6.1.

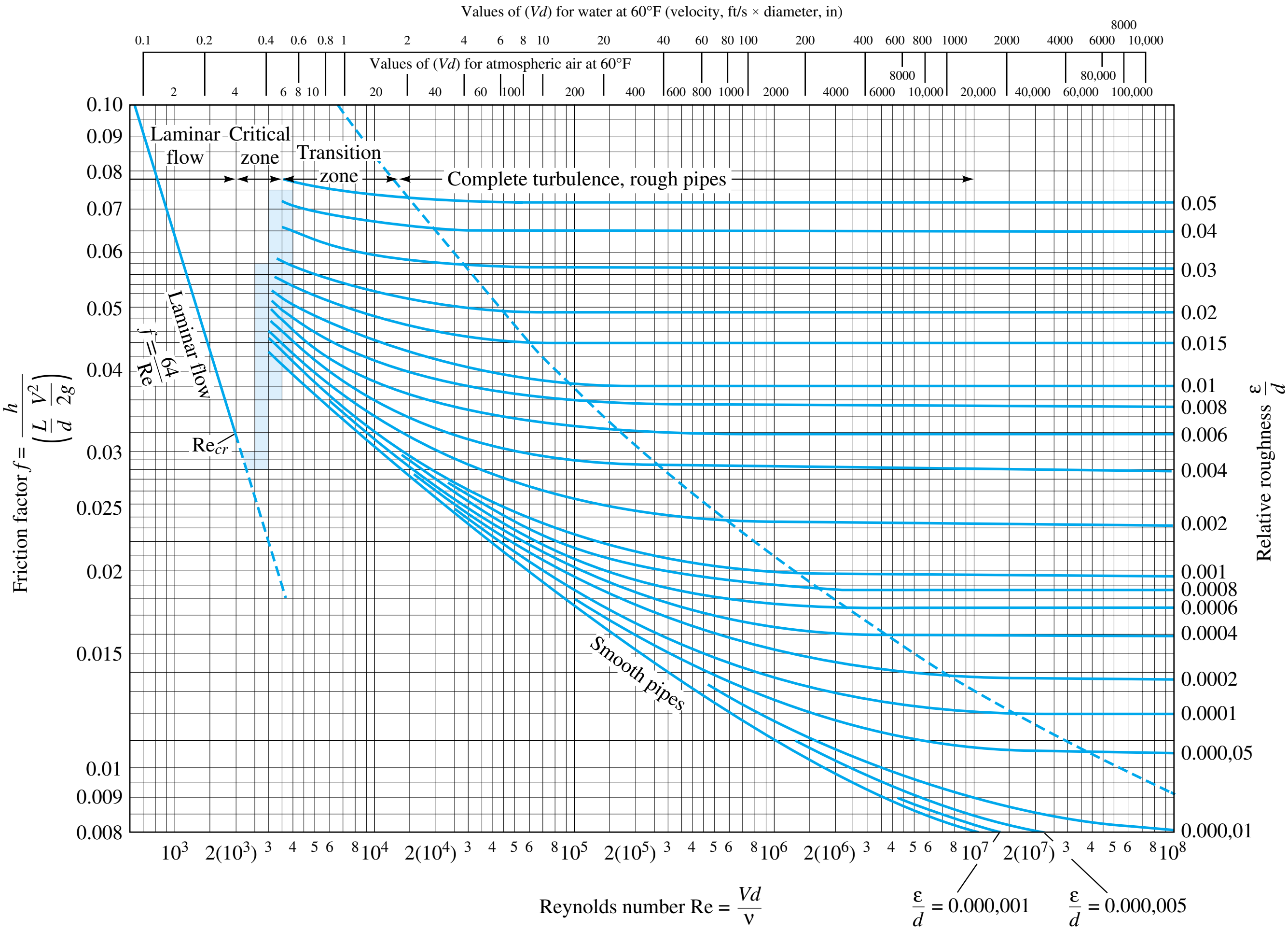

Fig. 6.13 The Moody chart for pipe friction with smooth and rough walls. This chart is identical to Eq. (6.64) for turbulent flow. *(From Ref. 8, by permission of the ASME.)*

Table 6.1 Recommended Roughness Values for Commercial Ducts

Material	Condition	ϵ ft	ϵ mm	Uncertainty, %
Steel	Sheet metal, new	0.00016	0.05	± 60
	Stainless, new	0.000007	0.002	± 50
	Commercial, new	0.00015	0.046	± 30
	Riveted	0.01	3.0	± 70
	Rusted	0.007	2.0	± 50
Iron	Cast, new	0.00085	0.26	± 50
	Wrought, new	0.00015	0.046	± 20
	Galvanized, new	0.0005	0.15	± 40
	Asphalted cast	0.0004	0.12	± 50
Brass	Drawn, new	0.000007	0.002	± 50
Plastic	Drawn tubing	0.000005	0.0015	± 60
Glass	—	Smooth	Smooth	
Concrete	Smoothed	0.00013	0.04	± 60
	Rough	0.007	2.0	± 50
Rubber	Smoothed	0.000033	0.01	± 60
Wood	Stave	0.0016	0.5	± 40

EXAMPLE 6.6[3]

Compute the loss of head and pressure drop in 200 ft of horizontal 6-in-diameter asphalted cast-iron pipe carrying water with a mean velocity of 6 ft/s.

Solution

One can estimate the Reynolds number of water and air from the Moody chart. Look across the top of the chart to V (ft/s) $\times$ d (in) = 36, and then look directly down to the bottom abscissa to find that $\mathrm{Re}_d(\text{water}) \approx 2.7 \times 10^5$. The roughness ratio for asphalted cast iron ($\epsilon = 0.0004$ ft) is

$$\frac{\epsilon}{d} = \frac{0.0004}{\frac{6}{12}} = 0.0008$$

Find the line on the right side for $\epsilon/d = 0.0008$, and follow it to the left until it intersects the vertical line for $\mathrm{Re} = 2.7 \times 10^5$. Read, approximately, $f = 0.02$ [or compute $f = 0.0197$ from Eq. (6.64a)]. Then the head loss is

$$h_f = f\frac{L}{d}\frac{V^2}{2g} = (0.02)\frac{200}{0.5}\frac{(6\text{ ft/s})^2}{2(32.2\text{ ft/s}^2)} = 4.5\text{ ft} \qquad \textit{Ans.}$$

The pressure drop for a horizontal pipe ($z_1 = z_2$) is

$$\Delta p = \rho g h_f = (62.4\text{ lbf/ft}^3)(4.5\text{ ft}) = 280\text{ lbf/ft}^2 \qquad \textit{Ans.}$$

Moody points out that this computation, even for clean new pipe, can be considered accurate only to about $\pm$ 10 percent.

EXAMPLE 6.7

Oil, with $\rho = 900$ kg/m^3 and $\nu = 0.00001$ m^2/s, flows at 0.2 m^3/s through 500 m of 200-mm-diameter cast-iron pipe. Determine (a) the head loss and (b) the pressure drop if the pipe slopes down at 10° in the flow direction.

Solution

First compute the velocity from the known flow rate

$$V = \frac{Q}{\pi R^2} = \frac{0.2\text{ m}^3/\text{s}}{\pi(0.1\text{ m})^2} = 6.4\text{ m/s}$$

Then the Reynolds number is

$$\mathrm{Re}_d = \frac{Vd}{\nu} = \frac{(6.4\text{ m/s})(0.2\text{ m})}{0.00001\text{ m}^2/\text{s}} = 128{,}000$$

From Table 6.1, $\epsilon = 0.26$ mm for cast-iron pipe. Then

$$\frac{\epsilon}{d} = \frac{0.26\text{ mm}}{200\text{ mm}} = 0.0013$$

[3]This example was given by Moody in his 1944 paper [8].

Enter the Moody chart on the right at $\epsilon/d = 0.0013$ (you will have to interpolate), and move to the left to intersect with Re = 128,000. Read $f \approx 0.0225$ [from Eq. (6.64) for these values we could compute $f = 0.0227$]. Then the head loss is

$$h_f = f\frac{L}{d}\frac{V^2}{2g} = (0.0225)\frac{500\text{ m}}{0.2\text{ m}}\frac{(6.4\text{ m/s})^2}{2(9.81\text{ m/s}^2)} = 117\text{ m} \qquad \textit{Ans. (a)}$$

From Eq. (6.25) for the inclined pipe,

$$h_f = \frac{\Delta p}{\rho g} + z_1 - z_2 = \frac{\Delta p}{\rho g} + L\sin 10°$$

or $$\Delta p = \rho g[h_f - (500\text{ m})\sin 10°] = \rho g(117\text{ m} - 87\text{ m})$$

$$= (900\text{ kg/m}^3)(9.81\text{ m/s}^2)(30\text{ m}) = 265{,}000\text{ kg/(m}\cdot\text{s}^2) = 265{,}000\text{ Pa} \qquad \textit{Ans. (b)}$$

EXAMPLE 6.8

Repeat Example 6.5 to see whether there is any possible turbulent-flow solution for a smooth-walled pipe.

Solution

In Example 6.5 we estimated a head loss $h_f \approx 1.66$ ft, assuming laminar exit flow ($\alpha \approx 2.0$). For this condition the friction factor is

$$f = h_f\frac{d}{L}\frac{2g}{V^2} = (1.66\text{ ft})\frac{(0.004\text{ ft})(2)(32.2\text{ ft/s}^2)}{(1.0\text{ ft})(3.32\text{ ft/s})^2} \approx 0.0388$$

For laminar flow, $\text{Re}_d = 64/f = 64/0.0388 \approx 1650$, as we showed in Example 6.5. However, from the Moody chart (Fig. 6.13), we see that $f = 0.0388$ also corresponds to a *turbulent* smooth-wall condition, at $\text{Re}_d \approx 4500$. If the flow actually were turbulent, we should change our kinetic-energy factor to $\alpha \approx 1.06$ [Eq. (3.73)], whence the corrected $h_f \approx 1.82$ ft and $f \approx 0.0425$. With f known, we can estimate the Reynolds number from our formulas:

$$\text{Re}_d \approx 3250 \quad [\text{Eq. (6.54)}] \qquad \text{or} \qquad \text{Re}_d \approx 3400 \quad [\text{Eq. (6.55}b)]$$

So the flow *might* have been turbulent, in which case the viscosity of the fluid would have been

$$\mu = \frac{\rho V d}{\text{Re}_d} = \frac{1.80(3.32)(0.004)}{3300} = 7.2 \times 10^{-6}\text{ slug/(ft}\cdot\text{s)} \qquad \textit{Ans.}$$

This is about 55 percent less than our laminar estimate in Example 6.5. The moral is to keep the capillary-flow Reynolds number below about 1000 to avoid such duplicate solutions.

6.5 Three Types of Pipe-Flow Problems

The Moody chart (Fig. 6.13) can be used to solve almost any problem involving friction losses in long pipe flows. However, many such problems involve considerable iteration and repeated calculations using the chart because the standard Moody chart is essentially a *head-loss chart.* One is supposed to know all other variables, compute

Re_d, enter the chart, find f, and hence compute h_f. This is one of three fundamental problems which are commonly encountered in pipe-flow calculations:

1. Given d, L, and V or Q, ρ, μ, and g, compute the head loss h_f (head-loss problem).
2. Given d, L, h_f, ρ, μ, and g, compute the velocity V or flow rate Q (flow-rate problem).
3. Given Q, L, h_f, ρ, μ, and g, compute the diameter d of the pipe (sizing problem).

Only problem 1 is well suited to the Moody chart. We have to iterate to compute velocity or diameter because both d and V are contained in the ordinate *and* the abscissa of the chart.

There are two alternatives to iteration for problems of type 2 and 3: (*a*) preparation of a suitable new Moody-type chart (see Prob. 6.62 and 6.73); or (*b*) the use of *solver* software, especially the Engineering Equation Solver, known as EES [47], which gives the answer directly if the proper data are entered. Examples 6.9 and 6.11 include the EES approach to these problems.

Type 2 Problem: Find the Flow Rate

Even though velocity (or flow rate) appears in both the ordinate and the abscissa on the Moody chart, iteration for turbulent flow is nevertheless quite fast, because f varies so slowly with Re_d. Alternately, in the spirit of Example 5.7, we could change the scaling variables to (ρ, μ, d) and thus arrive at dimensionless head loss versus dimensionless *velocity*. The result is[4]

$$\zeta = \mathrm{fcn}(\mathrm{Re}_d) \qquad \text{where} \qquad \zeta = \frac{gd^3h_f}{L\nu^2} = \frac{f\,\mathrm{Re}_d^2}{2} \tag{6.65}$$

Example 5.7 did this and offered the simple correlation $\zeta \approx 0.155\,\mathrm{Re}_d^{1.75}$, which is valid for turbulent flow with smooth walls and $\mathrm{Re}_d \le 1$ E5.

A formula valid for all turbulent pipe flows is found by simply rewriting the Colebrook interpolation, Eq. (6.64), in the form of Eq. (6.65):

$$\mathrm{Re}_d = -(8\zeta)^{1/2} \log\left(\frac{\epsilon/d}{3.7} + \frac{1.775}{\sqrt{\zeta}}\right) \qquad \zeta = \frac{gd^3h_f}{L\nu^2} \tag{6.66}$$

Given ζ, we compute Re_d (and hence velocity) directly. Let us illustrate these two approaches with the following example.

EXAMPLE 6.9

Oil, with $\rho = 950\ \mathrm{kg/m^3}$ and $\nu = 2$ E-5 $\mathrm{m^2/s}$, flows through a 30-cm-diameter pipe 100 m long with a head loss of 8 m. The roughness ratio is $\epsilon/d = 0.0002$. Find the average velocity and flow rate.

Direct Solution

First calculate the dimensionless head-loss parameter:

$$\zeta = \frac{gd^3h_f}{L\nu^2} = \frac{(9.81\ \mathrm{m/s^2})(0.3\ \mathrm{m})^3(8.0\ \mathrm{m})}{(100\ \mathrm{m})(2\ \mathrm{E\text{-}5}\ \mathrm{m^2/s})^2} = 5.30\ \mathrm{E7}$$

[4]The parameter ζ was suggested by H. Rouse in 1942.

Now enter Eq. (6.66) to find the Reynolds number:

$$\mathrm{Re}_d = -[8(5.3\ \mathrm{E}7)]^{1/2} \log\left(\frac{0.0002}{3.7} + \frac{1.775}{\sqrt{5.3\ \mathrm{E}7}}\right) = 72{,}600$$

The velocity and flow rate follow from the Reynolds number:

$$V = \frac{\nu\,\mathrm{Re}_d}{d} = \frac{(2\ \mathrm{E}\text{-}5\ \mathrm{m^2/s})(72{,}600)}{0.3\ \mathrm{m}} \approx 4.84\ \mathrm{m/s}$$

$$Q = V\frac{\pi}{4}d^2 = \left(4.84\frac{\mathrm{m}}{\mathrm{s}}\right)\frac{\pi}{4}(0.3\ \mathrm{m})^2 \approx 0.342\ \mathrm{m^3/s} \qquad \textit{Ans.}$$

No iteration is required, but this idea falters if additional losses are present.

Iterative Solution

By definition, the friction factor is known except for V:

$$f = h_f\frac{d}{L}\frac{2g}{V^2} = (8\ \mathrm{m})\left(\frac{0.3\ \mathrm{m}}{100\ \mathrm{m}}\right)\left[\frac{2(9.81\ \mathrm{m/s^2})}{V^2}\right] \qquad \text{or} \qquad fV^2 \approx 0.471 \qquad \text{(SI units)}$$

To get started, we only need to guess f, compute $V = \sqrt{0.471/f}$, then get Re_d, compute a better f from the Moody chart, and repeat. The process converges fairly rapidly. A good first guess is the "fully rough" value for $\epsilon/d = 0.0002$, or $f \approx 0.014$ from Fig. 6.13. The iteration would be as follows:

Guess $f \approx 0.014$, then $V = \sqrt{0.471/0.014} = 5.80$ m/s and $\mathrm{Re}_d = Vd/\nu \approx 87{,}000$. At $\mathrm{Re}_d =$ 87,000 and $\epsilon/d = 0.0002$, compute $f_{\text{new}} \approx 0.0195$ [Eq. (6.64)].

New $f \approx 0.0195$, $V = \sqrt{0.481/0.0195} = 4.91$ m/s and $\mathrm{Re}_d = Vd/\nu = 73{,}700$. At $\mathrm{Re}_d =$ 73,700 and $\epsilon/d = 0.0002$, compute $f_{\text{new}} \approx 0.0201$ [Eq. (6.64)].

Better $f \approx 0.0201$, $V = \sqrt{0.471/0.0201} = 4.84$ m/s and $\mathrm{Re}_d \approx 72{,}600$. At $\mathrm{Re}_d = 72{,}600$ and $\epsilon/d = 0.0002$, compute $f_{\text{new}} \approx 0.0201$ [Eq. (6.64)].

We have converged to three significant figures. Thus our iterative solution is

$$V = 4.84\ \mathrm{m/s}$$

$$Q = V\left(\frac{\pi}{4}\right)d^2 = (4.84)\left(\frac{\pi}{4}\right)(0.3)^2 \approx 0.342\ \mathrm{m^3/s} \qquad \textit{Ans.}$$

The iterative approach is straightforward and not too onerous, so it is routinely used by engineers. Obviously this repetitive procedure is ideal for a personal computer.

Engineering Equation Solver (EES) Solution

In EES, one simply enters the data and the appropriate equations, letting the software do the rest. Correct units must of course be used. For the present example, the data could be entered as SI:

```
rho=950    nu=2E-5    d=0.3    L=100    epsod=0.0002    hf=8.0    g=9.81
```

The appropriate equations are the Moody formula (6.64) plus the definitions of Reynolds number, volume flow rate as determined from velocity, and the Darcy head-loss formula (6.30):

```
Re = V*d/nu
 Q = V*pi*d^2/4
 f = (−2.0*log10(epsod/3.7 + 2.51/Re/f^0.5))^(−2)
hf = f*L/d*V^2/2/g
```

EES understands that "pi" represents 3.141593. Then hit "SOLVE" from the menu. If errors have been entered, EES will complain that the system cannot be solved and attempt to explain why. Otherwise, the software will iterate, and in this case EES prints the correct solution:

```
Q=0.342    V=4.84    f=0.0201    Re=72585
```

The units are spelled out in a separate list as [m, kg, s, N]. This elegant approach to engineering problem-solving has one drawback, namely, that the user fails to check the solution for engineering viability. For example, are the data typed correctly? Is the Reynolds number turbulent?

EXAMPLE 6.10

Work Moody's problem (Example 6.6) backward, assuming that the head loss of 4.5 ft is known and the velocity (6.0 ft/s) is unknown.

Direct Solution

Find the parameter ζ, and compute the Reynolds number from Eq. (6.66):

$$\zeta = \frac{gd^3h_f}{L\nu^2} = \frac{(32.2\text{ ft/s}^2)(0.5\text{ ft})^3(4.5\text{ ft})}{(200\text{ ft})(1.1\text{ E-5 ft}^2\text{/s})^2} = 7.48\text{ E8}$$

Eq. (6.66): $$\text{Re}_d = -[8(7.48\text{ E8})]^{1/2}\log\left(\frac{0.0008}{3.7} + \frac{1.775}{\sqrt{7.48\text{ E8}}}\right) \approx 274{,}800$$

Then $$V = \nu\frac{\text{Re}_d}{d} = \frac{(1.1\text{ E-5})(274{,}800)}{0.5} \approx 6.05\text{ ft/s}$$ *Ans.*

We did not get 6.0 ft/s exactly because the 4.5-ft head loss was rounded off in Example 6.6.

Iterative Solution

As in Eq. (6.9) the friction factor is related to velocity:

$$f = h_f\frac{d}{L}\frac{2g}{V^2} = (4.5\text{ ft})\left(\frac{0.5\text{ ft}}{200\text{ ft}}\right)\left[\frac{2(32.2\text{ ft/s}^2)}{V^2}\right] \approx \frac{0.7245}{V^2}$$

or $$V = \sqrt{0.7245/f}$$

Knowing $\epsilon/d = 0.0008$, we can guess f and iterate until the velocity converges. Begin with the fully rough estimate $f \approx 0.019$ from Fig. 6.13. The resulting iterates are

$$f_1 = 0.019: \qquad V_1 = \sqrt{0.7245/f_1} = 6.18\text{ ft/s} \qquad \text{Re}_{d_1} = \frac{Vd}{\nu} = 280{,}700$$

$f_2 = 0.0198$: $V_2 = 6.05$ ft/s $\mathrm{Re}_{d_2} = 274{,}900$

$f_3 = 0.01982$: $V_3 = 6.046$ ft/s *Ans.*

The calculation converges rather quickly to the same result as that obtained through direct computation.

Type 3 Problem: Find the Pipe Diameter

The Moody chart is especially awkward for finding the pipe size, since d occurs in all three parameters f, Re_d, and ϵ/d. Further, it depends upon whether we know the velocity or the flow rate. We cannot know both, or else we could immediately compute $d = \sqrt{4Q/(\pi V)}$.

Let us assume that we know the flow rate Q. Note that this requires us to redefine the Reynolds number in terms of Q:

$$\mathrm{Re}_d = \frac{Vd}{\nu} = \frac{4Q}{\pi d \nu} \tag{6.67}$$

Then, if we choose (Q, ρ, μ) as scaling parameters (to eliminate d), we obtain the functional relationship

$$\mathrm{Re}_d = \frac{4Q}{\pi d \nu} = \mathrm{fcn}\left(\frac{gh_f}{L\nu^5}, \frac{\epsilon \nu}{Q}\right) \tag{6.68}$$

and can thus solve d when the right-hand side is known. Unfortunately, the writer knows of no *formula* for this relation, nor is he able to rearrange Eq. (6.64) into the explicit form of Eq. (6.68). One could recalculate and *plot* the relation, and indeed an ingenious "pipe-sizing" plot is given in Ref. 13. Here it seems reasonable to forgo a plot or curve fitted formula and to simply set up the problem as an iteration in terms of the Moody-chart variables. In this case we also have to set up the friction factor in terms of the flow rate:

$$f = h_f \frac{d}{L} \frac{2g}{V^2} = \frac{\pi^2}{8} \frac{g h_f d^5}{LQ^2} \tag{6.69}$$

The following two examples illustrate the iteration.

EXAMPLE 6.11

Work Example 6.9 backward, assuming that $Q = 0.342$ m^3/s and $\epsilon = 0.06$ mm are known but that d (30 cm) is unknown. Recall $L = 100$ m, $\rho = 950$ kg/m^3, $\nu = 2$ E-5 m^2/s, and $h_f = 8$ m.

Iterative Solution

First write the diameter in terms of the friction factor:

$$f = \frac{\pi^2}{8} \frac{(9.81 \text{ m/s}^2)(8 \text{ m})d^5}{(100 \text{ m})(0.342 \text{ m}^3/\text{s})^2} = 8.28 d^5 \qquad \text{or} \qquad d \approx 0.655 f^{1/5} \tag{1}$$

in SI units. Also write the Reynolds number and roughness ratio in terms of the diameter:

$$\mathrm{Re}_d = \frac{4(0.342\ \mathrm{m^3/s})}{\pi(2\ \mathrm{E\text{-}5}\ \mathrm{m^2/s})d} = \frac{21{,}800}{d} \tag{2}$$

$$\frac{\epsilon}{d} = \frac{6\ \mathrm{E\text{-}5\ m}}{d} \tag{3}$$

Guess f, compute d from (1), then compute Re_d from (2) and ϵ/d from (3), and compute a better f from the Moody chart or Eq. (6.64). Repeat until (fairly rapid) convergence. Having no initial estimate for f, the writer guesses $f \approx 0.03$ (about in the middle of the turbulent portion of the Moody chart). The following calculations result:

$$f \approx 0.03 \qquad d \approx 0.655(0.03)^{1/5} \approx 0.325\ \mathrm{m}$$

$$\mathrm{Re}_d \approx \frac{21{,}800}{0.325} \approx 67{,}000 \qquad \frac{\epsilon}{d} \approx 1.85\ \mathrm{E\text{-}4}$$

Eq. (6.54): $$f_{\mathrm{new}} \approx 0.0203 \qquad \text{then} \qquad d_{\mathrm{new}} \approx 0.301\ \mathrm{m}$$

$$\mathrm{Re}_{d,\mathrm{new}} \approx 72{,}500 \qquad \frac{\epsilon}{d} \approx 2.0\ \mathrm{E\text{-}4}$$

Eq. (6.54): $$f_{\mathrm{better}} \approx 0.0201 \qquad \text{and} \qquad d = 0.300\ \mathrm{m}$$ *Ans.*

The procedure has converged to the correct diameter of 30 cm given in Example 6.9.

EES Solution

EES

For an EES solution, enter the data and the appropriate equations. The diameter is unknown. Correct units must of course be used. For the present example, the data should use SI units:

```
rho=950    nu=2E-5    L=100    eps=6E-5    hf=8.0    g=9.81    Q=0.342
```

The appropriate equations are the Moody formula, the definition of Reynolds number, volume flow rate as determined from velocity, the Darcy head-loss formula, and the roughness ratio:

```
   Re = V*d/nu
    Q = V*pi*d^2/4
    f = (-2.0*log10(epsod/3.7 + 2.51/Re/f^0.5))^(-2)
   hf = f*L/d*V^2/2/g
epsod = eps/d
```

Hit *Solve* from the menu. Unlike Example 6.9, this time EES complains that the system *cannot* be solved and reports "logarithm of a negative number." The reason is that we allowed EES to assume that f could be a negative number. Bring down *Variable Information* from the menu and change the limits of f so that it cannot be negative. EES agrees and iterates to the solution:

```
d = 0.300    V = 4.84    f = 0.0201    Re = 72,585
```

The unit system is spelled out as (m, kg, s, N). As always when using software, the user should check the solution for engineering viability. For example, is the Reynolds number turbulent? (Yes)

EXAMPLE 6.12

Work Moody's problem, Example 6.6, backward to find the unknown (6 in) diameter if the flow rate $Q = 1.18$ ft^3/s is known. Recall $L = 200$ ft, $\epsilon = 0.0004$ ft, and $\nu = 1.1$ E-5 ft^2/s.

Solution

Write f, Re_d, and ϵ/d in terms of the diameter:

$$f = \frac{\pi^2}{8}\frac{gh_f d^5}{LQ^2} = \frac{\pi^2}{8}\frac{(32.2\ \text{ft/s}^2)(4.5\ \text{ft})d^5}{(200\ \text{ft})(1.18\ \text{ft}^3/\text{s})^2} = 0.642d^5 \quad \text{or} \quad d \approx 1.093 f^{1/5} \tag{1}$$

$$\text{Re}_d = \frac{4(1.18\ \text{ft}^3/\text{s})}{\pi(1.1\ \text{E-5 ft}^2/\text{s})\ d} = \frac{136{,}600}{d} \tag{2}$$

$$\frac{\epsilon}{d} = \frac{0.0004\ \text{ft}}{d} \tag{3}$$

with everything in BG units, of course. Guess f; compute d from (1), Re_d from (2), and ϵ/d from (3); and then compute a better f from the Moody chart. Repeat until convergence. The writer traditionally guesses an initial $f \approx 0.03$:

$$f \approx 0.03 \qquad d \approx 1.093(0.03)^{1/5} \approx 0.542\ \text{ft}$$

$$\text{Re}_d = \frac{136{,}600}{0.542} \approx 252{,}000 \qquad \frac{\epsilon}{d} \approx 7.38\ \text{E-4}$$

$$f_{\text{new}} \approx 0.0196 \qquad d_{\text{new}} \approx 0.498\ \text{ft} \qquad \text{Re}_d \approx 274{,}000 \qquad \frac{\epsilon}{d} \approx 8.03\ \text{E-4}$$

$$f_{\text{better}} \approx 0.0198 \qquad d \approx 0.499\ \text{ft} \qquad \textit{Ans.}$$

Convergence is rapid, and the predicted diameter is correct, about 6 in. The slight discrepancy (0.499 rather than 0.500 ft) arises because h_f was rounded to 4.5 ft.

In discussing pipe-sizing problems, we should remark that commercial pipes are made only in certain sizes. Table 6.2 lists standard water-pipe sizes in the United States. If the sizing calculation gives an intermediate diameter, the next largest pipe size should be selected.

Table 6.2 Nominal and Actual Sizes of Schedule 40 Wrought-Steel Pipe*

Nominal size, in	Actual ID, in
$\frac{1}{8}$	0.269
$\frac{1}{4}$	0.364
$\frac{3}{8}$	0.493
$\frac{1}{2}$	0.622
$\frac{3}{4}$	0.824
1	1.049
$1\frac{1}{2}$	1.610
2	2.067
$2\frac{1}{2}$	2.469
3	3.068

*Nominal size within 1 percent for 4 in or larger.

6.6 Flow in Noncircular Ducts[5]

If the duct is noncircular, the analysis of fully developed flow follows that of the circular pipe but is more complicated algebraically. For laminar flow, one can solve the exact equations of continuity and momentum. For turbulent flow, the logarithm-law velocity profile can be used, or (better and simpler) the hydraulic diameter is an excellent approximation.

The Hydraulic Diameter

For a noncircular duct, the control-volume concept of Fig. 6.10 is still valid, but the cross-sectional area A does not equal πR^2 and the cross-sectional perimeter wetted by the shear stress $\mathcal{P}$ does not equal $2\pi R$. The momentum equation (6.26) thus becomes

$$\Delta p\ A + \rho g A\ \Delta L \sin\phi - \bar{\tau}_w \mathcal{P}\ \Delta L = 0$$

[5]This section may be omitted without loss of continuity.

or
$$h_f = \frac{\Delta p}{\rho g} + \Delta z = \frac{\bar{\tau}_w}{\rho g}\frac{\Delta L}{A/\mathcal{P}} \tag{6.70}$$

This is identical to Eq. (6.27) except that (1) the shear stress is an average value integrated around the perimeter and (2) the length scale $A/\mathcal{P}$ takes the place of the pipe radius R. For this reason a noncircular duct is said to have a *hydraulic radius* R_h, defined by

$$R_h = \frac{A}{\mathcal{P}} = \frac{\text{cross-sectional area}}{\text{wetted perimeter}} \tag{6.71}$$

This concept receives constant use in open-channel flow (Chap. 10), where the channel cross section is almost never circular. If, by comparison to Eq. (6.29) for pipe flow, we define the friction factor in terms of average shear

$$f_{\text{NCD}} = \frac{8\bar{\tau}_w}{\rho V^2} \tag{6.72}$$

where NCD stands for noncircular duct and $V = Q/A$ as usual, Eq. (6.70) becomes

$$h_f = f\frac{L}{4R_h}\frac{V^2}{2g} \tag{6.73}$$

This is equivalent to Eq. (6.30) for pipe flow except that d is replaced by $4R_h$. Therefore we customarily define the *hydraulic diameter* as

$$D_h = \frac{4A}{\mathcal{P}} = \frac{4 \times \text{area}}{\text{wetted perimeter}} = 4R_h \tag{6.74}$$

We should stress that the wetted perimeter includes all surfaces acted upon by the shear stress. For example, in a circular annulus, both the outer and the inner perimeter should be added. The fact that D_h equals $4R_h$ is just one of those things: Chalk it up to an engineer's sense of humor. Note that for the degenerate case of a circular pipe, $D_h = 4\pi R^2/(2\pi R) = 2R$, as expected.

We would therefore expect by dimensional analysis that this friction factor f, based upon hydraulic diameter as in Eq. (6.72), would correlate with the Reynolds number and roughness ratio based upon the hydraulic diameter

$$f = F\left(\frac{VD_h}{\nu}, \frac{\epsilon}{D_h}\right) \tag{6.75}$$

and this is the way the data are correlated. But we should not necessarily expect the Moody chart (Fig. 6.13) to hold exactly in terms of this new length scale. And it does not, but it is surprisingly accurate:

$$f \approx \begin{cases} \dfrac{64}{\text{Re}_{D_h}} & \pm 40\% \quad \text{laminar flow} \\ f_{\text{Moody}}\left(\text{Re}_{D_h}, \dfrac{\epsilon}{D_h}\right) & \pm 15\% \quad \text{turbulent flow} \end{cases} \tag{6.76}$$

Now let us look at some particular cases.

Flow between Parallel Plates

As shown in Fig. 6.14, flow between parallel plates a distance h apart is the limiting case of flow through a very wide rectangular channel. For fully developed flow, $u = u(y)$ only, which satisfies continuity identically. The momentum equation in cartesian coordinates reduces to

$$0 = -\frac{dp}{dx} + \rho g_x + \frac{d\tau}{dy} \qquad \tau_{\text{lam}} = \mu\frac{du}{dy} \tag{6.77}$$

subject to no-slip conditions: $u = 0$ at $y = \pm h$. The laminar-flow solution was given as an example in Eq. (4.143). Here we also allow for the possibility of a sloping channel, with a pressure gradient due to gravity. The solution is

$$u = \frac{1}{2\mu}\left[-\frac{d}{dx}(p + \rho g z)\right](h^2 - y^2) \tag{6.78}$$

If the channel has width b, the volume flow is

$$Q = \int_{-h}^{+h} u(y)b\,dy = \frac{bh^3}{3\mu}\left[-\frac{d}{dx}(p + \rho g z)\right]$$

or

$$V = \frac{Q}{bh} = \frac{h^2}{3\mu}\left[-\frac{d}{dx}(p + \rho g z)\right] = \frac{2}{3}u_{\max} \tag{6.79}$$

Note the difference between a parabola [Eq. (6.79)] and a paraboloid [Eq. (6.43)]: the average is two-thirds of the maximum velocity in plane flow and one-half in axisymmetric flow.

The wall shear stress in developed channel flow is a constant:

$$\tau_w = \mu\left|\frac{du}{dy}\right|_{y=+h} = h\left[-\frac{d}{dx}(p + \rho g z)\right] \tag{6.80}$$

This may be nondimensionalized as a friction factor:

$$f = \frac{8\tau_w}{\rho V^2} = \frac{24\mu}{\rho V h} = \frac{24}{\text{Re}_h} \tag{6.81}$$

These are exact analytic laminar-flow results, so there is no reason to resort to the hydraulic-diameter concept. However, if we did use D_h, a discrepancy would arise. The hydraulic diameter of a wide channel is

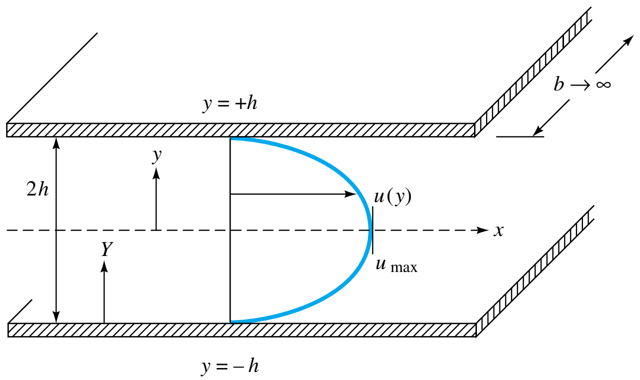

Fig. 6.14 Fully developed flow between parallel plates.

$$D_h = \frac{4A}{\rho} = \lim_{b\to\infty} \frac{4(2bh)}{2b + 4h} = 4h \tag{6.82}$$

or twice the distance between the plates. Substituting into Eq. (6.81), we obtain the interesting result

Parallel plates:
$$f_{\text{lam}} = \frac{96\mu}{\rho V(4h)} = \frac{96}{\text{Re}_{D_h}} \tag{6.83}$$

Thus, if we could not work out the laminar theory and chose to use the approximation $f \approx 64/\text{Re}_{D_h}$, we would be 33 percent low. The hydraulic-diameter approximation is relatively crude in laminar flow, as Eq. (6.76) states.

Just as in circular-pipe flow, the laminar solution above becomes unstable at about $\text{Re}_{D_h} \approx 2000$; transition occurs and turbulent flow results.

For turbulent flow between parallel plates, we can again use the logarithm law, Eq. (6.21), as an approximation across the entire channel, using not y but a wall coordinate Y, as shown in Fig. 6.14:

$$\frac{u(Y)}{u^*} \approx \frac{1}{\kappa}\ln\frac{Yu^*}{\nu} + B \qquad 0 < Y < h \tag{6.84}$$

This distribution looks very much like the flat turbulent profile for pipe flow in Fig. 6.11b, and the mean velocity is

$$V = \frac{1}{h}\int_0^h u\, dY = u^*\left(\frac{1}{\kappa}\ln\frac{hu^*}{\nu} + B - \frac{1}{\kappa}\right) \tag{6.85}$$

Recalling that $V/u^* = (8/f)^{1/2}$, we see that Eq. (6.85) is equivalent to a parallel-plate friction law. Rearranging and cleaning up the constant terms, we obtain

$$\frac{1}{f^{1/2}} \approx 2.0 \log\,(\text{Re}_{D_h} f^{1/2}) - 1.19 \tag{6.86}$$

where we have introduced the hydraulic diameter $D_h = 4h$. This is remarkably close to the pipe-friction law, Eq. (6.54). Therefore we conclude that the use of the hydraulic diameter in this turbulent case is quite successful. That turns out to be true for other noncircular turbulent flows also.

Equation (6.86) can be brought into exact agreement with the pipe law by rewriting it in the form

$$\frac{1}{f^{1/2}} = 2.0 \log\,(0.64\ \text{Re}_{D_h} f^{1/2}) - 0.8 \tag{6.87}$$

Thus the turbulent friction is predicted most accurately when we use an effective diameter D_{eff} equal to 0.64 times the hydraulic diameter. The effect on f itself is much less, about 10 percent at most. We can compare with Eq. (6.83) for laminar flow, which predicted

Parallel plates:
$$D_{\text{eff}} = \frac{64}{96}D_h = \frac{2}{3}D_h \tag{6.88}$$

This close resemblance ($0.64D_h$ versus $0.667D_h$) occurs so often in noncircular duct flow that we take it to be a general rule for computing turbulent friction in ducts:

$$D_{\text{eff}} = D_h = \frac{4A}{\mathcal{P}} \quad \text{reasonable accuracy}$$

$$D_{\text{eff}}(\text{laminar theory}) \quad \text{extreme accuracy} \tag{6.89}$$

Jones [10] shows that the effective-laminar-diameter idea collapses all data for rectangular ducts of arbitrary height-to-width ratio onto the Moody chart for pipe flow. We recommend this idea for all noncircular ducts.

EXAMPLE 6.13

Fluid flows at an average velocity of 6 ft/s between horizontal parallel plates a distance of 2.4 in apart. Find the head loss and pressure drop for each 100 ft of length for $\rho = 1.9$ slugs/ft^3 and (*a*) $\nu = 0.00002$ ft^3/s and (*b*) $\nu = 0.002$ ft^3/s. Assume smooth walls.

Solution

Part (a) The viscosity $\mu = \rho\nu = 3.8 \times 10^{-5}$ slug/(ft · s). The spacing is $2h = 2.4$ in $= 0.2$ ft, and $D_h = 4h = 0.4$ ft. The Reynolds number is

$$\text{Re}_{D_h} = \frac{VD_h}{\nu} = \frac{(6.0 \text{ ft/s})(0.4 \text{ ft})}{0.00002 \text{ ft}^2/\text{s}} = 120{,}000$$

The flow is therefore turbulent. For reasonable accuracy, simply look on the Moody chart (Fig. 6.13) for smooth walls

$$f \approx 0.0173 \quad h_f \approx f\frac{L}{D_h}\frac{V^2}{2g} = 0.0173\frac{100}{0.4}\frac{(6.0)^2}{2(32.2)} \approx 2.42 \text{ ft} \qquad \textit{Ans. (a)}$$

Since there is no change in elevation,

$$\Delta p = \rho g h_f = 1.9(32.2)(2.42) = 148 \text{ lbf/ft}^2 \qquad \textit{Ans. (a)}$$

This is the head loss and pressure drop per 100 ft of channel. For more accuracy, take $D_{\text{eff}} = \frac{2}{3}D_h$ from laminar theory; then

$$\text{Re}_{\text{eff}} = \tfrac{2}{3}(120{,}000) = 80{,}000$$

and from the Moody chart read $f \approx 0.0189$ for smooth walls. Thus a better estimate is

$$h_f = 0.0189\frac{100}{0.4}\frac{(6.0)^2}{2(32.2)} = 2.64 \text{ ft}$$

and $$\Delta p = 1.9(32.2)(2.64) = 161 \text{ lbf/ft}^2 \qquad \textit{Better ans. (a)}$$

The more accurate formula predicts friction about 9 percent higher.

Part (b) Compute $\mu = \rho\nu = 0.0038$ slug/(ft · s). The Reynolds number is $6.0(0.4)/0.002 = 1200$; therefore the flow is laminar, since Re is less than 2300.

You could use the laminar-flow friction factor, Eq. (6.83)

$$f_{\text{lam}} = \frac{96}{\text{Re}_{D_h}} = \frac{96}{1200} = 0.08$$

from which $$h_f = 0.08\frac{100}{0.4}\frac{(6.0)^2}{2(32.2)} = 11.2 \text{ ft}$$

and $$\Delta p = 1.9(32.2)(11.2) = 684 \text{ lbf/ft}^2 \qquad \textit{Ans. (b)}$$

Alternately you can finesse the Reynolds number and go directly to the appropriate laminar-flow formula, Eq. (6.79)

$$V = \frac{h^2}{3\mu}\frac{\Delta p}{L}$$

or $$\Delta p = \frac{3(6.0\ \text{ft/s})[0.0038\ \text{slug/(ft}\cdot\text{s)}](100\ \text{ft})}{(0.1\ \text{ft})^2} = 684\ \text{slugs/(ft}\cdot\text{s}^2) = 684\ \text{lbf/ft}^2$$

and $$h_f = \frac{\Delta p}{\rho g} = \frac{684}{1.9(32.2)} = 11.2\ \text{ft}$$

This is one of those—perhaps unexpected—problems where the laminar friction is greater than the turbulent friction.

Flow through a Concentric Annulus

Consider steady axial laminar flow in the annular space between two concentric cylinders, as in Fig. 6.15. There is no slip at the inner ($r = b$) and outer radius ($r = a$). For $u = u(r)$ only, the governing relation is Eq. (6.34)

$$\frac{d}{dr}\left(r\mu\frac{du}{dr}\right) = Kr \qquad K = \frac{d}{dx}(p + \rho gz) \tag{6.90}$$

Integrate this twice

$$u = \frac{1}{4}r^2\frac{K}{\mu} + C_1 \ln r + C_2$$

The constants are found from the two no-slip conditions

$$u(r = a) = 0 = \frac{1}{4}a^2\frac{K}{\mu} + C_1 \ln a + C_2$$

$$u(r = b) = 0 = \frac{1}{4}b^2\frac{K}{\mu} + C_1 \ln b + C_2$$

The final solution for the velocity profile is

$$u = \frac{1}{4\mu}\left[-\frac{d}{dx}(p + \rho gz)\right]\left[a^2 - r^2 + \frac{a^2 - b^2}{\ln (b/a)}\ln\frac{a}{r}\right] \tag{6.91}$$

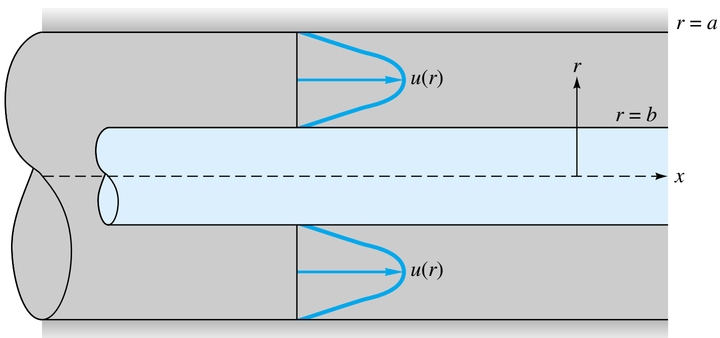

Fig. 6.15 Fully developed flow through a concentric annulus.

The volume flow is given by

$$Q = \int_b^a u 2\pi r \, dr = \frac{\pi}{8\mu}\left[-\frac{d}{dx}(p + \rho g z)\right]\left[a^4 - b^4 - \frac{(a^2 - b^2)^2}{\ln (a/b)}\right] \tag{6.92}$$

The velocity profile $u(r)$ resembles a parabola wrapped around in a circle to form a split doughnut, as in Fig. 6.15. The maximum velocity occurs at the radius

$$r' = \left[\frac{a^2 - b^2}{2 \ln (a/b)}\right]^{1/2} \qquad u = u_{max} \tag{6.93}$$

This maximum is closer to the inner radius but approaches the midpoint between cylinders as the clearance $a - b$ becomes small. Some numerical values are as follows:

$\frac{b}{a}$	0.01	0.1	0.2	0.5	0.8	0.9	0.99
$\frac{r' - b}{a - b}$	0.323	0.404	0.433	0.471	0.491	0.496	0.499

Also, as the clearance becomes small, the profile approaches a parabolic distribution, as if the flow were between two parallel plates [Eq. (4.143)].

It is confusing to base the friction factor on the wall shear because there are two shear stresses, the inner stress being greater than the outer. It is better to define f with respect to the head loss, as in Eq. (6.73),

$$f = h_f \frac{D_h}{L}\frac{2g}{V^2} \qquad \text{where } V = \frac{Q}{\pi(a^2 - b^2)} \tag{6.94}$$

The hydraulic diameter for an annulus is

$$D_h = \frac{4\pi(a^2 - b^2)}{2\pi(a + b)} = 2(a - b) \tag{6.95}$$

It is twice the clearance, rather like the parallel-plate result of twice the distance between plates [Eq. (6.82)].

Substituting h_f, D_h, and V into Eq. (6.94), we find that the friction factor for laminar flow in a concentric annulus is of the form

$$f = \frac{64\zeta}{\text{Re}_{D_h}} \qquad \zeta = \frac{(a - b)^2(a^2 - b^2)}{a^4 - b^4 - (a^2 - b^2)^2/\ln (a/b)} \tag{6.96}$$

The dimensionless term ζ is a sort of correction factor for the hydraulic diameter. We could rewrite Eq. (6.96) as

$$\text{Concentric annulus:} \qquad f = \frac{64}{\text{Re}_{\text{eff}}} \qquad \text{Re}_{\text{eff}} = \frac{1}{\zeta}\text{Re}_{D_h} \tag{6.97}$$

Some numerical values of $f\,\text{Re}_{D_h}$ and $D_{\text{eff}}/D_h = 1/\zeta$ are given in Table 6.3.

For turbulent flow through a concentric annulus, the analysis might proceed by patching together two logarithmic-law profiles, one going out from the inner wall to meet the other coming in from the outer wall. We omit such a scheme here and proceed directly to the friction factor. According to the general rule proposed in Eq. (6.89), turbulent friction is predicted with excellent accuracy by replacing d in the Moody chart

Table 6.3 Laminar Friction Factors for a Concentric Annulus

b/a	$f\,\mathrm{Re}_{D_h}$	$D_{\mathrm{eff}}/D_h = 1/\zeta$
0.0	64.0	1.000
0.00001	70.09	0.913
0.0001	71.78	0.892
0.001	74.68	0.857
0.01	80.11	0.799
0.05	86.27	0.742
0.1	89.37	0.716
0.2	92.35	0.693
0.4	94.71	0.676
0.6	95.59	0.670
0.8	95.92	0.667
1.0	96.0	0.667

by $D_{\mathrm{eff}} = 2(a - b)/\zeta$, with values listed in Table 6.3.[6] This idea includes roughness also (replace ϵ/d in the chart by $\epsilon/D_{\mathrm{eff}}$). For a quick design number with about 10 percent accuracy, one can simply use the hydraulic diameter $D_h = 2(a - b)$.

EXAMPLE 6.14

What should the reservoir level h be to maintain a flow of 0.01 m^3/s through the commercial steel annulus 30 m long shown in Fig. E6.14? Neglect entrance effects and take $\rho = 1000$ kg/m^3 and $\nu = 1.02 \times 10^{-6}$ m^2/s for water.

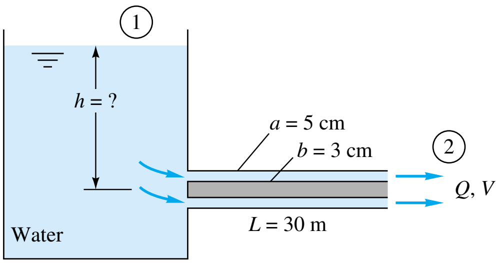

E6.14

Solution

Compute the average velocity and hydraulic diameter

$$V = \frac{Q}{A} = \frac{0.01\ \mathrm{m^3/s}}{\pi[(0.05\ \mathrm{m})^2 - (0.03\ \mathrm{m})^2]} = 1.99\ \mathrm{m/s}$$

$$D_h = 2(a - b) = 2(0.05 - 0.03)\ \mathrm{m} = 0.04\ \mathrm{m}$$

Apply the steady-flow energy equation between sections 1 and 2:

$$\frac{p_1}{\rho} + \frac{1}{2}V_1^2 + gz_1 = \left(\frac{p_2}{\rho} + \frac{1}{2}V_2^2 + gz_2\right) + gh_f$$

But $p_1 = p_2 = p_a$, $V_1 \approx 0$, and $V_2 = V$ in the pipe. Therefore solve for

$$h_f = f\frac{L}{D_h}\frac{V^2}{2g} = z_1 - z_2 - \frac{V^2}{2g}$$

But $z_1 - z_2 = h$, the desired reservoir height. Thus, finally,

$$h = \frac{V^2}{2g}\left(1 + f\frac{L}{D_h}\right) \tag{1}$$

Since V, L, and D_h are known, our only remaining problem is to compute the annulus friction factor f. For a quick approximation, take $D_{\mathrm{eff}} = D_h = 0.04$ m. Then

$$\mathrm{Re}_{D_h} = \frac{VD_h}{\nu} = \frac{1.99(0.04)}{1.02 \times 10^{-6}} = 78{,}000$$

$$\frac{\epsilon}{D_h} = \frac{0.046\ \mathrm{mm}}{40\ \mathrm{mm}} = 0.00115$$

[6]Jones and Leung [44] show that data for annular flow also satisfy the effective-laminar-diameter idea.

where $\epsilon = 0.046$ mm has been read from Table 6.1 for commercial steel surfaces. From the Moody chart, read $f = 0.0232$. Then, from Eq. (1) above,

$$h \approx \frac{(1.99 \text{ m/s})^2}{2(9.81 \text{ m/s}^2)}\left(1 + 0.0232\,\frac{30 \text{ m}}{0.04 \text{ m}}\right) = 3.71 \text{ m} \qquad \textit{Crude ans.}$$

For better accuracy, take $D_{\text{eff}} = D_h/\zeta = 0.670D_h = 2.68$ cm, where the correction factor 0.670 has been read from Table 6.3 for $b/a = \frac{3}{5} = 0.6$. Then the corrected Reynolds number and roughness ratio are

$$\text{Re}_{\text{eff}} = \frac{VD_{\text{eff}}}{\nu} = 52{,}300 \qquad \frac{\epsilon}{D_{\text{eff}}} = 0.00172$$

From the Moody chart, read $f = 0.0257$. Then the improved computation for reservoir height is

$$h = \frac{(1.99 \text{ m/s})^2}{2(9.81 \text{ m/s}^2)}\left(1 + 0.0257\,\frac{30 \text{ m}}{0.04 \text{ m}}\right) = 4.09 \text{ m} \qquad \textit{Better ans.}$$

The uncorrected hydraulic-diameter estimate is about 9 percent low. Note that we do *not* replace D_h by D_{eff} in the ratio L/D_h in Eq. (1) since this is implicit in the definition of friction factor.

Other Noncircular Cross Sections

In principle, any duct cross section can be solved analytically for the laminar-flow velocity distribution, volume flow, and friction factor. This is because any cross section can be mapped onto a circle by the methods of complex variables, and other powerful analytical techniques are also available. Many examples are given by White [3, pp. 119–122], Berker [11], and Olson and Wright [12, pp. 315–317]. Reference 34 is devoted entirely to laminar duct flow.

In general, however, most unusual duct sections have strictly academic and not commercial value. We list here only the rectangular and isosceles-triangular sections, in Table 6.4, leaving other cross sections for you to find in the references.

For turbulent flow in a duct of unusual cross section, one should replace d by D_h on the Moody chart if no laminar theory is available. If laminar results are known, such as Table 6.4, replace d by $D_{\text{eff}} = [64/(f\,\text{Re})]D_h$ for the particular geometry of the duct.

For laminar flow in rectangles and triangles, the wall friction varies greatly, being largest near the midpoints of the sides and zero in the corners. In turbulent flow through the same sections, the shear is nearly constant along the sides, dropping off sharply to zero in the corners. This is because of the phenomenon of turbulent *secondary flow*, in which there are nonzero mean velocities v and w in the plane of the cross section. Some measurements of axial velocity and secondary-flow patterns are shown in Fig. 6.16, as sketched by Nikuradse in his 1926 dissertation. The secondary-flow "cells" drive the mean flow toward the corners, so that the axial-velocity contours are similar to the cross section and the wall shear is nearly constant. This is why the hydraulic-diameter concept is so successful for turbulent flow. Laminar flow in a straight noncircular duct has no secondary flow. An accurate theoretical prediction of turbulent secondary flow has yet to be achieved, although numerical models are improving [36].

Table 6.4 Laminar Friction Constants $f\,\text{Re}$ for Rectangular and Triangular Ducts

Rectangular

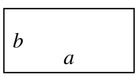

Isosceles triangle

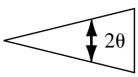

b/a	$f\text{Re}_{D_h}$	θ, deg	$f\text{Re}_{D_h}$
0.0	96.00	0	48.0
0.05	89.91	10	51.6
0.1	84.68	20	52.9
0.125	82.34	30	53.3
0.167	78.81	40	52.9
0.25	72.93	50	52.0
0.4	65.47	60	51.1
0.5	62.19	70	49.5
0.75	57.89	80	48.3
1.0	56.91	90	48.0

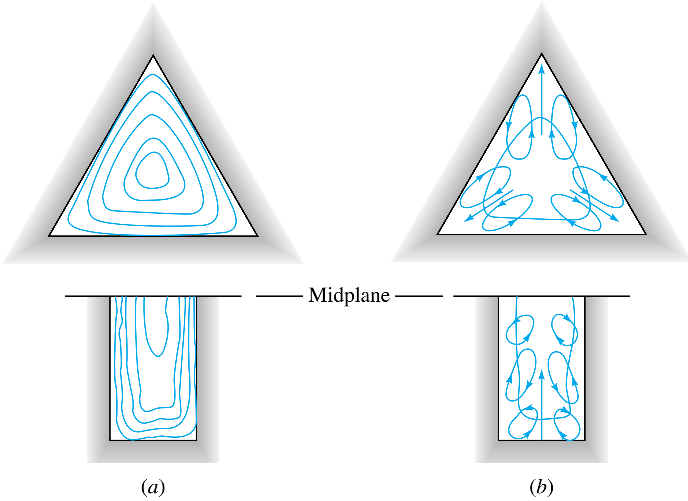

Fig. 6.16 Illustration of secondary turbulent flow in noncircular ducts: (*a*) axial mean-velocity contours; (*b*) secondary-flow cellular motions. *(After J. Nikuradse, dissertation, Göttingen, 1926.)*

EXAMPLE 6.15

Air, with $\rho = 0.00237$ slug/ft^3 and $\nu = 0.000157$ ft^2/s, is forced through a horizontal square 9-by 9-in duct 100 ft long at 25 ft^3/s. Find the pressure drop if $\epsilon = 0.0003$ ft.

Solution

Compute the mean velocity and hydraulic diameter

$$V = \frac{25 \text{ ft}^3/\text{s}}{(0.75 \text{ ft})^2} = 44.4 \text{ ft/s}$$

$$D_h = \frac{4A}{\mathcal{P}} = \frac{4(81 \text{ in}^2)}{36 \text{ in}} = 9 \text{ in} = 0.75 \text{ ft}$$

From Table 6.4, for $b/a = 1.0$, the effective diameter is

$$D_{\text{eff}} = \frac{64}{56.91} D_h = 0.843 \text{ ft}$$

whence
$$\text{Re}_{\text{eff}} = \frac{VD_{\text{eff}}}{\nu} = \frac{44.4(0.843)}{0.000157} = 239{,}000$$

$$\frac{\epsilon}{D_{\text{eff}}} = \frac{0.0003}{0.843} = 0.000356$$

From the Moody chart, read $f = 0.0177$. Then the pressure drop is

$$\Delta p = \rho g h_f = \rho g \left(f \frac{L}{D_h} \frac{V^2}{2g} \right) = 0.00237(32.2)\left[0.0177 \frac{100}{0.75} \frac{44.4^2}{2(32.2)}\right]$$

or
$$\Delta p = 5.5 \text{ lbf/ft}^2 \qquad \textit{Ans.}$$

Pressure drop in air ducts is usually small because of the low density.

6.7 Minor Losses in Pipe Systems[7]

For any pipe system, in addition to the Moody-type friction loss computed for the length of pipe, there are additional so-called *minor losses* due to

1. Pipe entrance or exit
2. Sudden expansion or contraction
3. Bends, elbows, tees, and other fittings
4. Valves, open or partially closed
5. Gradual expansions or contractions

The losses may not be so minor; e.g., a partially closed valve can cause a greater pressure drop than a long pipe.

Since the flow pattern in fittings and valves is quite complex, the theory is very weak. The losses are commonly measured experimentally and correlated with the pipe-flow parameters. The data, especially for valves, are somewhat dependent upon the particular manufacturer's design, so that the values listed here must be taken as average design estimates [15, 16, 35, 43, 46].

The measured minor loss is usually given as a ratio of the head loss $h_m = \Delta p/(\rho g)$ through the device to the velocity head $V^2/(2g)$ of the associated piping system

$$\text{Loss coefficient } K = \frac{h_m}{V^2/(2g)} = \frac{\Delta p}{\frac{1}{2}\rho V^2} \tag{6.98}$$

Although K is dimensionless, it unfortunately is not correlated in the literature with the Reynolds number and roughness ratio but rather simply with the raw size of the pipe in, say, inches. Almost all data are reported for turbulent-flow conditions.

An alternate, and less desirable, procedure is to report the minor loss as if it were an *equivalent length* L_{eq} of pipe, satisfying the Darcy friction-factor relation

$$h_m = f\frac{L_{eq}}{d}\frac{V^2}{2g} = K\frac{V^2}{2g}$$

or

$$L_{eq} = \frac{Kd}{f} \tag{6.99}$$

Although the equivalent length should take some of the variability out of the loss data, it is an artificial concept and will not be pursued here.

A single pipe system may have many minor losses. Since all are correlated with $V^2/(2g)$, they can be summed into a single total system loss if the pipe has constant diameter

$$\Delta h_{tot} = h_f + \sum h_m = \frac{V^2}{2g}\left(\frac{fL}{d} + \sum K\right) \tag{6.100}$$

Note, however, that we must sum the losses separately if the pipe size changes so that V^2 changes. The length L in Eq. (6.100) is the total length of the pipe axis, including any bends.

There are many different valve designs in commercial use. Figure 6.17 shows five typical designs: (*a*) the *gate*, which slides down across the section; (*b*) the *globe*, which closes a hole in a special insert; (*c*) the *angle*, similar to a globe but with a 90° turn;

[7]This section may be omitted without loss of continuity.

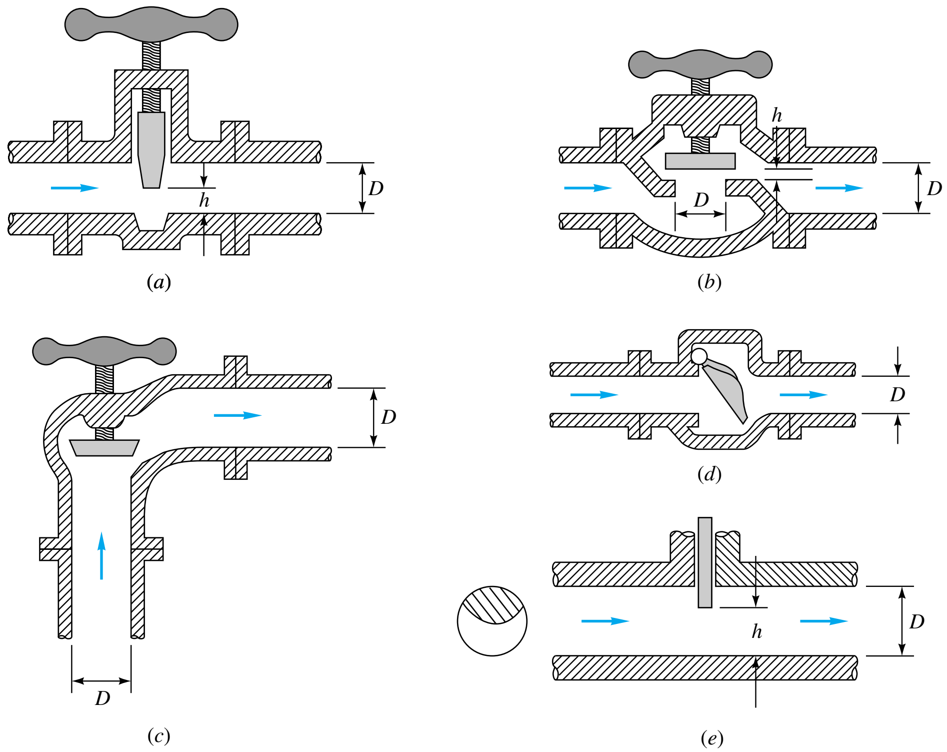

Fig. 6.17 Typical commercial valve geometries: (*a*) gate valve; (*b*) globe valve; (*c*) angle valve; (*d*) swing-check valve; (*e*) disk-type gate valve.

(*d*) the *swing-check* valve, which allows only one-way flow; and (*e*) the *disk*, which closes the section with a circular gate. The globe, with its tortuous flow path, has the highest losses when fully open. Many excellent details about these and other valves are given in the handbook by Lyons [35].

Table 6.5 lists loss coefficients K for four types of valve, three angles of elbow fit-

Table 6.5 Resistance Coefficients $K = h_m/[V^2/(2g)]$ for Open Valves, Elbows, and Tees

	Nominal diameter, in								
	Screwed				Flanged				
	$\frac{1}{2}$	1	2	4	1	2	4	8	20
Valves (fully open):									
Globe	14	8.2	6.9	5.7	13	8.5	6.0	5.8	5.5
Gate	0.30	0.24	0.16	0.11	0.80	0.35	0.16	0.07	0.03
Swing check	5.1	2.9	2.1	2.0	2.0	2.0	2.0	2.0	2.0
Angle	9.0	4.7	2.0	1.0	4.5	2.4	2.0	2.0	2.0
Elbows:									
45° regular	0.39	0.32	0.30	0.29					
45° long radius					0.21	0.20	0.19	0.16	0.14
90° regular	2.0	1.5	0.95	0.64	0.50	0.39	0.30	0.26	0.21
90° long radius	1.0	0.72	0.41	0.23	0.40	0.30	0.19	0.15	0.10
180° regular	2.0	1.5	0.95	0.64	0.41	0.35	0.30	0.25	0.20
180° long radius					0.40	0.30	0.21	0.15	0.10
Tees:									
Line flow	0.90	0.90	0.90	0.90	0.24	0.19	0.14	0.10	0.07
Branch flow	2.4	1.8	1.4	1.1	1.0	0.80	0.64	0.58	0.41

ting, and two tee connections. Fittings may be connected by either internal screws or flanges, hence the two listings. We see that K generally decreases with pipe size, which is consistent with the higher Reynolds number and decreased roughness ratio of large pipes. We stress that Table 6.5 represents losses *averaged among various manufacturers*, so there is an uncertainty as high as ± 50 percent.

In addition, most of the data in Table 6.5 are relatively old [15, 16] and therefore based upon fittings manufactured in the 1950s. Modern forged and molded fittings may yield somewhat different loss factors, often less than listed in Table 6.5. An example, shown in Fig. 6.18*a*, gives very recent data [48] for fairly short (bend-radius/elbow-diameter = 1.2) flanged 90° elbows. The elbow diameter was 1.69 in. Notice first that K is plotted versus Reynolds number, rather than versus the raw (dimensional) pipe diameters in Table 6.5, and therefore Fig. 6.18*a* has more generality. Then notice that the K values of 0.23 ± 0.05 are significantly less than the values for 90° elbows in Table 6.5, indicating smoother walls and/or better design. One may conclude that (1) Table 6.5 data are probably conservative and (2) loss factors are highly dependent upon actual design and manufacturing factors, with Table 6.5 only serving as a rough guide.

The valve losses in Table 6.5 are for the fully open condition. Losses can be much higher for a partially open valve. Figure 6.18*b* gives average losses for three valves as a function of "percentage open," as defined by the opening-distance ratio h/D (see Fig. 6.17 for the geometries). Again we should warn of a possible uncertainty of ± 50 percent. Of all minor losses, valves, because of their complex geometry, are most sensitive to manufacturers' design details. For more accuracy, the particular design and manufacturer should be consulted [35].

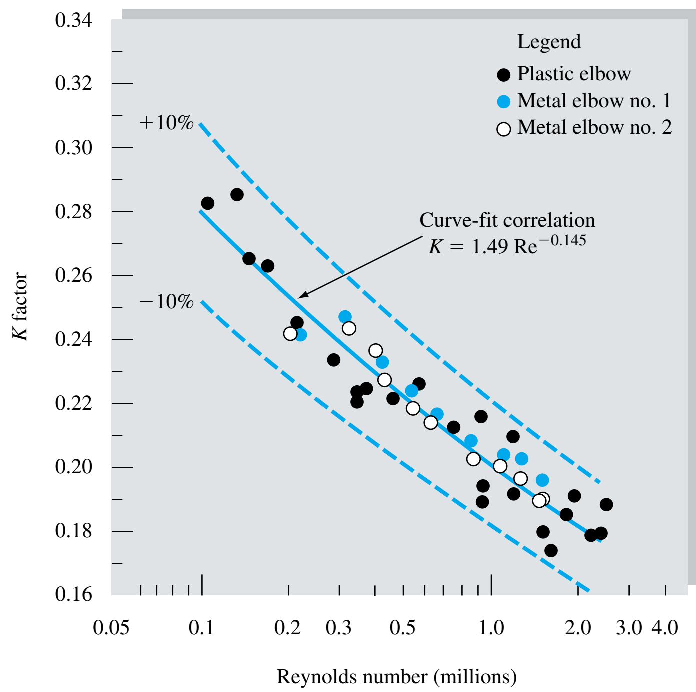

Fig. 6.18a Recent measured loss coefficients for 90° elbows. These values are less than those reported in Table 6.5. *[From Ref. 48, courtesy of R. D. Coffield.]*

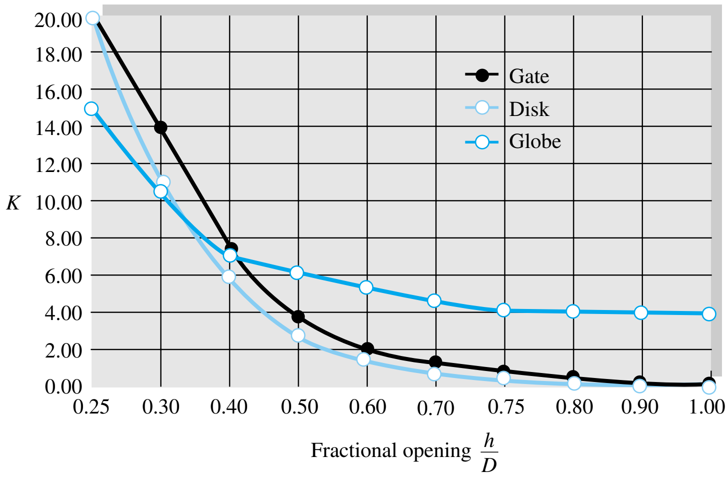

Fig. 6.18b Average-loss coefficients for partially open valves (see sketches in Fig. 6.17).

(*a*)

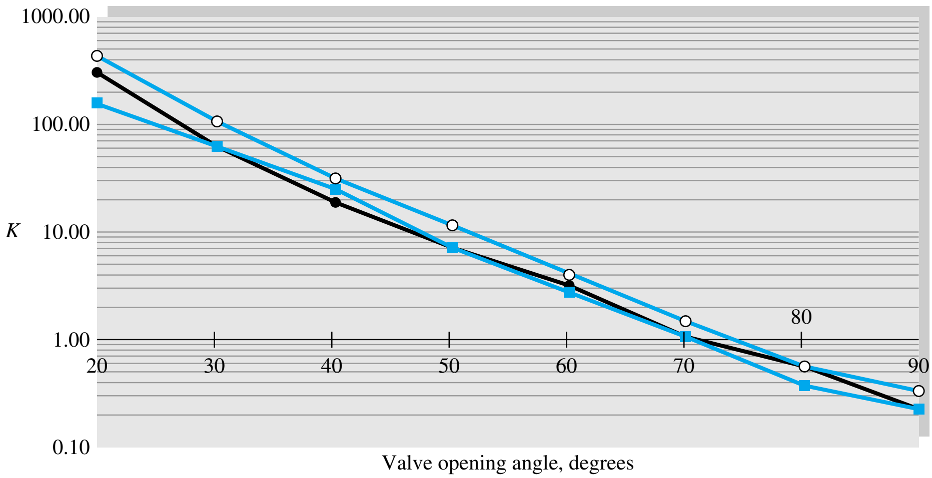

(*b*)

Fig. 6.19 Performance of butterfly valves: (*a*) typical geometry *(courtesy of Grinnell Corp., Cranston, R.I.);* (*b*) loss coefficients for three different manufacturers.

The *butterfly* valve of Fig. 6.19*a* is a stem-mounted disk which, when closed, seats against an O-ring or compliant seal near the pipe surface. A single 90° turn opens the valve completely, hence the design is ideal for controllable quick-opening and quick-closing situations such as occur in fire protection and the electric power industry. However, considerable dynamic torque is needed to close these valves, and losses are high when the valves are nearly closed.

Figure 6.19*b* shows butterfly-valve loss coefficients as a function of the opening angle θ for turbulent-flow conditions ($\theta = 0$ is closed). The losses are huge when the opening is small, and K drops off nearly exponentially with the opening angle. There is a factor of 2 spread among the various manufacturers. Note that K in Fig. 6.19*b* is, as usual, based on the average *pipe* velocity $V = Q/A$, not on the increased velocity of the flow as it passes through the narrow valve passage.

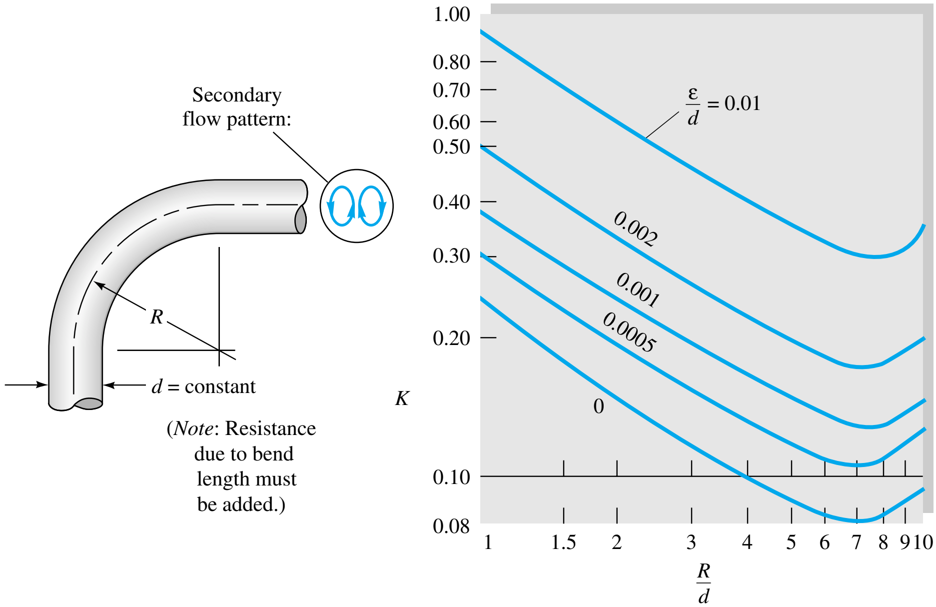

Fig. 6.20 Resistance coefficients for 90° bends.

A bend or curve in a pipe, as in Fig. 6.20, always induces a loss larger than the simple Moody friction loss, due to flow separation at the walls and a swirling secondary flow arising from the centripetal acceleration. The loss coefficients K in Fig. 6.20 are for this additional bend loss. The Moody loss due to the axial length of the bend must be computed separately; i.e., the bend length should be added to the pipe length.

As shown in Fig. 6.21, entrance losses are highly dependent upon entrance geometry, but exit losses are not. Sharp edges or protrusions in the entrance cause large zones of flow separation and large losses. A little rounding goes a long way, and a well-rounded entrance ($r = 0.2d$) has a nearly negligible loss $K = 0.05$. At a submerged exit, on the other hand, the flow simply passes out of the pipe into the large downstream reservoir and loses all its velocity head due to viscous dissipation. Therefore $K = 1.0$ for all *submerged exits,* no matter how well rounded.

If the entrance is from a finite reservoir, it is termed a *sudden contraction* (SC) between two sizes of pipe. If the exit is to finite-sized pipe, it is termed a *sudden expansion* (SE). The losses for both are graphed in Fig. 6.22. For the sudden expansion, the shear stress in the corner separated flow, or deadwater region, is negligible, so that a control-volume analysis between the expansion section and the end of the separation zone gives a theoretical loss

$$K_{SE} = \left(1 - \frac{d^2}{D^2}\right)^2 = \frac{h_m}{V^2/(2g)} \tag{6.101}$$

Note that K is based on the velocity head in the small pipe. Equation (6.101) is in excellent agreement with experiment.

For the sudden contraction, however, flow separation in the downstream pipe causes the main stream to contract through a minimum diameter d_{min}, called the *vena contracta*, as sketched in Fig. 6.22. Because the theory of the vena contracta is not well developed, the loss coefficient in the figure for sudden contraction is experimental. It

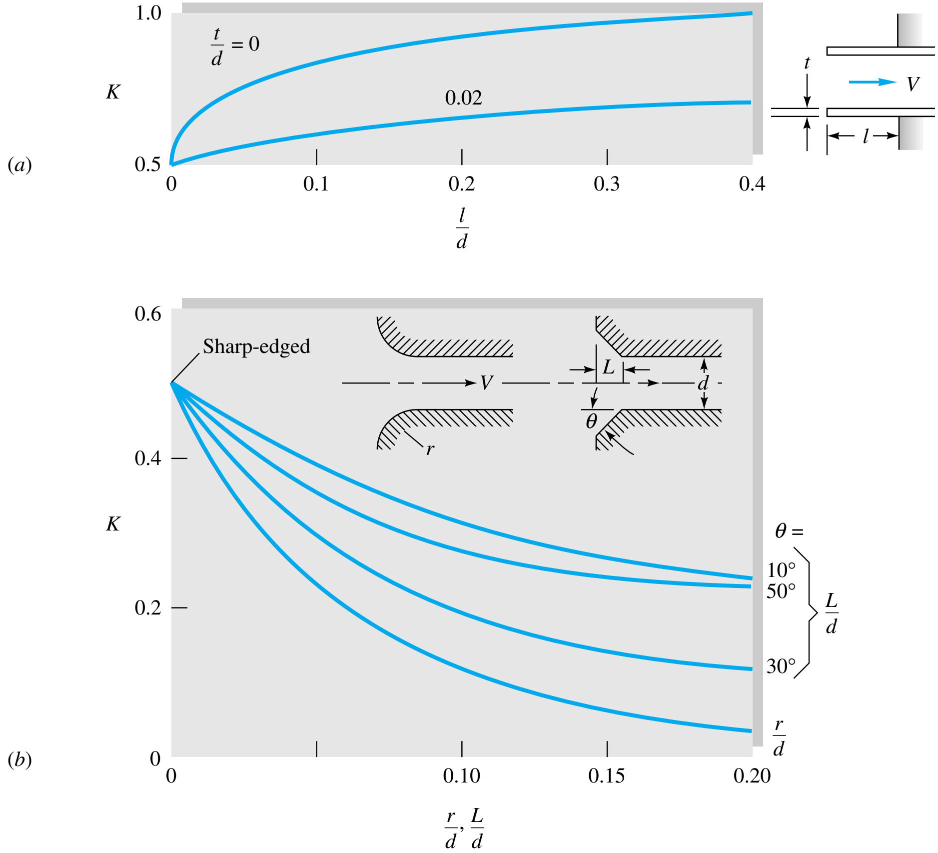

Fig. 6.21 Entrance and exit loss coefficients: (*a*) reentrant inlets; (*b*) rounded and beveled inlets. Exit losses are $K \approx 1.0$ for all shapes of exit (reentrant, sharp, beveled, or rounded). *(From Ref. 37.)*

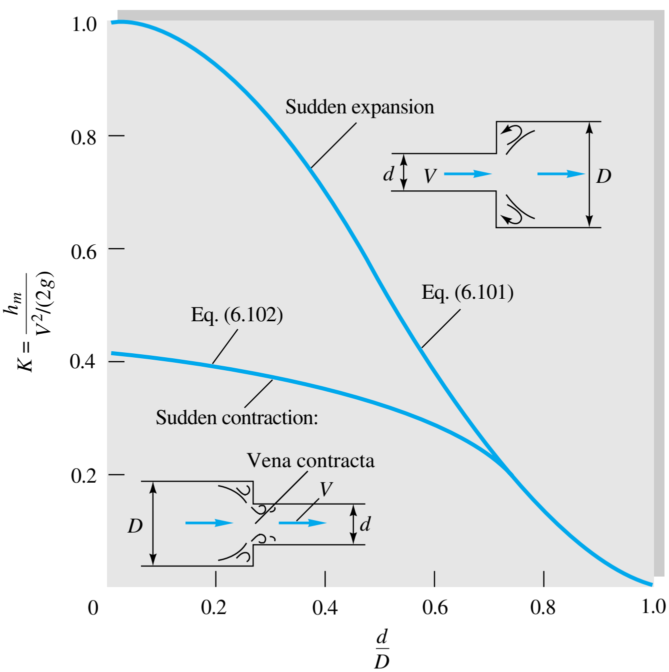

Fig. 6.22 Sudden expansion and contraction losses. Note that the loss is based on velocity head in the small pipe.

fits the empirical formula

$$K_{SC} \approx 0.42\left(1 - \frac{d^2}{D^2}\right) \tag{6.102}$$

up to the value $d/D = 0.76$, above which it merges into the sudden-expansion prediction, Eq. (6.101).

If the expansion or contraction is gradual, the losses are quite different. Figure 6.23 shows the loss through a gradual conical expansion, usually called a *diffuser* [14]. There is a spread in the data, depending upon the boundary-layer conditions in the upstream pipe. A thinner entrance boundary layer, like the entrance profile in Fig. 6.6, gives a smaller loss. Since a diffuser is intendsed to raise the static pressure of the flow, diffuser data list the pressure-recovery coefficient of the flow

$$C_p = \frac{p_2 - p_1}{\frac{1}{2}\rho V_1^2} \tag{6.103}$$

The loss coefficient is related to this parameter by

$$K = \frac{h_m}{V^2/(2g)} = 1 - \frac{d_1^4}{d_2^4} - C_p \tag{6.104}$$

For a given area ratio, the higher the pressure recovery, the lower the loss; hence large C_p means a successful diffuser. From Fig. 6.23 the minimum loss (maximum recovery) occurs for a cone angle 2θ equal to about 5°. Angles smaller than this give a large Moody-type loss because of their excessive length. For cone angles greater than 40 to 60°, the loss is so excessive that it would actually be better to use a sudden expansion.

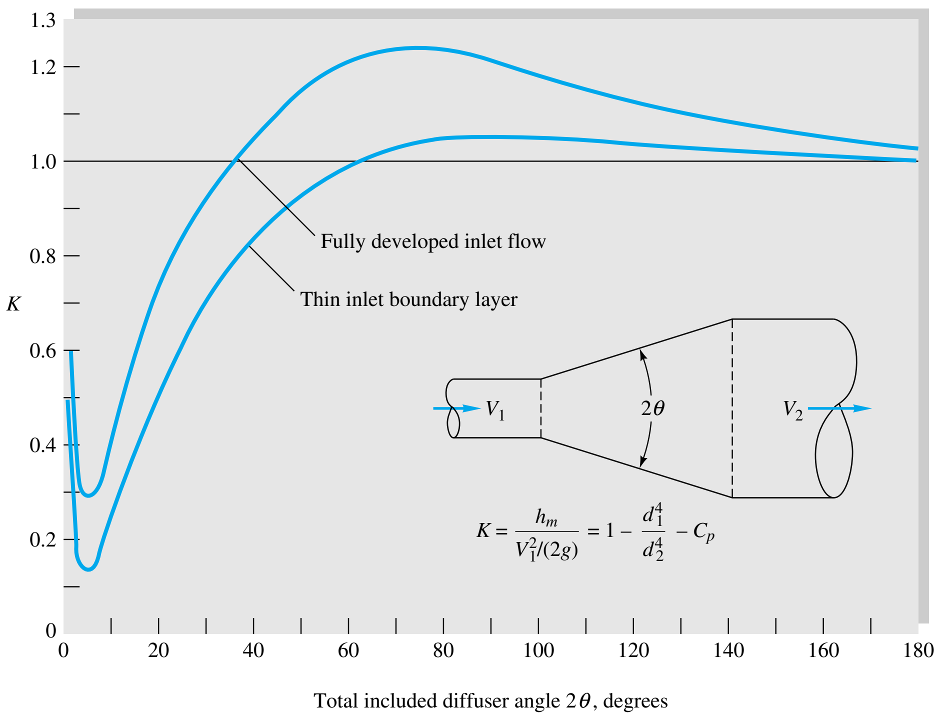

Fig. 6.23 Flow losses in a gradual conical expansion region.

This unexpected effect is due to gross flow separation in a wide-angle diffuser, as we shall see soon when we study boundary layers. Reference 14 has extensive data on diffusers.

For a gradual *contraction,* the loss is very small, as seen from the following experimental values [15]:

Contraction cone angle 2θ, deg	30	45	60
K for gradual contraction	0.02	0.04	0.07

References 15, 16, 43, and 46 contain additional data on minor losses.

EXAMPLE 6.16

Water, $\rho = 1.94$ slugs/ft^3 and $\nu = 0.000011$ ft^2/s, is pumped between two reservoirs at 0.2 ft^3/s through 400 ft of 2-in-diameter pipe and several minor losses, as shown in Fig. E6.16. The roughness ratio is $\epsilon/d = 0.001$. Compute the pump horsepower required.

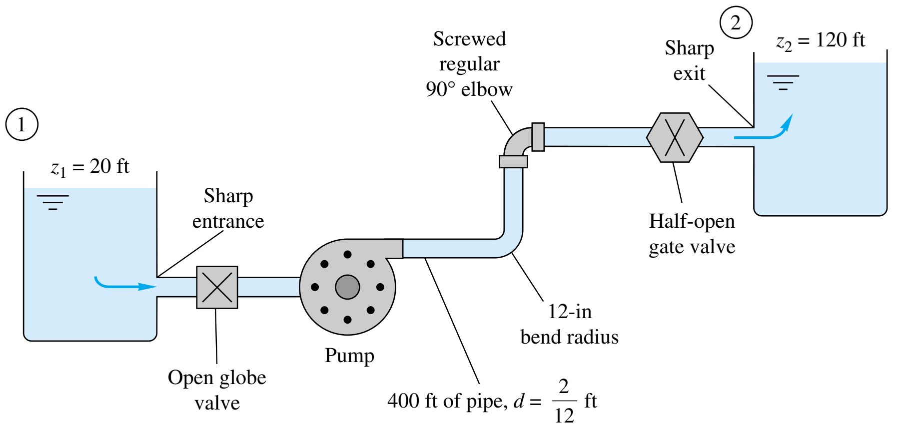

E6.16

Solution

Write the steady-flow energy equation between sections 1 and 2, the two reservoir surfaces:

$$\frac{p_1}{\rho g} + \frac{V_1^2}{2g} + z_1 = \left(\frac{p_2}{\rho g} + \frac{V_2^2}{2g} + z_2\right) + h_f + \sum h_m - h_p$$

where h_p is the head increase across the pump. But since $p_1 = p_2$ and $V_1 = V_2 \approx 0$, solve for the pump head

$$h_p = z_2 - z_1 + h_f + \sum h_m = 120 \text{ ft} - 20 \text{ ft} + \frac{V^2}{2g}\left(\frac{fL}{d} + \sum K\right) \tag{1}$$

Now with the flow rate known, calculate

$$V = \frac{Q}{A} = \frac{0.2 \text{ ft}^3/\text{s}}{\frac{1}{4}\pi(\frac{2}{12}\text{ ft})^2} = 9.17 \text{ ft/s}$$

Now list and sum the minor loss coefficients:

Loss	K
Sharp entrance (Fig. 6.21)	0.5
Open globe valve (2 in, Table 6.5)	6.9
12-in bend (Fig. 6.20)	0.15
Regular 90° elbow (Table 6.5)	0.95
Half-closed gate valve (from Fig. 6.18*b*)	2.7
Sharp exit (Fig. 6.21)	1.0
	$\sum K = 12.2$

Calculate the Reynolds number and pipe-friction factor

$$\mathrm{Re}_d = \frac{Vd}{\nu} = \frac{9.17(\frac{2}{12})}{0.000011} = 139{,}000$$

For $\epsilon/d = 0.001$, from the Moody chart read $f = 0.0216$. Substitute into Eq. (1)

$$h_p = 100 \text{ ft} + \frac{(9.17 \text{ ft/s})^2}{2(32.2 \text{ ft/s}^2)}\left[\frac{0.0216(400)}{\frac{2}{12}} + 12.2\right]$$

$$= 100 \text{ ft} + 84 \text{ ft} = 184 \text{ ft} \quad \text{pump head}$$

The pump must provide a power to the water of

$$P = \rho g Q h_p = [1.94(32.2) \text{ lbf/ft}^3](0.2 \text{ ft}^3/\text{s})(184 \text{ ft}) = 2300 \text{ ft} \cdot \text{lbf/s}$$

The conversion factor is 1 hp = 550 ft · lbf/s. Therefore

$$P = \frac{2300}{550} = 4.2 \text{ hp} \qquad \textit{Ans.}$$

Allowing for an efficiency of 70 to 80 percent, a pump is needed with an input of about 6 hp.

6.8 Multiple-Pipe Systems[8]

If you can solve the equations for one-pipe systems, you can solve them all; but when systems contain two or more pipes, certain basic rules make the calculations very smooth. Any resemblance between these rules and the rules for handling electric circuits is not coincidental.

Figure 6.24 shows three examples of multiple-pipe systems. The first is a set of three (or more) pipes in series. Rule 1 is that the flow rate is the same in all pipes

$$Q_1 = Q_2 = Q_3 = \text{const}$$

or

$$V_1 d_1^2 = V_2 d_2^2 = V_3 d_3^2 \tag{6.105}$$

Rule 2 is that the total head loss through the system equals the sum of the head loss in each pipe

$$\Delta h_{A\to B} = \Delta h_1 + \Delta h_2 + \Delta h_3 \tag{6.106}$$

In terms of the friction and minor losses in each pipe, we could rewrite this as

[8]This section may be omitted without loss of continuity.

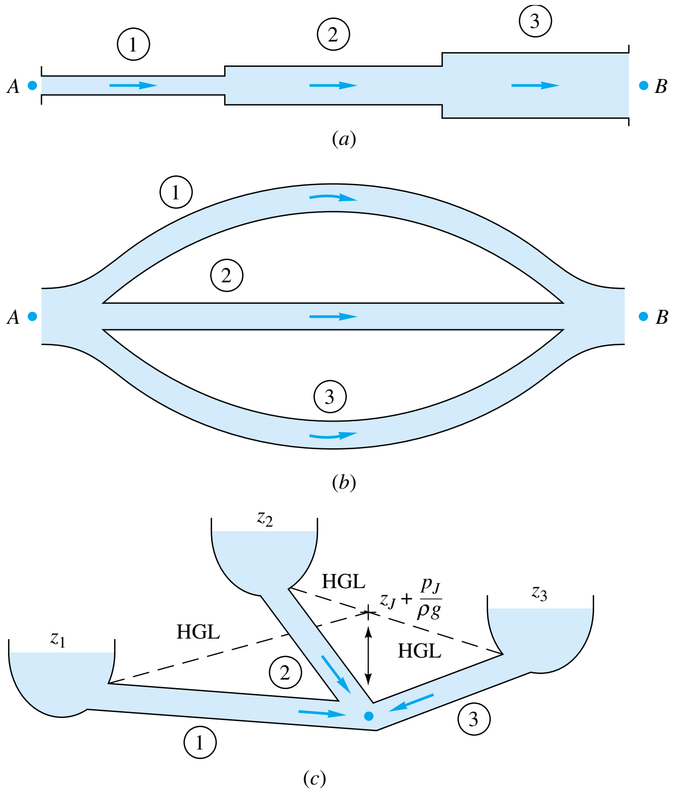

Fig. 6.24 Examples of multiple-pipe systems: (*a*) pipes in series; (*b*) pipes in parallel; (*c*) the three-reservoir junction problem.

$$\Delta h_{A\to B} = \frac{V_1^2}{2g}\left(\frac{f_1 L_1}{d_1} + \sum K_1\right) + \frac{V_2^2}{2g}\left(\frac{f_2 L_2}{d_2} + \sum K_2\right) + \frac{V_3^2}{2g}\left(\frac{f_3 L_3}{d_3} + \sum K_3\right) \tag{6.107}$$

and so on for any number of pipes in the series. Since V_2 and V_3 are proportional to V_1 from Eq. (6.105), Eq. (6.107) is of the form

$$\Delta h_{A\to B} = \frac{V_1^2}{2g}(\alpha_0 + \alpha_1 f_1 + \alpha_2 f_2 + \alpha_3 f_3) \tag{6.108}$$

where the α_i are dimensionless constants. If the flow rate is given, we can evaluate the right-hand side and hence the total head loss. If the head loss is given, a little iteration is needed, since f_1, f_2, and f_3 all depend upon V_1 through the Reynolds number. Begin by calculating f_1, f_2, and f_3, assuming fully rough flow, and the solution for V_1 will converge with one or two iterations. EES is ideal for this purpose.

EXAMPLE 6.17

Given is a three-pipe series system, as in Fig. 6.24*a*. The total pressure drop is $p_A - p_B = 150{,}000$ Pa, and the elevation drop is $z_A - z_B = 5$ m. The pipe data are

Pipe	L, m	d, cm	ϵ, mm	ϵ/d
1	100	8	0.24	0.003
2	150	6	0.12	0.002
3	80	4	0.20	0.005

The fluid is water, $\rho = 1000$ kg/m^3 and $\nu = 1.02 \times 10^{-6}$ m^2/s. Calculate the flow rate Q in m^3/h through the system.

Solution

The total head loss across the system is

$$\Delta h_{A \to B} = \frac{p_A - p_B}{\rho g} + z_A - z_B = \frac{150{,}000}{1000(9.81)} + 5 \text{ m} = 20.3 \text{ m}$$

From the continuity relation (6.105) the velocities are

$$V_2 = \frac{d_1^2}{d_2^2} V_1 = \frac{16}{9} V_1 \qquad V_3 = \frac{d_1^2}{d_3^2} V_1 = 4V_1$$

and

$$\text{Re}_2 = \frac{V_2 d_2}{V_1 d_1} \text{Re}_1 = \frac{4}{3} \text{Re}_1 \qquad \text{Re}_3 = 2 \text{ Re}_1$$

Neglecting minor losses and substituting into Eq. (6.107), we obtain

$$\Delta h_{A \to B} = \frac{V_1^2}{2g} \left[1250 f_1 + 2500 \left(\frac{16}{9} \right)^2 f_2 + 2000(4)^2 f_3 \right]$$

or

$$20.3 \text{ m} = \frac{V_1^2}{2g} (1250 f_1 + 7900 f_2 + 32{,}000 f_3) \qquad (1)$$

This is the form which was hinted at in Eq. (6.108). It seems to be dominated by the third pipe loss $32{,}000 f_3$. Begin by estimating f_1, f_2, and f_3 from the Moody-chart fully rough regime

$$f_1 = 0.0262 \qquad f_2 = 0.0234 \qquad f_3 = 0.0304$$

Substitute in Eq. (1) to find $V_1^2 \approx 2g(20.3)/(33 + 185 + 973)$. The first estimate thus is $V_1 = 0.58$ m/s, from which

$$\text{Re}_1 \approx 45{,}400 \qquad \text{Re}_2 = 60{,}500 \qquad \text{Re}_3 = 90{,}800$$

Hence, from the Moody chart,

$$f_1 = 0.0288 \qquad f_2 = 0.0260 \qquad f_3 = 0.0314$$

Substitution into Eq. (1) gives the better estimate

$$V_1 = 0.565 \text{ m/s} \qquad Q = \tfrac{1}{4}\pi d_1^2 V_1 = 2.84 \times 10^{-3} \text{ m}^3\text{/s}$$

or

$$Q_1 = 10.2 \text{ m}^3\text{/h} \qquad \textit{Ans.}$$

A second iteration gives $Q = 10.22$ m^3/h, a negligible change.

The second multiple-pipe system is the *parallel*-flow case shown in Fig. 6.24b. Here the loss is the same in each pipe, and the total flow is the sum of the individual flows

$$\Delta h_{A \to B} = \Delta h_1 = \Delta h_2 = \Delta h_3 \tag{6.109a}$$

$$Q = Q_1 + Q_2 + Q_3 \tag{6.109b}$$

If the total head loss is known, it is straightforward to solve for Q_i in each pipe and sum them, as will be seen in Example 6.18. The reverse problem, of determining ΣQ_i when h_f is known, requires iteration. Each pipe is related to h_f by the Moody relation $h_f = f(L/d)(V^2/2g) = fQ^2/C$, where $C = \pi^2 g d^5/8L$. Thus each pipe has nearly quadratic nonlinear parallel resistance, and head loss is related to total flow rate by

$$h_f = \frac{Q^2}{\left(\sum\sqrt{C_i/f_i}\right)^2} \qquad \text{where } C_i = \frac{\pi^2 g d_i^5}{8L_i} \tag{6.109c}$$

Since the f_i vary with Reynolds number and roughness ratio, one begins Eq. (6.109*c*) by guessing values of f_i (fully rough values are recommended) and calculating a first estimate of h_f. Then each pipe yields a flow-rate estimate $Q_i \approx (C_i h_f/f_i)^{1/2}$ and hence a new Reynolds number and a better estimate of f_i. Then repeat Eq. (6.109*c*) to convergence.

It should be noted that both of these parallel-pipe cases—finding either ΣQ or h_f—are easily solved by EES if reasonable initial guesses are given.

EXAMPLE 6.18

Assume that the same three pipes in Example 6.17 are now in parallel with the same total head loss of 20.3 m. Compute the total flow rate Q, neglecting minor losses.

Solution

From Eq. (6.109*a*) we can solve for each V separately

$$20.3 \text{ m} = \frac{V_1^2}{2g}1250f_1 = \frac{V_2^2}{2g}2500f_2 = \frac{V_3^2}{2g}2000f_3 \tag{1}$$

Guess fully rough flow in pipe 1: $f_1 = 0.0262$, $V_1 = 3.49$ m/s; hence $\text{Re}_1 = V_1 d_1/\nu = 273{,}000$. From the Moody chart read $f_1 = 0.0267$; recompute $V_1 = 3.46$ m/s, $Q_1 = 62.5$ m^3/h. [This problem can also be solved from Eq. (6.66).]

Next guess for pipe 2: $f_2 \approx 0.0234$, $V_2 \approx 2.61$ m/s; then $\text{Re}_2 = 153{,}000$, and hence $f_2 = 0.0246$, $V_2 = 2.55$ m/s, $Q_2 = 25.9$ m^3/h.

Finally guess for pipe 3: $f_3 \approx 0.0304$, $V_3 \approx 2.56$ m/s; then $\text{Re}_3 = 100{,}000$, and hence $f_3 = 0.0313$, $V_3 = 2.52$ m/s, $Q_3 = 11.4$ m^3/h.

This is satisfactory convergence. The total flow rate is

$$Q = Q_1 + Q_2 + Q_3 = 62.5 + 25.9 + 11.4 = 99.8 \text{ m}^3/\text{h} \qquad \textit{Ans.}$$

These three pipes carry 10 times more flow in parallel than they do in series.

This example is ideal for EES. One enters the pipe data (L_i, d_i, ϵ_i); the fluid properties (ρ, μ); the definitions $Q_i = (\pi/4)d_i^2V_i$, $\text{Re}_i = \rho V_i d_i/\mu$, and $h_f = f_i(L_i/d_i)(V_i^2/2g)$; plus the Colebrook formula (6.74) for each friction factor f_i. There is no need to use resistance ideas such as Eq. (6.109*c*). Specify that $f_i > 0$ and $\text{Re}_i > 4000$. Then, if one enters $Q = \Sigma Q_i = (99.8/3600)$ m^3/s, EES quickly solves for $h_f = 20.3$ m. Conversely, if one enters $h_f = 20.3$ m, EES solves for $Q = 99.8$ m^3/h.

Consider the third example of a *three-reservoir pipe junction,* as in Fig. 6.24*c*. If all flows are considered positive toward the junction, then

$$Q_1 + Q_2 + Q_3 = 0 \tag{6.110}$$

which obviously implies that one or two of the flows must be away from the junction. The pressure must change through each pipe so as to give the same static pressure p_J at the junction. In other words, let the HGL at the junction have the elevation

$$h_J = z_J + \frac{p_J}{\rho g}$$

where p_J is in gage pressure for simplicity. Then the head loss through each, assuming $p_1 = p_2 = p_3 = 0$ (gage) at each reservoir surface, must be such that

$$\Delta h_1 = \frac{V_1^2}{2g}\frac{f_1 L_1}{d_1} = z_1 - h_J$$
$$\Delta h_2 = \frac{V_2^2}{2g}\frac{f_2 L_2}{d_2} = z_2 - h_J \tag{6.111}$$
$$\Delta h_3 = \frac{V_3^2}{2g}\frac{f_3 L_3}{d_3} = z_3 - h_J$$

We guess the position h_J and solve Eqs. (6.111) for V_1, V_2, and V_3 and hence Q_1, Q_2, and Q_3, iterating until the flow rates balance at the junction according to Eq. (6.110). If we guess h_J too *high*, the sum $Q_1 + Q_2 + Q_3$ will be *negative* and the remedy is to reduce h_J, and vice versa.

EXAMPLE 6.19

Take the same three pipes as in Example 6.17, and assume that they connect three reservoirs at these surface elevations

$$z_1 = 20 \text{ m} \qquad z_2 = 100 \text{ m} \qquad z_3 = 40 \text{ m}$$

Find the resulting flow rates in each pipe, neglecting minor losses.

Solution

As a first guess, take h_J equal to the middle reservoir height, $z_3 = h_J = 40$ m. This saves one calculation ($Q_3 = 0$) and enables us to get the lay of the land:

Reservoir	h_J, m	$z_i - h_J$, m	f_i	V_i, m/s	Q_i, m³/h	L_i/d_i
1	40	−20	0.0267	−3.43	−62.1	1250
2	40	60	0.0241	4.42	45.0	2500
3	40	0		0	0	2000
					$\sum Q = -17.1$	

Since the sum of the flow rates toward the junction is negative, we guessed h_J too high. Reduce h_J to 30 m and repeat:

Reservoir	h_J, m	$z_i - h_J$, m	f_i	V_i, m/s	Q_i, m^3/h
1	30	−10	0.0269	−2.42	−43.7
2	30	70	0.0241	4.78	48.6
3	30	10	0.0317	1.76	8.0
					$\sum Q = 12.9$

This is positive ΣQ, and so we can linearly interpolate to get an accurate guess: $h_J \approx 34.3$ m. Make one final list:

Reservoir	h_J, m	$z_i - h_J$, m	f_i	V_i, m/s	Q_i, m^3/h
1	34.3	−14.3	0.0268	−2.90	−52.4
2	34.3	65.7	0.0241	4.63	47.1
3	34.3	5.7	0.0321	1.32	6.0
					$\sum Q = 0.7$

This is close enough; hence we calculate that the flow rate is 52.4 m^3/h toward reservoir 3, balanced by 47.1 m^3/h away from reservoir 1 and 6.0 m^3/h away from reservoir 3.

One further iteration with this problem would give $h_J = 34.53$ m, resulting in $Q_1 = -52.8$, $Q_2 = 47.0$, and $Q_3 = 5.8$ m^3/h, so that $\Sigma Q = 0$ to three-place accuracy. Pedagogically speaking, we would then be exhausted.

The ultimate case of a multipipe system is the *piping network* illustrated in Fig. 6.25. This might represent a water supply system for an apartment or subdivision or even a city. This network is quite complex algebraically but follows the same basic rules:

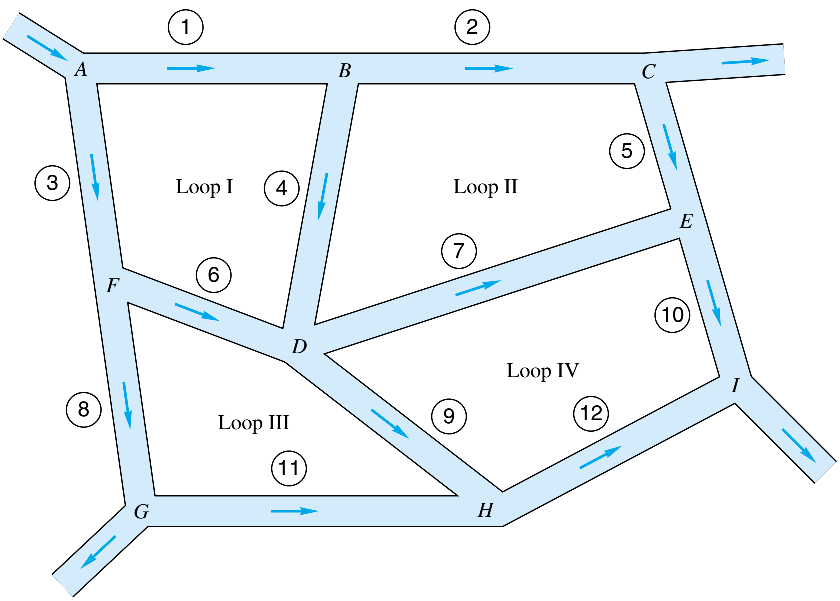

Fig. 6.25 Schematic of a piping network.

1. The net flow into any junction must be zero.
2. The net head loss around any closed loop must be zero. In other words, the HGL at each junction must have one and only one elevation.
3. All head losses must satisfy the Moody and minor-loss friction correlations.

By supplying these rules to each junction and independent loop in the network, one obtains a set of simultaneous equations for the flow rates in each pipe leg and the HGL (or pressure) at each junction. Solution may then be obtained by numerical iteration, as first developed in a hand-calculation technique by Prof. Hardy Cross in 1936 [17]. Computer solution of pipe-network problems is now quite common and covered in at least one specialized text [18]. Solution on microcomputers is also a reality. Some explicit numerical algorithms have been developed by Ormsbee and Wood [19]. Network analysis is quite useful for real water distribution systems if well calibrated with the actual system head-loss data.

6.9 Experimental Duct Flows: Diffuser Performance

The Moody chart is such a great correlation for tubes of any cross section with any roughness or flow rate that we may be deluded into thinking that the world of internal-flow prediction is at our feet. Not so. The theory is reliable only for ducts of constant cross section. As soon as the section varies, we must rely principally upon experiment to determine the flow properties. As mentioned many times before, experiment is a vital part of fluid mechanics.

Literally thousands of papers in the literature report experimental data for specific internal and external viscous flows. We have already seen several examples:

1. Vortex shedding from a cylinder (Fig. 5.2)
2. Drag of a sphere and a cylinder (Fig. 5.3)
3. Hydraulic model of an estuary (Fig. 5.9)
4. Rough-wall pipe flows (Fig. 6.12)
5. Secondary flow in ducts (Fig. 6.16)
6. Minor-duct-loss coefficients (Sec. 6.7)

Chapter 7 will treat a great many more external-flow experiments, especially in Sec. 7.5. Here we shall show data for one type of internal flow, the diffuser.

Diffuser Performance

A diffuser, shown in Fig. 6.26*a* and *b*, is an expansion or area increase intended to reduce velocity in order to recover the pressure head of the flow. Rouse and Ince [6] relate that it may have been invented by customers of the early Roman (about 100 A.D.) water supply system, where water flowed continuously and was billed according to pipe size. The ingenious customers discovered that they could increase the flow rate at no extra cost by flaring the outlet section of the pipe.

Engineers have always designed diffusers to increase pressure and reduce kinetic energy of ducted flows, but until about 1950, diffuser design was a combination of art, luck, and vast amounts of empiricism. Small changes in design parameters caused large changes in performance. The Bernoulli equation seemed highly suspect as a useful tool.

Neglecting losses and gravity effects, the incompressible Bernoulli equation predicts that

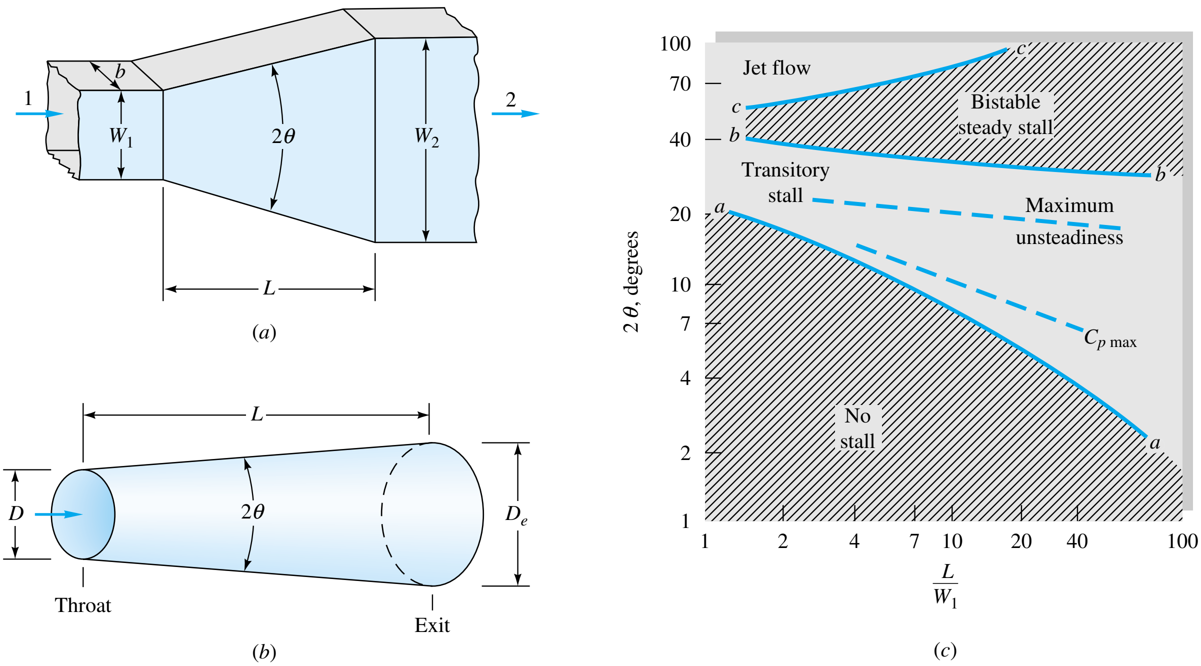

Fig. 6.26 Diffuser geometry and typical flow regimes: (a) geometry of a flat-walled diffuser; (b) geometry of a conical diffuser; (c) flat-diffuser stability map. *(From Ref. 14, by permission of Creare, Inc.)*

$$p + \tfrac{1}{2}\rho V^2 = p_0 = \text{const} \qquad (6.112)$$

where p_0 is the stagnation pressure which the fluid would achieve if the fluid were slowed to rest ($V = 0$) without losses.

The basic output of a diffuser is the *pressure-recovery coefficient* C_p, defined as

$$C_p = \frac{p_e - p_t}{p_{0t} - p_t} \qquad (6.113)$$

where subscripts e and t mean the exit and the throat (or inlet), respectively. Higher C_p means better performance.

Consider the flat-walled diffuser in Fig. 6.26a, where section 1 is the inlet and section 2 the exit. Application of Bernoulli's equation (6.112) to this diffuser predicts that

$$p_{01} = p_1 + \tfrac{1}{2}\rho V_1^2 = p_2 + \tfrac{1}{2}\rho V_2^2 = p_{02}$$

or

$$C_{p,\text{frictionless}} = 1 - \left(\frac{V_2}{V_1}\right)^2 \qquad (6.114)$$

Meanwhile, steady one-dimensional continuity would require that

$$Q = V_1 A_1 = V_2 A_2 \qquad (6.115)$$

Combining (6.114) and (6.115), we can write the performance in terms of the *area ratio* AR $= A_2/A_1$, which is a basic parameter in diffuser design:

$$C_{p,\text{frictionless}} = 1 - (\text{AR})^{-2} \qquad (6.116)$$

A typical design would have AR $= 5{:}1$, for which Eq. (6.116) predicts $C_p = 0.96$, or nearly full recovery. But, in fact, measured values of C_p for this area ratio [14] are only as high as 0.86 and can be as low as 0.24.

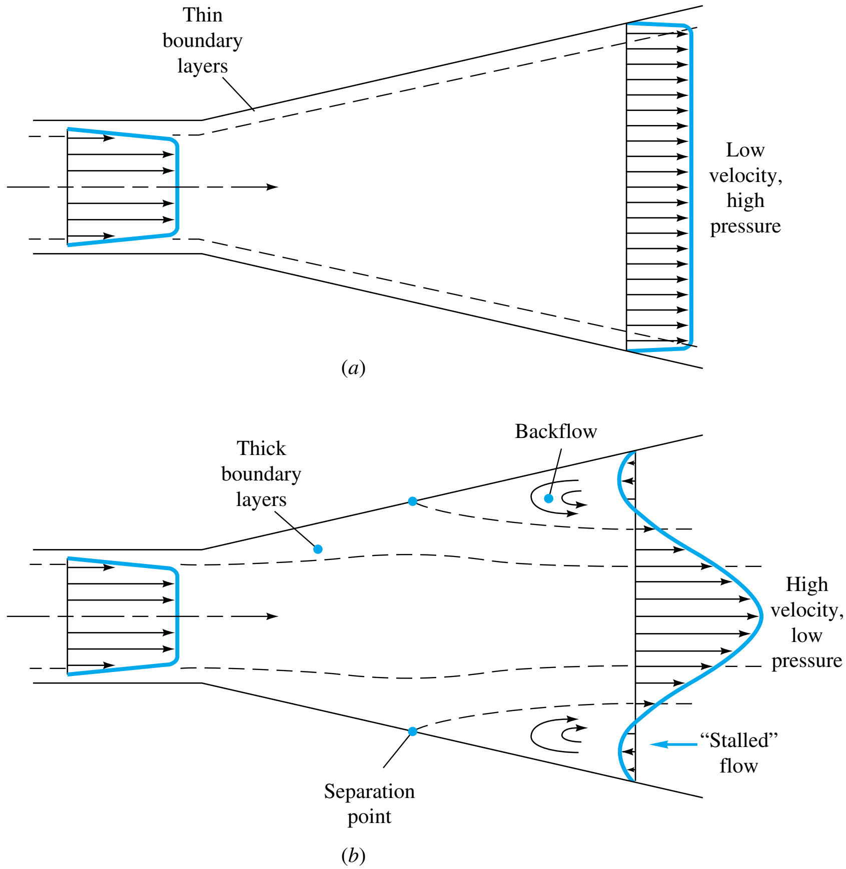

Fig. 6.27 Diffuser performance: (*a*) ideal pattern with good performance; (*b*) actual measured pattern with boundary-layer separation and resultant poor performance.

The basic reason for the discrepancy is flow separation, as sketched in Fig. 6.27. The increasing pressure in the diffuser is an unfavorable gradient (Sec. 7.4), which causes the viscous boundary layers to break away from the walls and greatly reduces the performance. Theories can now predict this behavior (see, e.g., Ref. 20).

As an added complication to boundary-layer separation, the flow patterns in a diffuser are highly variable and were considered mysterious and erratic until 1955, when Kline revealed the structure of these patterns with flow-visualization techniques in a simple water channel.

A complete *stability map* of diffuser flow patterns was published in 1962 by Fox and Kline [21], as shown in Fig. 6.26*c*. There are four basic regions. Below line *aa* there is steady viscous flow, no separation, and moderately good performance. Note that even a very short diffuser will separate, or stall, if its half-angle is greater than 10°.

Between lines *aa* and *bb* is a transitory stall pattern with strongly unsteady flow. Best performance, i.e., highest C_p, occurs in this region. The third pattern, between *bb* and *cc*, is steady bistable stall from one wall only. The stall pattern may flip-flop from one wall to the other, and performance is poor.

The fourth pattern, above line *cc*, is *jet flow*, where the wall separation is so gross and pervasive that the mainstream ignores the walls and simply passes on through at nearly constant area. Performance is extremely poor in this region.

Dimensional analysis of a flat-walled or conical diffuser shows that C_p should depend upon the following parameters:

1. Any two of the following geometric parameters:
   a. Area ratio AR $= A_2/A_1$ or $(D_e/D)^2$
   b. Divergence angle 2θ
   c. Slenderness L/W_1 or L/D
2. Inlet Reynolds number $\mathrm{Re}_t = V_1W_1/\nu$ or $\mathrm{Re}_t = V_1D/\nu$
3. Inlet Mach number $\mathrm{Ma}_t = V_1/a_1$
4. Inlet boundary-layer *blockage factor* $B_t = A_{BL}/A_1$, where A_{BL} is the wall area blocked, or displaced, by the retarded boundary-layer flow in the inlet (typically B_t varies from 0.03 to 0.12)

A flat-walled diffuser would require an additional shape parameter to describe its cross section:

5. Aspect ratio AS $= b/W_1$

Even with this formidable list, we have omitted five possible important effects: inlet turbulence, inlet swirl, inlet profile vorticity, superimposed pulsations, and downstream obstruction, all of which occur in practical machinery applications.

The three most important parameters are AR, θ, and B. Typical performance maps for diffusers are shown in Fig. 6.28. For this case of 8 to 9 percent blockage, both the flat-walled and conical types give about the same maximum performance, $C_p = 0.70$, but at different divergence angles (9° flat versus 4.5° conical). Both types fall far short of the Bernoulli estimates of $C_p = 0.93$ (flat) and 0.99 (conical), primarily because of the blockage effect.

From the data of Ref. 14 we can determine that, in general, performance decreases with blockage and is approximately the same for both flat-walled and conical diffusers, as shown in Table 6.6. In all cases, the best conical diffuser is 10 to 80 percent longer than the best flat-walled design. Therefore, if length is limited in the design, the flat-walled design will give the better performance.

The experimental design of a diffuser is an excellent example of a successful attempt to minimize the undesirable effects of adverse pressure gradient and flow separation.

Table 6.6 Maximum Diffuser-Performance Data [14]

Inlet blockage	Flat-walled		Conical	
B_t	$C_{p,\max}$	L/W_1	$C_{p,\max}$	L/d
0.02	0.86	18	0.83	20
0.04	0.80	18	0.78	22
0.06	0.75	19	0.74	24
0.08	0.70	20	0.71	26
0.10	0.66	18	0.68	28
0.12	0.63	16	0.65	30

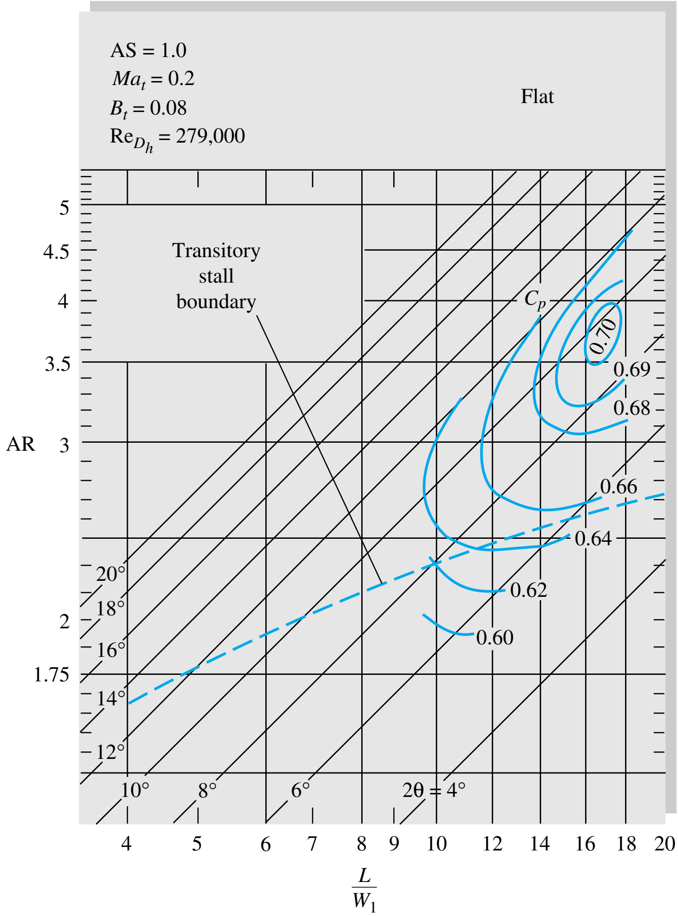

Fig. 6.28a Typical performance maps for flat-wall and conical diffusers at similar operating conditions: (*a*) flat wall. *(From Ref. 14, by permission of Creare, Inc.)*

6.10 Fluid Meters

Almost all practical fluids engineering problems are associated with the need for an accurate flow measurement. There is a need to measure *local* properties (velocity, pressure, temperature, density, viscosity, turbulent intensity), *integrated* properties (mass flow and volume flow), and *global* properties (visualization of the entire flow field). We shall concentrate in this section on velocity and volume-flow measurements.

We have discussed pressure measurement in Sec. 2.10. Measurement of other thermodynamic properties, such as density, temperature, and viscosity, is beyond the scope of this text and is treated in specialized books such as Refs. 22 and 23. Global visualization techniques were discussed in Sec. 1.7 for low-speed flows, and the special optical techniques used in high-speed flows are treated in Ref. 21 of Chap. 1. Flow-measurement schemes suitable for open-channel and other free-surface flows are treated in Chap. 10.

Local-Velocity Measurements

Velocity averaged over a small region, or point, can be measured by several different physical principles, listed in order of increasing complexity and sophistication:

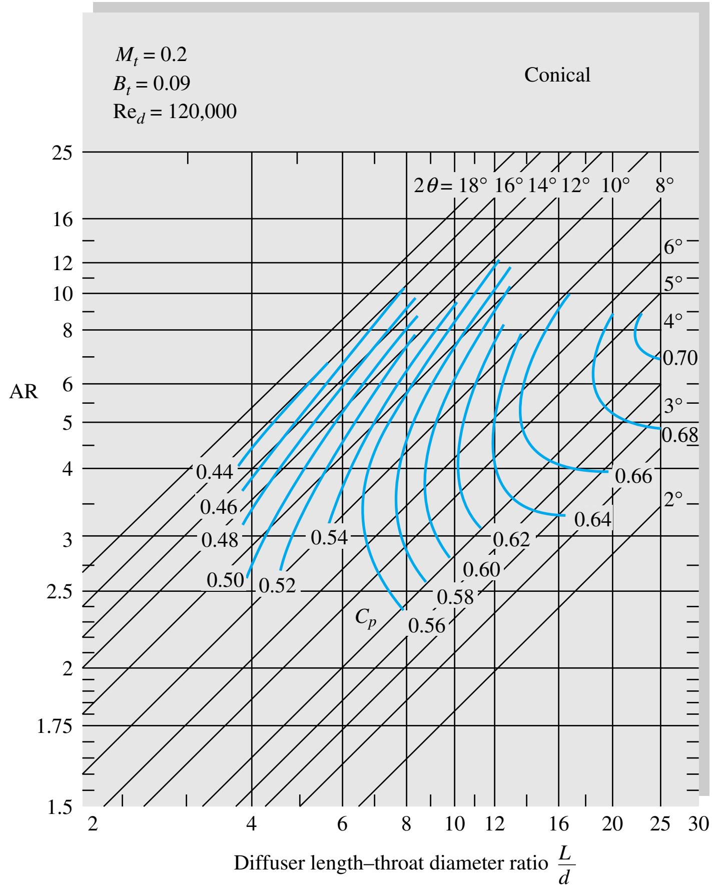

(*b*)

Fig. 6.28b Typical performance maps for flat-wall and conical diffusers at similar operating conditions: (*b*) conical wall. *(From Ref. 14, by permission of Creare, Inc.)*

1. Trajectory of floats or neutrally buoyant particles
2. Rotating mechanical devices
   a. Cup anemometer
   b. Savonius rotor
   c. Propeller meter
   d. Turbine meter
3. Pitot-static tube (Fig. 6.30)
4. Electromagnetic current meter
5. Hot wires and hot films
6. Laser-doppler anemometer (LDA)

Some of these meters are sketched in Fig. 6.29.

Floats or buoyant particles. A simple but effective estimate of flow velocity can be found from visible particles entrained in the flow. Examples include flakes on the surface of a channel flow, small neutrally buoyant spheres mixed with a liquid, or hydro-

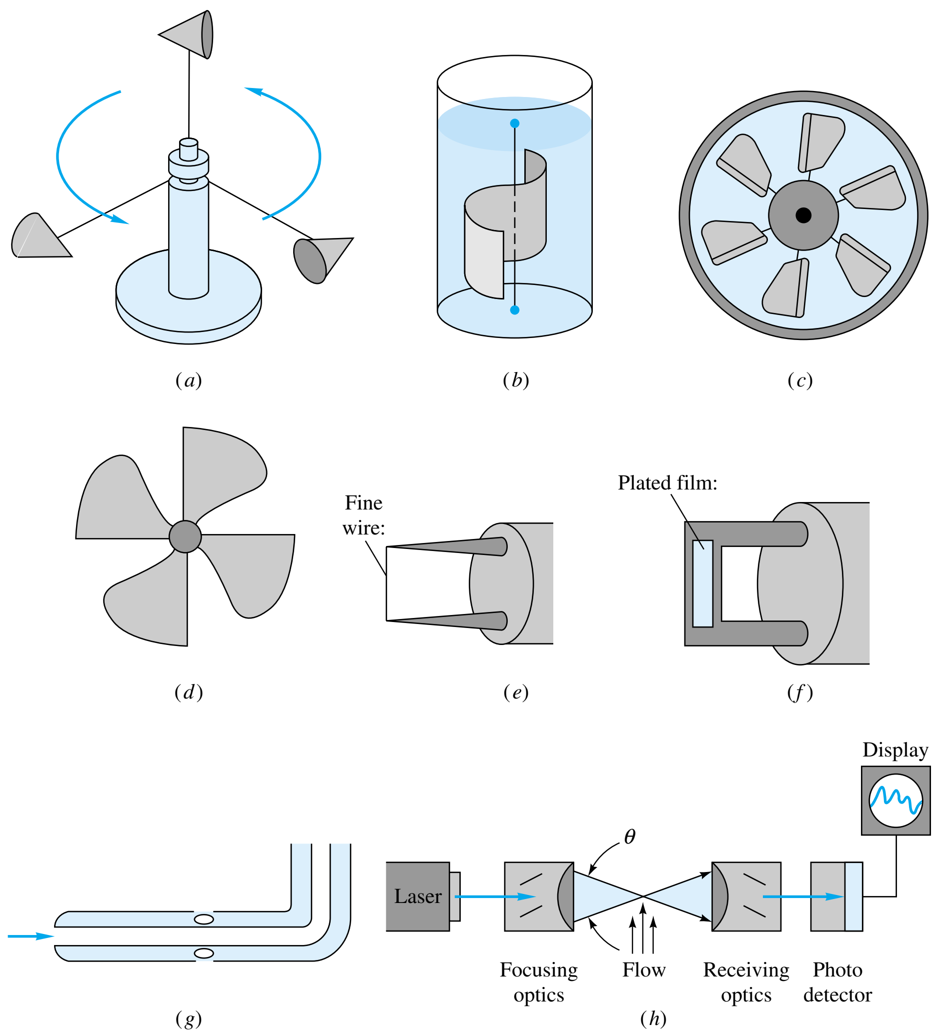

Fig. 6.29 Eight common velocity meters: (*a*) three-cup anemometer; (*b*) Savonius rotor; (*c*) turbine mounted in a duct; (*d*) free-propeller meter; (*e*) hot-wire anemometer; (*f*) hot-film anemometer; (*g*) pitot-static tube; (*h*) laser-doppler anemometer.

gen bubbles. Sometimes gas flows can be estimated from the motion of entrained dust particles. One must establish whether the particle motion truly simulates the fluid motion. Floats are commonly used to track the movement of ocean waters and can be designed to move at the surface, along the bottom, or at any given depth [24]. Many official tidal-current charts [25] were obtained by releasing and timing a floating spar attached to a length of string. One can release whole groups of spars to determine a flow pattern.

Rotating sensors. The rotating devices of Fig. 6.29*a* to *d* can be used in either gases or liquids, and their rotation rate is approximately proportional to the flow velocity. The cup anemometer (Fig. 6.29*a*) and Savonius rotor (Fig. 6.29*b*) always rotate the same way, regardless of flow direction. They are popular in atmospheric and oceanographic applications and can be fitted with a direction vane to align themselves with the flow. The ducted-propeller (Fig. 6.29*c*) and free-propeller (Fig. 6.29*d*) meters must be aligned with the flow parallel to their axis of rotation. They can sense reverse flow because they will then rotate in the opposite direction. All these rotating sensors can be attached to counters or sensed by electromagnetic or slip-ring devices for either a continuous or a digital reading of flow velocity. All have the disadvantage of being relatively large and thus not representing a "point."

Pitot-static tube. A slender tube aligned with the flow (Figs. 6.29*g* and 6.30) can measure local velocity by means of a pressure difference. It has sidewall holes to measure the static pressure p_s in the moving stream and a hole in the front to measure the *stagnation* pressure p_0, where the stream is decelerated to zero velocity. Instead of measuring p_0 or p_s separately, it is customary to measure their difference with, say, a transducer, as in Fig. 6.30.

If $Re_D > 1000$, where D is the probe diameter, the flow around the probe is nearly frictionless and Bernoulli's relation, Eq. (3.77), applies with good accuracy. For incompressible flow

$$p_s + \tfrac{1}{2}\rho V^2 + \rho g z_s \approx p_0 + \tfrac{1}{2}\rho(0)^2 + \rho g z_0$$

Assuming that the elevation pressure difference $\rho g(z_s - z_0)$ is negligible, this reduces to

$$V \approx \left[2\frac{(p_0 - p_s)}{\rho}\right]^{1/2} \tag{6.117}$$

This is the *Pitot formula,* named after the French engineer who designed the device in 1732.

The primary disadvantage of the pitot tube is that it must be aligned with the flow direction, which may be unknown. For yaw angles greater than 5°, there are substantial errors in both the p_0 and p_s measurements, as shown in Fig. 6.30. The pitot-static tube is useful in liquids and gases; for gases a compressibility correction is necessary if the stream Mach number is high (Chap. 9). Because of the slow response of the fluid-filled tubes leading to the pressure sensors, it is not useful for unsteady-flow measurements. It does resemble a point and can be made small enough to measure, e.g.,

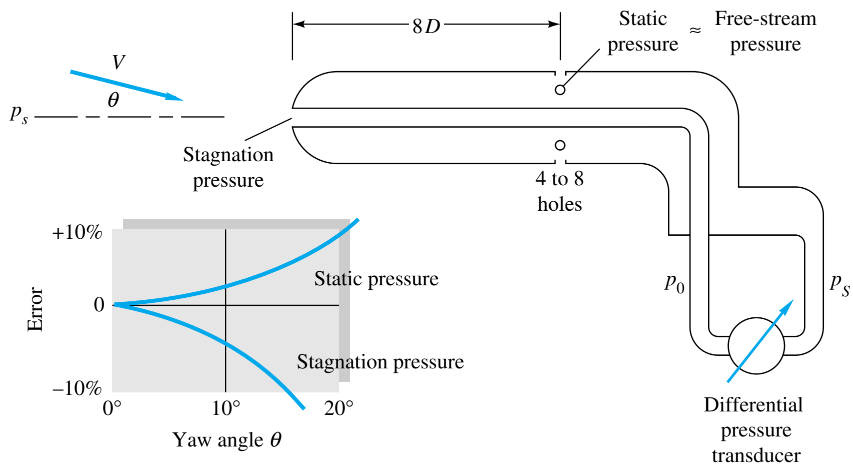

Fig. 6.30 Pitot-static tube for combined measurement of static and stagnation pressure in a moving stream.

blood flow in arteries and veins. It is not suitable for low-velocity measurement in gases because of the small pressure differences developed. For example, if $V = 1$ ft/s in standard air, from Eq. (6.117) we compute $p_0 - p$ equal to only 0.001 lbf/ft^2 (0.048 Pa). This is beyond the resolution of most pressure gages.

Electromagnetic meter. If a magnetic field is applied across a conducting fluid, the fluid motion will induce a voltage across two electrodes placed in or near the flow. The electrodes can be streamlined or built into the wall, and they cause little or no flow resistance. The output is very strong for highly conducting fluids such as liquid metals. Seawater also gives good output, and electromagnetic current meters are in common use in oceanography. Even low-conductivity fresh water can be measured by amplifying the output and insulating the electrodes. Commercial instruments are available for most liquid flows but are relatively costly. Electromagnetic flowmeters are treated in Ref. 26.

Hot-wire anemometer. A very fine wire ($d = 0.01$ mm or less) heated between two small probes, as in Fig. 6.29*e*, is ideally suited to measure rapidly fluctuating flows such as the turbulent boundary layer. The idea dates back to work by L. V. King in 1914 on heat loss from long thin cylinders. If electric power is supplied to heat the cylinder, the loss varies with flow velocity across the cylinder according to *King's law*

$$q = I^2R \approx a + b(\rho V)^n \tag{6.118}$$

where $n \approx \frac{1}{3}$ at very low Reynolds numbers and equals $\frac{1}{2}$ at high Reynolds numbers. The hot wire normally operates in the high-Reynolds-number range but should be calibrated in each situation to find the best-fit a, b, and n. The wire can be operated either at constant current I, so that resistance R is a measure of V, or at constant resistance R (constant temperature), with I a measure of velocity. In either case, the output is a nonlinear function of V, and the equipment should contain a *linearizer* to produce convenient velocity data. Many varieties of commercial hot-wire equipment are available, as are do-it-yourself designs [27]. Excellent detailed discussions of the hot wire are given in Refs. 1 and 28.

Because of its frailty, the hot wire is not suited to liquid flows, whose high density and entrained sediment will knock the wire right off. A more stable yet quite sensitive alternative for liquid-flow measurement is the hot-film anemometer (Fig. 6.29*f*). A thin metallic film, usually platinum, is plated onto a relatively thick support which can be a wedge, a cone, or a cylinder. The operation is similar to the hot wire. The cone gives best response but is liable to error when the flow is yawed to its axis.

Hot wires can easily be arranged in groups to measure two- and three-dimensional velocity components.

Laser-doppler anemometer. In the LDA a laser beam provides highly focused, coherent monochromatic light which is passed through the flow. When this light is scattered from a moving particle in the flow, a stationary observer can detect a change, or *doppler shift*, in the frequency of the scattered light. The shift Δf is proportional to the velocity of the particle. There is essentially zero disturbance of the flow by the laser.

Figure 6.29*h* shows the popular dual-beam mode of the LDA. A focusing device splits the laser into two beams, which cross the flow at an angle θ. Their intersection, which is the measuring volume or resolution of the measurement, resembles an ellipsoid about 0.5 mm wide and 0.1 mm in diameter. Particles passing through this measuring volume scatter the beams; they then pass through receiving optics to a photodetector which converts the light to an electric signal. A signal processor then converts electric frequency to a voltage which can be either displayed or stored. If λ is the wavelength of the laser light, the measured velocity is given by

$$V = \frac{\lambda\,\Delta f}{2\sin(\theta/2)} \tag{6.119}$$

Multiple components of velocity can be detected by using more than one photodetector and other operating modes. Either liquids or gases can be measured as long as scattering particles are present. In liquids, normal impurities serve as scatterers, but gases may have to be seeded. The particles may be as small as the wavelength of the light. Although the measuring volume is not as small as with a hot wire, the LDA is capable of measuring turbulent fluctuations.

The advantages of the LDA are as follows:

1. No disturbance of the flow
2. High spatial resolution of the flow field
3. Velocity data that are independent of the fluid thermodynamic properties
4. An output voltage that is linear with velocity
5. No need for calibration

The disadvantages are that both the apparatus and the fluid must be transparent to light and that the cost is high (a basic system shown in Fig. 6.29*h* begins at about $50,000).

Once installed, an LDA can map the entire flow field in minutest detail. To truly appreciate the power of the LDA, one should examine, e.g., the amazingly detailed three-dimensional flow profiles measured by Eckardt [29] in a high-speed centrifugal compressor impeller. Extensive discussions of laser velocimetry are given in Refs. 38 and 39.

EXAMPLE 6.20

The pitot-static tube of Fig. 6.30 uses mercury as a manometer fluid. When it is placed in a water flow, the manometer height reading is $h = 8.4$ in. Neglecting yaw and other errors, what is the flow velocity V in ft/s?

Solution

From the two-fluid manometer relation (2.33), with $z_A = z_2$, the pressure difference is related to h by

$$p_0 - p_s = (\gamma_M - \gamma_w)h$$

Taking the specific weights of mercury and water from Table 2.1, we have

$$p_0 - p_s = (846 - 62.4\ \text{lbf/ft}^3)\,\frac{8.4}{12}\ \text{ft} = 549\ \text{lbf/ft}^2$$

The density of water is $62.4/32.2 = 1.94$ slugs/ft^3. Introducing these values into the pitot-static formula (6.117), we obtain

$$V = \left[\frac{2(549\ \text{lbf/ft}^2)}{1.94\ \text{slugs/ft}^3}\right]^{1/2} = 23.8\ \text{ft/s} \qquad \textit{Ans.}$$

Since this is a low-speed flow, no compressibility correction is needed.

Volume-Flow Measurements

It is often desirable to measure the integrated mass, or volume flow, passing through a duct. Accurate measurement of flow is vital in billing customers for a given amount of liquid or gas passing through a duct. The different devices available to make these measurements are discussed in great detail in the ASME text on fluid meters [30]. These devices split into two classes: mechanical instruments and head-loss instruments.

The mechanical instruments measure actual mass or volume of fluid by trapping it and counting it. The various types of measurement are

1. Mass measurement
   a. Weighing tanks
   b. Tilting traps
2. Volume measurement
   a. Volume tanks
   b. Reciprocating pistons
   c. Rotating slotted rings
   d. Nutating disk
   e. Sliding vanes
   f. Gear or lobed impellers
   g. Reciprocating bellows
   h. Sealed-drum compartments

The last three of these are suitable for gas flow measurement.

The head-loss devices obstruct the flow and cause a pressure drop which is a measure of flux:

1. Bernoulli-type devices
   a. Thin-plate orifice
   b. Flow nozzle
   c. Venturi tube
2. Friction-loss devices
   a. Capillary tube
   b. Porous plug

The friction-loss meters cause a large nonrecoverable head loss and obstruct the flow too much to be generally useful.

Six other widely used meters operate on different physical principles:

1. Turbine meter
2. Vortex meter
3. Ultrasonic flowmeter
4. Rotameter
5. Coriolis mass flowmeter
6. Laminar flow element

Turbine meter. The turbine meter, sometimes called a *propeller meter*, is a freely rotating propeller which can be installed in a pipeline. A typical design is shown in Fig. 6.31*a*. There are flow straighteners upstream of the rotor, and the rotation is measured by electric or magnetic pickup of pulses caused by passage of a point on the rotor. The rotor rotation is approximately proportional to the volume flow in the pipe.

A major advantage of the turbine meter is that each pulse corresponds to a finite incremental volume of fluid, and the pulses are digital and can be summed easily. Liquid-flow turbine meters have as few as two blades and produce a constant number of pulses per unit fluid volume over a 5:1 flow-rate range with ± 0.25 percent accuracy. Gas meters need many blades to produce sufficient torque and are accurate to ± 1 percent.

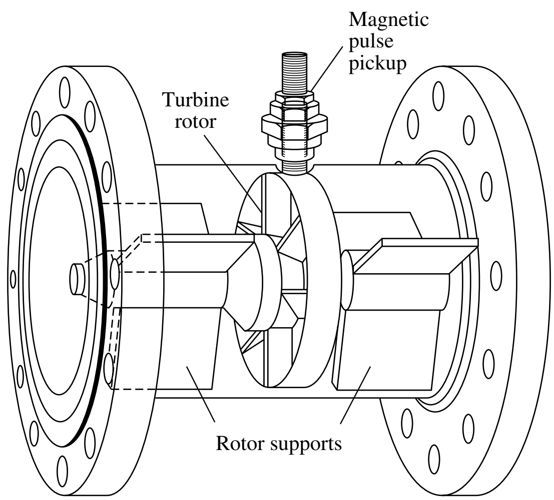

(*a*)

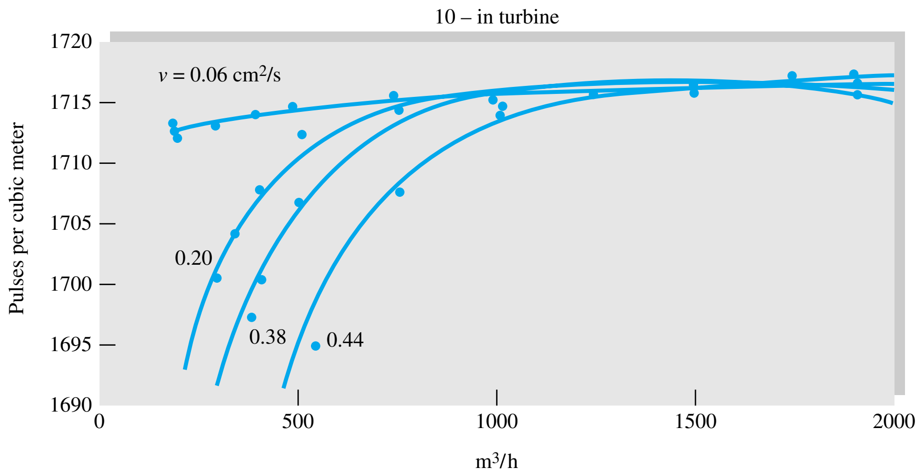

(*b*)

Fig. 6.31 The turbine meter widely used in the oil, gas, and water supply industries: (*a*) basic design; (*b*) typical calibration curve for a range of crude oils. *(Daniel Industries, Inc., Flow Products Division.)*

Fig. 6.32 A Commercial handheld wind-velocity turbine meter. *(Courtesy of Nielsen-Kellerman Company.)*

Since turbine meters are very individualistic, flow calibration is an absolute necessity. A typical liquid-meter calibration curve is shown in Fig. 6.31*b*. Researchers attempting to establish universal calibration curves have met with little practical success as a result of manufacturing variabilities.

Turbine meters can also be used in unconfined flow situations, such as winds or ocean currents. They can be compact, even microsize with two or three component directions. Figure 6.32 illustrates a handheld wind velocity meter which uses a seven-bladed turbine with a calibrated digital output. The accuracy of this device is quoted at $\pm$ 2 percent.

Vortex flowmeters. Recall from Fig. 5.2 that a bluff body placed in a uniform cross-flow sheds alternating vortices at a nearly uniform Strouhal number St $= fL/U$, where U is the approach velocity and L is a characteristic body width. Since L and St are constant, this means that the shedding frequency is proportional to velocity

$$f = (\text{const})(U) \tag{6.120}$$

The vortex meter introduces a shedding element across a pipe flow and picks up the shedding frequency downstream with a pressure, ultrasonic, or heat-transfer type of sensor. A typical design is shown in Fig. 6.33.

The advantages of a vortex meter are as follows:

1. Absence of moving parts
2. Accuracy to $\pm$ 1 percent over a wide flow-rate range (up to 100 : 1)
3. Ability to handle very hot or very cold fluids
4. Requirement of only a short pipe length
5. Calibration insensitive to fluid density or viscosity

For further details see Ref. 40.

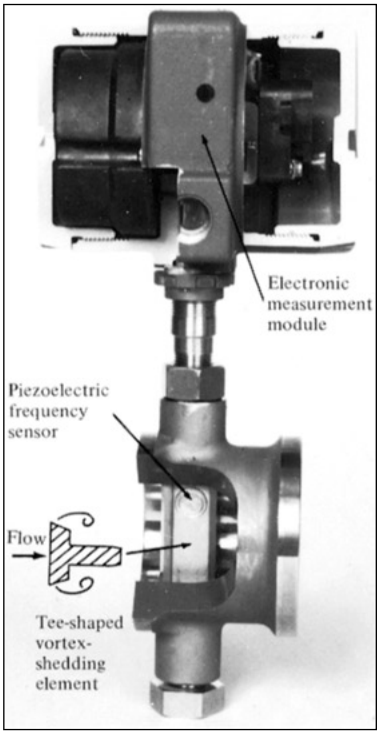

Fig. 6.33 A vortex flowmeter. *(The Foxboro Company.)*

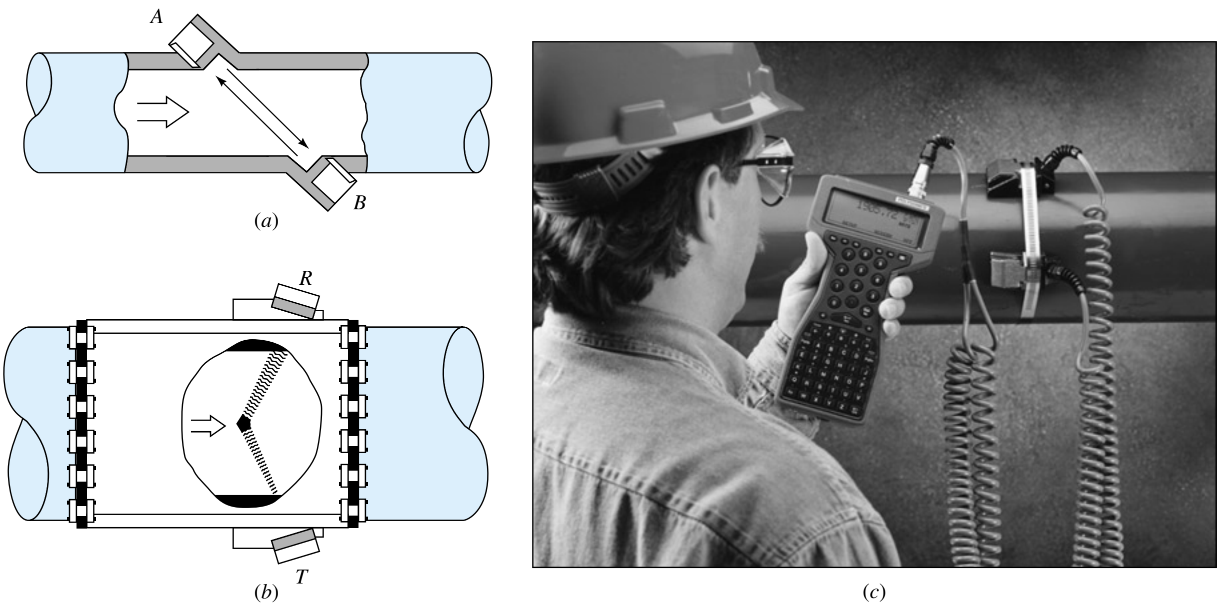

Fig. 6.34 Ultrasonic flowmeters: (*a*) pulse type; (*b*) doppler-shift type *(from Ref. 41)*; (*c*) a portable noninvasive installation *(courtesy of Polysonics Inc., Houston, TX)*.

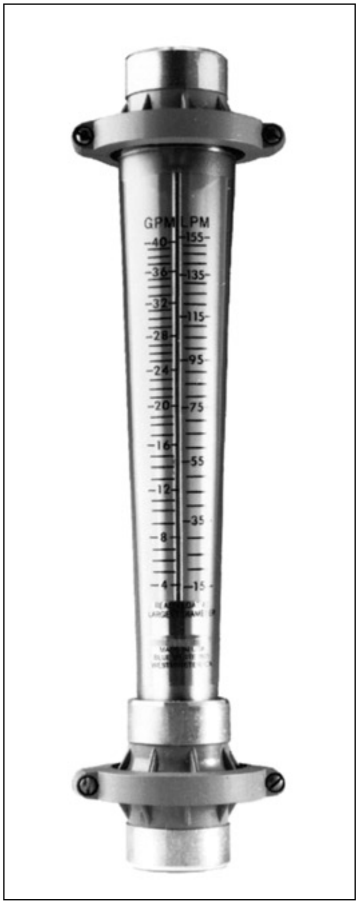

Fig. 6.35 A commercial rotameter. The float rises in the tapered tube to an equilibrium position which is a measure of the fluid-flow rate. *(Courtesy of Blue White Industries, Westminster, CA.)*

Ultrasonic flowmeters. The sound-wave analog of the laser velocimeter of Fig. 6.29*h* is the ultrasonic flowmeter. Two examples are shown in Fig. 6.34. The pulse-type flowmeter is shown in Fig. 6.34*a*. Upstream piezoelectric transducer *A* is excited with a short sonic pulse which propagates across the flow to downstream transducer *B*. The arrival at *B* triggers another pulse to be created at *A*, resulting in a regular pulse frequency f_A. The same process is duplicated in the reverse direction from *B* to *A*, creating frequency f_B. The difference $f_A - f_B$ is proportional to the flow rate. Figure 6.33*b* shows a doppler-type arrangement, where sound waves from transmitter *T* are scattered by particles or contaminants in the flow to receiver *R*. Comparison of the two signals reveals a doppler frequency shift which is proportional to the flow rate. Ultrasonic meters are nonintrusive and can be directly attached to pipe flows in the field (Fig. 6.34*c*). Their quoted uncertainty of $\pm$ 1 to 2 percent can rise to $\pm$ 5 percent or more due to irregularities in velocity profile, fluid temperature, or Reynolds number. For further details see Ref. 41.

Rotameter. The variable-area transparent *rotameter* of Fig. 6.35 has a float which, under the action of flow, rises in the vertical tapered tube and takes a certain equilibrium position for any given flow rate. A student exercise for the forces on the float would yield the approximate relation

$$Q = C_d A_a \left(\frac{2W_{\text{net}}}{A_{\text{float}} \rho_{\text{fluid}}} \right)^{1/2} \qquad (6.121)$$

where W_{net} is the float's net weight in the fluid, $A_a = A_{\text{tube}} - A_{\text{float}}$ is the annular area between the float and the tube, and C_d is a dimensionless discharge coefficient of order unity, for the annular constricted flow. For slightly tapered tubes, A_a varies nearly linearly with the float position, and the tube may be calibrated and marked with a flow-rate scale, as in Fig. 6.35. The rotameter thus provides a readily visible measure of the flow rate. Capacity may be changed by using different-sized floats. Obviously the tube must be vertical, and the device does not give accurate readings for fluids containing high concentrations of bubbles or particles.

Coriolis mass flowmeter. Most commercial meters measure *volume* flow, with mass flow then computed by multiplying by the nominal fluid density. An attractive modern alternative is a *mass* flowmeter which operates on the principle of the Coriolis acceleration associated with noninertial coordinates [recall Fig. 3.12 and the Coriolis term $2\Omega \times V$ in Eq. (3.48)]. The output of the meter is directly proportional to mass flow.

Figure 6.36 is a schematic of a Coriolis device, to be inserted into a piping system. The flow enters a double-loop, double-tube arrangement which is electromagnetically vibrated at a high natural frequency (amplitude $<$ 1 mm and frequency $>$ 100 Hz). The up flow induces inward loop motion, while the down flow creates outward loop motion, both due to the Coriolis effect. Sensors at both ends register a phase difference which is proportional to mass flow. Quoted accuracy is approximately $\pm$ 0.2 percent of full scale.

Laminar flow element. In many, perhaps most, commercial flowmeters, the flow through the meter is turbulent and the variation of flow rate with pressure drop is nonlinear. In laminar duct flow, however, Q is linearly proportional to Δp, as in Eq. (6.44): $Q = [\pi R^4/(8\mu L)]\,\Delta p$. Thus a *laminar* flow sensing element is attractive, since its calibration will be linear. To ensure laminar flow for what otherwise would be a turbu-

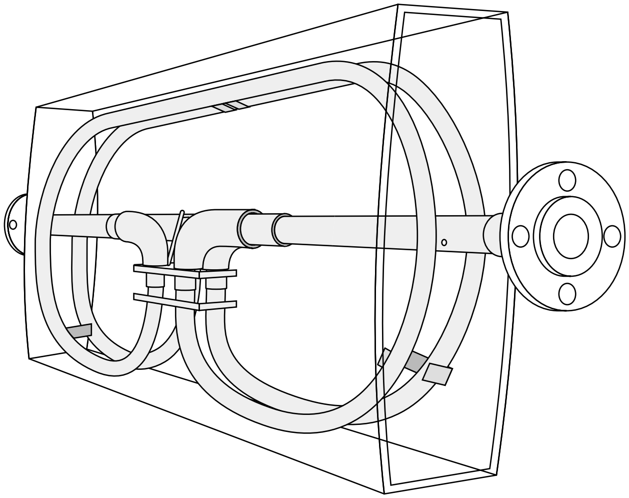

Fig. 6.36 A Coriolis mass flowmeter. *(Courtesy of ABB Instrumentation, Inc.)*

lent condition, all or part of the fluid is directed into small passages, each of which has a low (laminar) Reynolds number. A honeycomb is a popular design.

Figure 6.37 uses axial flow through a narrow annulus to effect laminar flow. The theory again predicts $Q \propto \Delta p$, as in Eq. (6.92). However, the flow is very sensitive to passage size; for example, halving the annulus clearance increases Δp more than eight

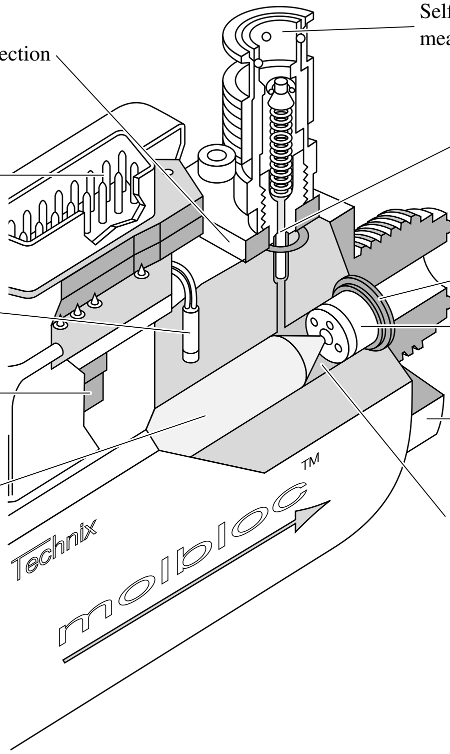

Fig. 6.37 A complete flowmeter system using a laminar-flow element (in this case a narrow annulus). The flow rate is linearly proportional to the pressure drop. *(Courtesy of Martin Girard, DH Instruments, Inc.)*

times. Careful calibration is thus necessary. In Fig. 6.37 the laminar-flow concept has been synthesized into a complete mass-flow system, with temperature control, differential pressure measurement, and a microprocessor all self-contained. The accuracy of this device is rated at $\pm$ 0.2 percent.

Bernoulli obstruction theory. Consider the generalized flow obstruction shown in Fig. 6.38. The flow in the basic duct of diameter D is forced through an obstruction of diameter d; the β ratio of the device is a key parameter

$$\beta = \frac{d}{D} \tag{6.122}$$

After leaving the obstruction, the flow may neck down even more through a vena contracta of diameter $D_2 < d$, as shown. Apply the Bernoulli and continuity equations for incompressible steady frictionless flow to estimate the pressure change:

Continuity: $$Q = \frac{\pi}{4}D^2V_1 = \frac{\pi}{4}D_2^2V_2$$

Bernoulli: $$p_0 = p_1 + \tfrac{1}{2}\rho V_1^2 = p_2 + \tfrac{1}{2}\rho V_2^2$$

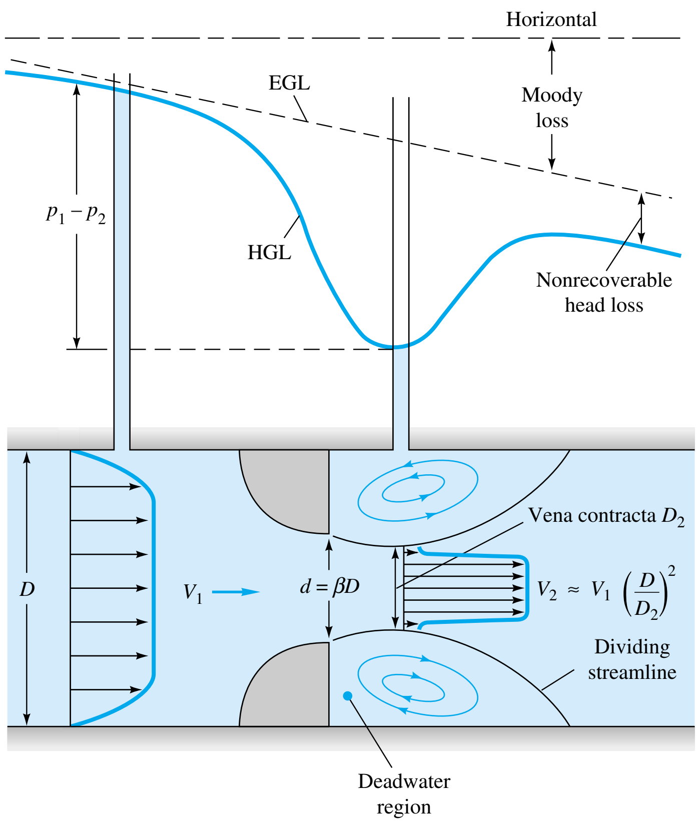

Fig. 6.38 Velocity and pressure change through a generalized Bernoulli obstruction meter.

Eliminating V_1, we solve these for V_2 or Q in terms of the pressure change $p_1 - p_2$:

$$\frac{Q}{A_2} = V_2 \approx \left[\frac{2(p_1 - p_2)}{\rho(1 - D_2^4/D^4)}\right]^{1/2} \tag{6.123}$$

But this is surely inaccurate because we have neglected friction in a duct flow, where we know friction will be very important. Nor do we want to get into the business of measuring vena contracta ratios D_2/d for use in (6.123). Therefore we assume that $D_2/D \approx \beta$ and then calibrate the device to fit the relation

$$Q = A_t V_t = C_d A_t \left[\frac{2(p_1 - p_2)/\rho}{1 - \beta^4}\right]^{1/2} \tag{6.124}$$

where subscript t denotes the throat of the obstruction. The dimensionless *discharge coefficient* C_d accounts for the discrepancies in the approximate analysis. By dimensional analysis for a given design we expect

$$C_d = f(\beta, \mathrm{Re}_D) \quad \text{where} \quad \mathrm{Re}_D = \frac{V_1 D}{\nu} \tag{6.125}$$

The geometric factor involving β in (6.124) is called the *velocity-of-approach factor*

$$E = (1 - \beta^4)^{-1/2} \tag{6.126}$$

One can also group C_d and E in Eq. (6.124) to form the dimensionless *flow coefficient* α

$$\alpha = C_d E = \frac{C_d}{(1 - \beta^4)^{1/2}} \tag{6.127}$$

Thus Eq. (6.124) can be written in the equivalent form

$$Q = \alpha A_t \left[\frac{2(p_1 - p_2)}{\rho}\right]^{1/2} \tag{6.128}$$

Obviously the flow coefficient is correlated in the same manner:

$$\alpha = f(\beta, \mathrm{Re}_D) \tag{6.129}$$

Occasionally one uses the throat Reynolds number instead of the approach Reynolds number

$$\mathrm{Re}_d = \frac{V_t d}{\nu} = \frac{\mathrm{Re}_D}{\beta} \tag{6.130}$$

Since the design parameters are assumed known, the correlation of α from Eq. (6.129) or of C_d from Eq. (6.125) is the desired solution to the fluid-metering problem.

The mass flow is related to Q by

$$\dot{m} = \rho Q \tag{6.131}$$

and is thus correlated by exactly the same formulas.

Figure 6.39 shows the three basic devices recommended for use by the International Organization for Standardization (ISO) [31]: the orifice, nozzle, and venturi tube.

Thin-plate orifice. The thin-plate orifice, Fig. 6.39*b*, can be made with β in the range of 0.2 to 0.8, except that the hole diameter d should not be less than 12.5 mm. To measure p_1 and p_2, three types of tappings are commonly used:

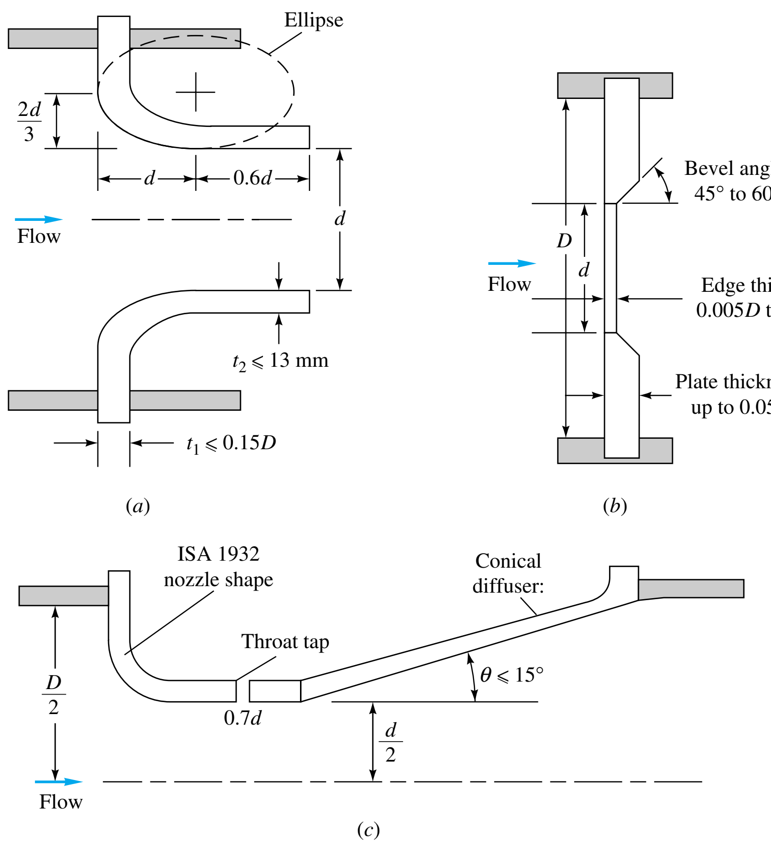

Fig. 6.39 International standard shapes for the three primary Bernoulli obstruction-type meters: (*a*) long radius nozzle; (*b*) thin-plate orifice; (*c*) venturi nozzle. *(From Ref. 31 by permission of the International Organization for Standardization.)*

1. Corner taps where the plate meets the pipe wall
2. D: $\frac{1}{2}D$ taps: pipe-wall taps at D upstream and $\frac{1}{2}D$ downstream
3. Flange taps: 1 in (25 mm) upstream and 1 in (25 mm) downstream of the plate, regardless of the size D

Types 1 and 2 approximate geometric similarity, but since the flange taps 3 do not, they must be correlated separately for every single size of pipe in which a flange-tap plate is used [30, 31].

Figure 6.40 shows the discharge coefficient of an orifice with D: $\frac{1}{2}D$ or type 2 taps in the Reynolds-number range $\mathrm{Re}_D = 10^4$ to 10^7 of normal use. Although detailed charts such as Fig. 6.37 are available for designers [30], the ASME recommends use of the curve-fit formulas developed by the ISO [31]. The basic form of the curve fit is [42]

$$C_d = f(\beta) + 91.71\beta^{2.5}\mathrm{Re}_D^{-0.75} + \frac{0.09\beta^4}{1-\beta^4}F_1 - 0.0337\beta^3 F_2 \qquad (6.132)$$

where $$f(\beta) = 0.5959 + 0.0312\beta^{2.1} - 0.184\beta^8$$

The correlation factors F_1 and F_2 vary with tap position:

Corner taps: $$F_1 = 0 \qquad F_2 = 0 \qquad (6.133a)$$

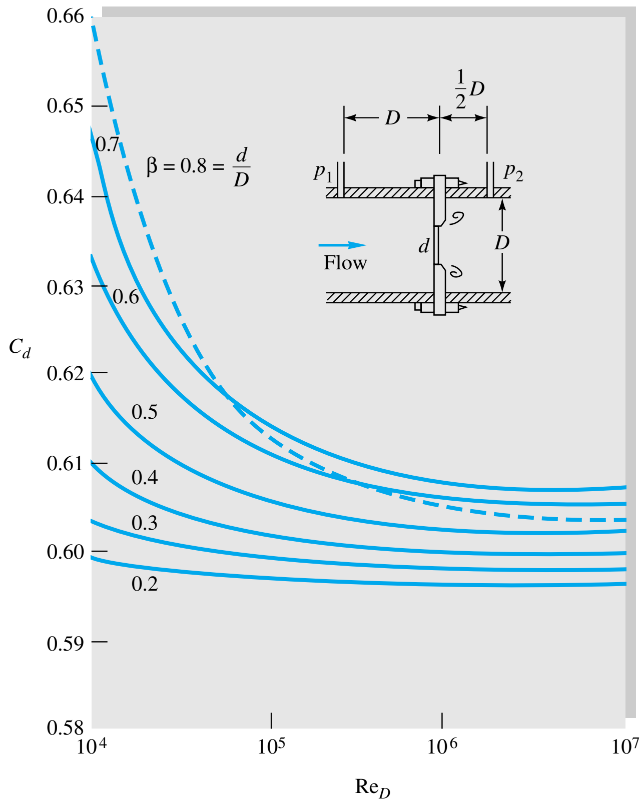

Fig. 6.40 Discharge coefficient for a thin-plate orifice with D: $\frac{1}{2}D$ taps, plotted from Eqs. (6.132) and (6.133b).

$$D\text{: } \tfrac{1}{2}D \text{ taps:} \qquad F_1 = 0.4333 \qquad F_2 = 0.47 \tag{6.133b}$$

$$\text{Flange taps:} \qquad F_2 = \frac{1}{D\ (\text{in})} \qquad F_1 = \begin{cases} \dfrac{1}{D\ (\text{in})} & D > 2.3 \text{ in} \\ 0.4333 & 2.0 \le D \le 2.3 \text{ in} \end{cases} \tag{6.133c}$$

Note that the flange taps (6.133c), not being geometrically similar, use raw diameter in inches in the formula. The constants will change if other diameter units are used. We cautioned against such dimensional formulas in Example 1.4 and Eq. (5.17) and give Eq. (6.133c) only because flange taps are widely used in the United States.

Flow nozzle. The flow nozzle comes in two types, a long-radius type shown in Fig. 6.39a and a short-radius type (not shown) called the ISA 1932 nozzle [30, 31]. The flow nozzle, with its smooth rounded entrance convergence, practically eliminates the vena contracta and gives discharge coefficients near unity. The nonrecoverable loss is still large because there is no diffuser provided for gradual expansion.

The ISO recommended correlation for long-radius-nozzle discharge coefficient is

$$C_d \approx 0.9965 - 0.00653\beta^{1/2}\left(\frac{10^6}{\mathrm{Re}_D}\right)^{1/2} = 0.9965 - 0.00653\left(\frac{10^6}{\mathrm{Re}_d}\right)^{1/2} \tag{6.134}$$

The second form is independent of the β ratio and is plotted in Fig. 6.41. A similar ISO correlation is recommended for the short-radius ISA 1932 flow nozzle

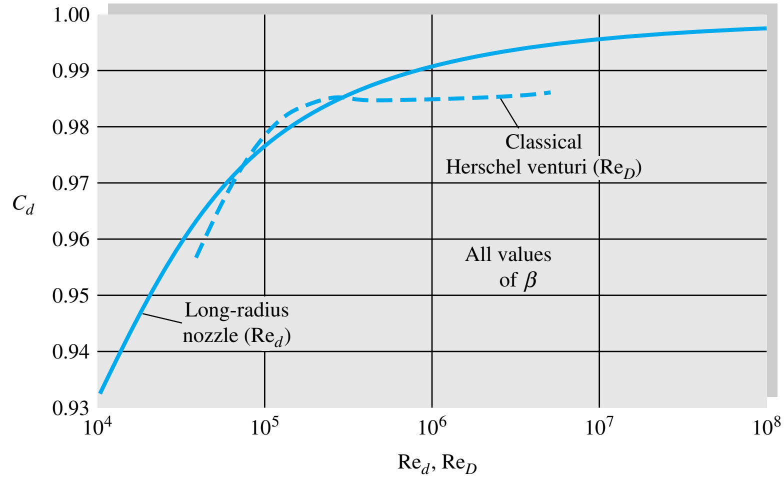

Fig. 6.41 Discharge coefficient for long-radius nozzle and classical Herschel-type venturi.

$$C_d \approx 0.9900 - 0.2262\beta^{4.1} + (0.000215 - 0.001125\beta + 0.00249\beta^{4.7})\left(\frac{10^6}{\mathrm{Re}_D}\right)^{1.15} \qquad (6.135)$$

Flow nozzles may have β values between 0.2 and 0.8.

Venturi meter. The third and final type of obstruction meter is the venturi, named in honor of Giovanni Venturi (1746–1822), an Italian physicist who first tested conical expansions and contractions. The original, or *classical*, venturi was invented by a U.S. engineer, Clemens Herschel, in 1898. It consisted of a 21° conical contraction, a straight throat of diameter d and length d, then a 7 to 15° conical expansion. The discharge coefficient is near unity, and the nonrecoverable loss is very small. Herschel venturis are seldom used now.

The modern venturi nozzle, Fig. 6.39*c*, consists of an ISA 1932 nozzle entrance and a conical expansion of half-angle no greater than 15°. It is intended to be operated in a narrow Reynolds-number range of 1.5×10^5 to 2×10^6. Its discharge coefficient, shown in Fig. 6.42, is given by the ISO correlation formula

$$C_d \approx 0.9858 - 0.196\beta^{4.5} \qquad (6.136)$$

It is independent of Re_D within the given range. The Herschel venturi discharge varies with Re_D but not with β, as shown in Fig. 6.41. Both have very low net losses.

The choice of meter depends upon the loss and the cost and can be illustrated by the following table:

Type of meter	Net head loss	Cost
Orifice	Large	Small
Nozzle	Medium	Medium
Venturi	Small	Large

As so often happens, the product of inefficiency and initial cost is approximately constant.

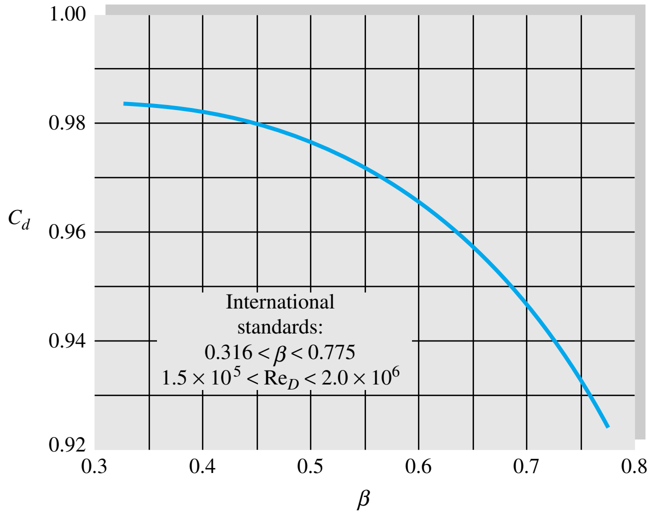

Fig. 6.42 Discharge coefficient for a venturi nozzle.

The average nonrecoverable head losses for the three types of meters, expressed as a fraction of the throat velocity head $V_t^2/(2g)$, are shown in Fig. 6.43. The orifice has the greatest loss and the venturi the least, as discussed. The orifice and nozzle simulate partially closed valves as in Fig. 6.18*b*, while the venturi is a very minor loss. When the loss is given as a fraction of the measured *pressure drop,* the orifice and nozzle have nearly equal losses, as Example 6.21 will illustrate.

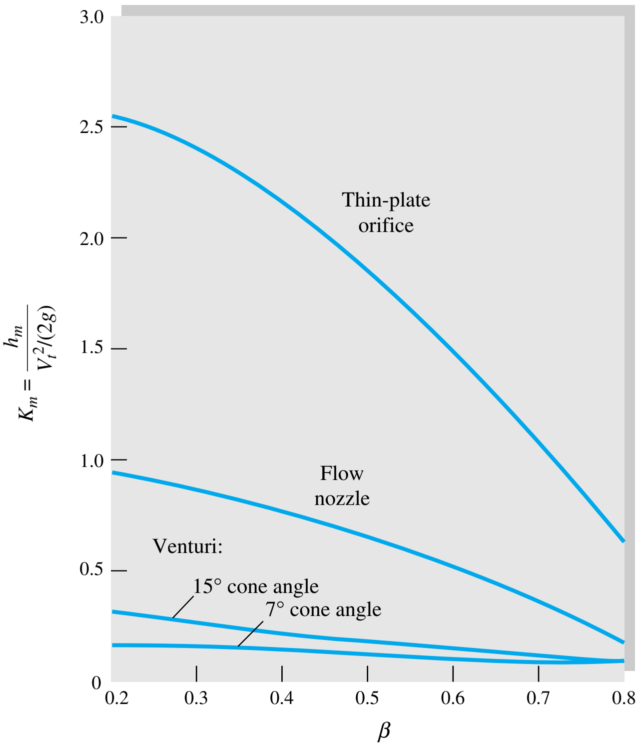

Fig. 6.43 Nonrecoverable head loss in Bernoulli obstruction meters. *(Adapted from Ref. 30.)*

The other types of instruments discussed earlier in this section can also serve as flowmeters if properly constructed. For example, a hot wire mounted in a tube can be calibrated to read volume flow rather than point velocity. Such hot-wire meters are commercially available, as are other meters modified to use velocity instruments. For further details see Ref. 30.

EXAMPLE 6.21

We want to meter the volume flow of water ($\rho = 1000$ kg/m^3, $\nu = 1.02 \times 10^{-6}$ m^2/s) moving through a 200-mm-diameter pipe at an average velocity of 2.0 m/s. If the differential pressure gage selected reads accurately at $p_1 - p_2 = 50{,}000$ Pa, what size meter should be selected for installing (*a*) an orifice with D: $\frac{1}{2}D$ taps, (*b*) a long-radius flow nozzle, or (*c*) a venturi nozzle? What would be the nonrecoverable head loss for each design?

Solution

Here the unknown is the β ratio of the meter. Since the discharge coefficient is a complicated function of β, iteration will be necessary. We are given $D = 0.2$ m and $V_1 = 2.0$ m/s. The pipe-approach Reynolds number is thus

$$\text{Re}_D = \frac{V_1 D}{\nu} = \frac{(2.0)(0.2)}{1.02 \times 10^{-6}} = 392{,}000$$

For all three cases [(*a*) to (*c*)] the generalized formula (6.128) holds:

$$V_t = \frac{V_1}{\beta^2} = \alpha\left[\frac{2(p_1 - p_2)}{\rho}\right]^{1/2} \qquad \alpha = \frac{C_d}{(1 - \beta^4)^{1/2}} \tag{1}$$

where the given data are $V_1 = 2.0$ m/s, $\rho = 1000$ kg/m^3, and $\Delta p = 50{,}000$ Pa. Inserting these known values into Eq. (1) gives a relation between β and α:

$$\frac{2.0}{\beta^2} = \alpha\left[\frac{2(50{,}000)}{1000}\right]^{1/2} \qquad \text{or} \qquad \beta^2 = \frac{0.2}{\alpha} \tag{2}$$

The unknowns are β (or α) and C_d. Parts (*a*) to (*c*) depend upon the particular chart or formula needed for $C_d = \text{fcn}(\text{Re}_D, \beta)$. We can make an initial guess $\beta \approx 0.5$ and iterate to convergence.

Part (a) For the orifice with D: $\frac{1}{2}D$ taps, use Eq. (6.132) or Fig. 6.40. The iterative sequence is

$$\beta_1 \approx 0.5,\ C_{d1} \approx 0.604,\ \alpha_1 \approx 0.624,\ \beta_2 \approx 0.566,\ C_{d2} \approx 0.606,\ \alpha_2 \approx 0.640,\ \beta_3 = \mathbf{0.559}$$

We have converged to three figures. The proper orifice diameter is

$$d = \beta D = \mathbf{112\ mm} \qquad \textit{Ans. (a)}$$

Part (b) For the long-radius flow nozzle, use Eq. (6.134) or Fig. 6.41. The iterative sequence is

$$\beta_1 \approx 0.5,\ C_{d1} \approx 0.9891,\ \alpha_1 \approx 1.022,\ \beta_2 \approx 0.442,\ C_{d2} \approx 0.9896,\ \alpha_2 \approx 1.009,\ \beta_3 = \mathbf{0.445}$$

We have converged to three figures. The proper nozzle diameter is

$$d = \beta D = \mathbf{89\ mm} \qquad \textit{Ans. (b)}$$

Part (c) For the venturi nozzle, use Eq. (6.136) or Fig. 6.42. The iterative sequence is

$$\beta_1 \approx 0.5,\ C_{d1} \approx 0.977,\ \alpha_1 \approx 1.009,\ \beta_2 \approx 0.445,\ C_{d2} \approx 0.9807,\ \alpha_2 \approx 1.0004,\ \beta_3 = \mathbf{0.447}$$

We have converged to three figures. The proper venturi diameter is

$$d = \beta D = \mathbf{89\ mm} \qquad \textit{Ans. (c)}$$

These meters are of similar size, but their head losses are not the same. From Fig. 6.43 for the three different shapes we may read the three K factors and compute

$$h_{m,\text{orifice}} \approx 3.5\text{ m} \qquad h_{m,\text{nozzle}} \approx 3.6\text{ m} \qquad h_{m,\text{venturi}} \approx 0.8\text{ m}$$

The venturi loss is only about 22 percent of the orifice and nozzle losses.

Solution

The iteration encountered in this example is ideal for the EES. Input the data in SI units:

```
Rho = 1000    Nu = 1.02E-6    D = 0.2    V = 2.0    DeltaP = 50000
```

Then write out the basic formulas for Reynolds number, throat velocity and flow coefficient:

```
Re = V*D/Nu
Vt = V/Beta^2
Alpha = Cd/(1-Beta^4)^0.5
Vt = Alpha*SQRT(2*DeltaP/Rho)
```

Finally, input the proper formula for the discharge coefficient. For example, for the flow nozzle,

```
Cd = 0.9965 – 0.00653*Beta^0.5*(1E6/Re)^0.5
```

When asked to Solve the equation, EES at first complains of dividing by zero. One must then tighten up the Variable Information by not allowing β, α, or C_d to be negative and, in particular, by confining β to its practical range $0.2 < \beta < 0.9$. EES then readily announces correct answers for the flow nozzle:

```
Alpha = 1.0096    Cd = 0.9895    Beta = 0.4451
```

Summary

This chapter is concerned with internal pipe and duct flows, which are probably the most common problems encountered in engineering fluid mechanics. Such flows are very sensitive to the Reynolds number and change from laminar to transitional to turbulent flow as the Reynolds number increases.

The various Reynolds-number regimes are outlined, and a semiempirical approach to turbulent-flow modeling is presented. The chapter then makes a detailed analysis of flow through a straight circular pipe, leading to the famous Moody chart (Fig. 6.13) for the friction factor. Possible uses of the Moody chart are discussed for flow-rate and sizing problems, as well as the application of the Moody chart to noncircular ducts using an equivalent duct "diameter." The addition of minor losses due to valves, elbows, fittings, and other devices is presented in the form of loss coefficients to be incorporated along with Moody-type friction losses. Multiple-pipe systems are discussed briefly and are seen to be quite complex algebraically and appropriate for computer solution.

Diffusers are added to ducts to increase pressure recovery at the exit of a system. Their behavior is presented as experimental data, since the theory of real diffusers is still not well developed. The chapter ends with a discussion of flowmeters, especially the pitot-static tube and the Bernoulli-obstruction type of meter. Flowmeters also require careful experimental calibration.

Problems

Most of the problems herein are fairly straightforward. More difficult or open-ended assignments are labeled with an asterisk. Problems labeled with an EES icon will benefit from the use of the Engineering Equation Solver (EES), while problems labeled with a computer disk may require the use of a computer. The standard end-of-chapter problems 6.1 to 6.160 (categorized in the problem list below) are followed by word problems W6.1 to W6.5, fundamentals of engineering exam problems FE6.1 to FE6.15, comprehensive problems C6.1 to C6.5, and design projects D6.1 and D6.2.

Problem distribution

Section	Topic	Problems
6.1	Reynolds-number regimes	6.1–6.7
6.2	Internal and external flow	6.8–6.10
6.3	Turbulent-shear correlations	6.11–6.18
6.4	Laminar pipe flow	6.19–6.41
6.4	Turbulent pipe flow	6.42–6.77
6.5	Flow-rate and pipe-sizing problems	6.78–6.85
6.6	Noncircular ducts	6.86–6.99
6.7	Minor losses	6.100–6.110
6.8	Series and parallel pipe systems	6.111–6.120
6.8	Three-reservoir and pipe-network systems	6.121–6.130
6.9	Diffuser performance	6.131–6.134
6.10	The pitot-static tube	6.135–6.139
6.10	Flowmeters: The orifice plate	6.140–6.148
6.10	Flowmeters: The flow nozzle	6.149–6.153
6.10	Flowmeters: The venturi meter	6.154–6.160

P6.1 In flow past a sphere, the boundary layer becomes turbulent at about $Re_D \approx 2.5$ E5. To what air speed in mi/h does this correspond for a golf ball whose diameter is 1.6 in? Do the pressure, temperature, and humidity of the air make any difference in your calculation?

P6.2 For a thin wing moving parallel to its chord line, transition to a turbulent boundary layer normally occurs at $Re_x = 2.8 \times 10^6$, where x is the distance from the leading edge [2, 3]. If the wing is moving at 20 m/s, at what point on the wing will transition occur at 20°C for (*a*) air and (*b*) water?

P6.3 If the wing of Prob. 6.2 is tested in a wind or water tunnel, it may undergo transition earlier than $Re_x = 2.8 \times 10^6$ if the test stream itself contains turbulent fluctuations. A semiempirical correlation for this case [3, p. 383] is

$$Re_{x_{crit}}^{1/2} \approx \frac{-1 + (1 + 13.25\zeta^2)^{1/2}}{0.00392\zeta^2}$$

where ζ is the tunnel-turbulence intensity in percent. If $V = 20$ m/s in air at 20°C, use this formula to plot the transition position on the wing versus stream turbulence for ζ between 0 and 2 percent. At what value of ζ is x_{crit} decreased 50 percent from its value at $\zeta = 0$?

P6.4 For flow of SAE 10 oil through a 5-cm-diameter pipe, from Fig. A.1, for what flow rate in m^3/h would we expect transition to turbulence at (*a*) 20°C and (*b*) 100°C?

P6.5 In flow past a body or wall, early transition to turbulence can be induced by placing a trip wire on the wall across the flow, as in Fig. P6.5. If the trip wire in Fig. P6.5 is placed where the local velocity is U, it will trigger turbulence if $Ud/\nu = 850$, where d is the wire diameter [3, p. 386]. If the sphere diameter is 20 cm and transition is observed at $Re_D = 90{,}000$, what is the diameter of the trip wire in mm?

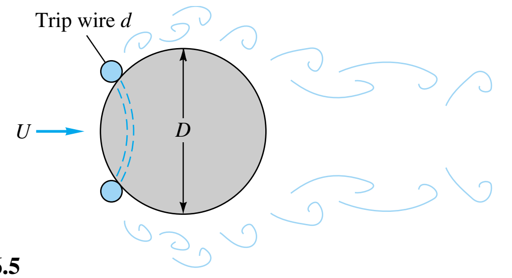

P6.5

P6.6 A fluid at 20°C flows at 850 cm^3/s through an 8-cm-diameter pipe. Determine whether the flow is laminar or turbulent if the fluid is (*a*) hydrogen, (*b*) air, (*c*) gasoline, (*d*) water, (*e*) mercury, or (*f*) glycerin.

P6.7 Cola, approximated as pure water at 20°C, is to fill an 8-oz container (1 U.S. gal = 128 fl oz) through a 5-mm-diameter tube. Estimate the minimum filling time if the tube flow is to remain laminar. For what cola (water) temperature would this minimum time be 1 min?

P6.8 When water at 20°C is in steady turbulent flow through an 8-cm-diameter pipe, the wall shear stress is 72 Pa. What is the axial pressure gradient ($\partial p/\partial x$) if the pipe is (*a*) horizontal and (*b*) vertical with the flow up?

P6.9 A light liquid ($\rho \approx 950$ kg/m^3) flows at an average velocity of 10 m/s through a horizontal smooth tube of diameter 5 cm. The fluid pressure is measured at 1-m intervals along the pipe, as follows:

x, m	0	1	2	3	4	5	6
p, kPa	304	273	255	240	226	213	200

Estimate (*a*) the average wall shear stress, in Pa, and (*b*) the wall shear stress in the fully developed region of the pipe.

P6.10 Water at 20°C flows through an inclined 8-cm-diameter pipe. At sections A and B the following data are taken: $p_A = 186$ kPa, $V_A = 3.2$ m/s, $z_A = 24.5$ m, and $p_B = 260$ kPa, $V_B = 3.2$ m/s, $z_B = 9.1$ m. Which way is the flow going? What is the head loss in meters?

P6.11 Derive the time-averaged x-momentum equation (6.14) by direct substitution of Eqs. (6.12) into the momentum equation (6.7). It is convenient to write the convective acceleration as

$$\frac{du}{dt} = \frac{\partial}{\partial x}(u^2) + \frac{\partial}{\partial y}(uv) + \frac{\partial}{\partial z}(uw)$$

which is valid because of the continuity relation, Eq. (6.7).

P6.12 By analogy with Eq. (6.14) write the turbulent mean-momentum differential equation for (*a*) the *y* direction and (*b*) the *z* direction. How many turbulent stress terms appear in each equation? How many unique turbulent stresses are there for the total of three directions?

P6.13 The following turbulent-flow velocity data $u(y)$, for air at 75°F and 1 atm near a smooth flat wall, were taken in the University of Rhode Island wind tunnel:

y, in	0.025	0.035	0.047	0.055	0.065
u, ft/s	51.2	54.2	56.8	57.6	59.1

Estimate (*a*) the wall shear stress and (*b*) the velocity *u* at $y = 0.22$ in.

P6.14 Two infinite plates a distance *h* apart are parallel to the *xz* plane with the upper plate moving at speed *V*, as in Fig. P6.14. There is a fluid of viscosity μ and constant pressure between the plates. Neglecting gravity and assuming incompressible turbulent flow $u(y)$ between the plates, use the logarithmic law and appropriate boundary conditions to derive a formula for dimensionless wall shear stress versus dimensionless plate velocity. Sketch a typical shape of the profile $u(y)$.

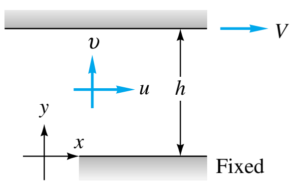

P6.14

P6.15 Suppose in Fig. P6.14 that $h = 3$ cm, the fluid in water at 20°C, and the flow is turbulent, so that the logarithmic law is valid. If the shear stress in the fluid is 15 Pa, what is *V* in m/s?

P6.16 By analogy with laminar shear, $\tau = \mu\, du/dy$, T. V. Boussinesq in 1877 postulated that turbulent shear could also be related to the mean-velocity gradient $\tau_{turb} = \epsilon\, du/dy$, where ϵ is called the *eddy viscosity* and is much larger than μ. If the logarithmic-overlap law, Eq. (6.21), is valid with $\tau \approx \tau_w$, show that $\epsilon \approx \kappa\rho u^* y$.

P6.17 Theodore von Kármán in 1930 theorized that turbulent shear could be represented by $\tau_{turb} = \epsilon\, du/dy$ where $\epsilon = \rho\kappa^2 y^2 |du/dy|$ is called the *mixing-length eddy viscosity* and $\kappa \approx 0.41$ is Kármán's dimensionless *mixing-length constant* [2, 3]. Assuming that $\tau_{turb} \approx \tau_w$ near the wall, show that this expression can be integrated to yield the logarithmic-overlap law, Eq. (6.21).

P6.18 Water at 20°C flows in a 9-cm-diameter pipe under fully developed conditions. The centerline velocity is 10 m/s. Compute (*a*) *Q*, (*b*) *V*, (*c*) τ_w, and (*d*) Δp for a 100-m pipe length.

In Probs. 6.19 to 6.99, neglect minor losses.

P6.19 A 5-mm-diameter capillary tube is used as a viscometer for oils. When the flow rate is 0.071 m^3/h, the measured pressure drop per unit length is 375 kPa/m. Estimate the viscosity of the fluid. Is the flow laminar? Can you also estimate the density of the fluid?

P6.20 A soda straw is 20 cm long and 2 mm in diameter. It delivers cold cola, approximated as water at 10°C, at a rate of 3 cm^3/s. (*a*) What is the head loss through the straw? What is the axial pressure gradient $\partial p/\partial x$ if the flow is (*b*) vertically up or (*c*) horizontal? Can the human lung deliver this much flow?

P6.21 Water at 20°C is to be siphoned through a tube 1 m long and 2 mm in diameter, as in Fig. P6.21. Is there any height *H* for which the flow might not be laminar? What is the flow rate if $H = 50$ cm? Neglect the tube curvature.

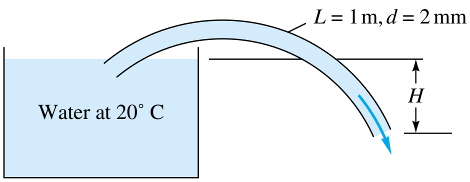

P6.21

P6.22 SAE 30W oil at 20°C flows through a long, horizontal, 12-cm-diameter tube. At section 1, the fluid pressure is 186 kPa. At section 2, which is 6 m further downstream, the pressure is 171 kPa. If the flow is laminar, estimate (*a*) the mass flow in kg/s and (*b*) the Reynolds number.

P6.23 Glycerin at 20°C is to be pumped through a horizontal smooth pipe at 3.1 m^3/s. It is desired that (1) the flow be laminar and (2) the pressure drop be no more than 100 Pa/m. What is the minimum pipe diameter allowable?

P6.24 The 6-cm-diameter pipe in Fig. P6.24 contains glycerin at 20°C flowing at a rate of 6 m^3/h. Verify that the flow is laminar. For the pressure measurements shown, is the flow up or down? What is the indicated head loss for these pressures?

P6.25 To determine the viscosity of a liquid of specific gravity 0.95, you fill, to a depth of 12 cm, a large container which drains through a 30-cm-long vertical tube attached to the bottom. The tube diameter is 2 mm, and the rate of drain-

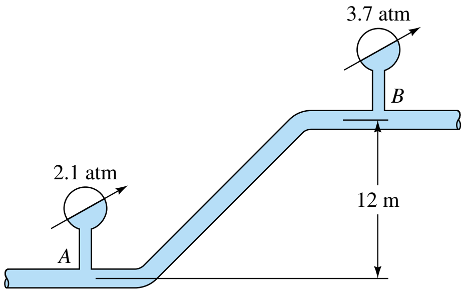

P6.24

ing is found to be 1.9 cm^3/s. What is your estimate of the fluid viscosity? Is the tube flow laminar?

P6.26 Water at 20°C is flowing through a 20-cm-square smooth duct at a (turbulent) Reynolds number of 100,000. For a "laminar flow element" measurement, it is desired to pack the pipe with a honeycomb array of small square passages (see Fig. P6.36 for an example). What passage width h will ensure that the flow in each tube will be laminar (Reynonds number less than 2000)?

P6.27 An oil (SG = 0.9) issues from the pipe in Fig. P6.27 at $Q = 35$ ft^3/h. What is the kinematic viscosity of the oil in ft^3/s? Is the flow laminar?

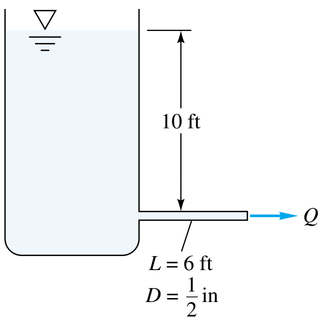

P6.27

P6.28 In Prob. 6.27 what will the flow rate be, in m^3/h, if the fluid is SAE 10 oil at 20°C?

P6.29 Oil, with $\rho = 890$ kg/m^3 and $\mu = 0.06$ kg/(m · s), is to be pumped through 1 km of straight horizontal pipe with a power input of 1 kW. What is the maximum possible mass flow rate, and corresponding pipe diameter, if laminar flow is to be maintained?

P6.30 A steady push on the piston in Fig. P6.30 causes a flow rate $Q = 0.15$ cm^3/s through the needle. The fluid has $\rho =$ 900 kg/m^3 and $\mu = 0.002$ kg/(m · s). What force F is required to maintain the flow?

P6.31 SAE 10 oil at 20°C flows in a vertical pipe of diameter 2.5 cm. It is found that the pressure is constant throughout the fluid. What is the oil flow rate in m^3/h? Is the flow up or down?

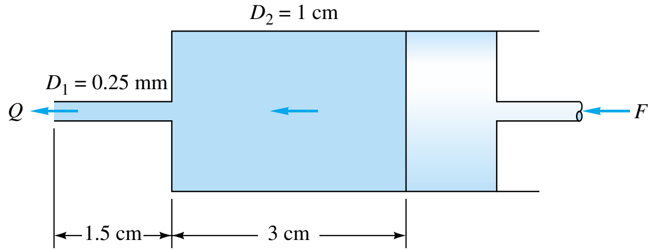

P6.30

P6.32 SAE 30 oil at 20°C flows at 0.001 m^3/s through 100 m of 1-cm-diameter pipe and then for another 100 m at an increased $d = 2$ cm. The double-pipe system slopes upward at 35° in the flow direction. Estimate (a) the total pressure change and (b) the power required to drive the flow.

P6.33 For the configuration shown in Fig. P6.33, the fluid is ethyl alcohol at 20°C, and the tanks are very wide. Find the flow rate which occurs in m^3/h. Is the flow laminar?

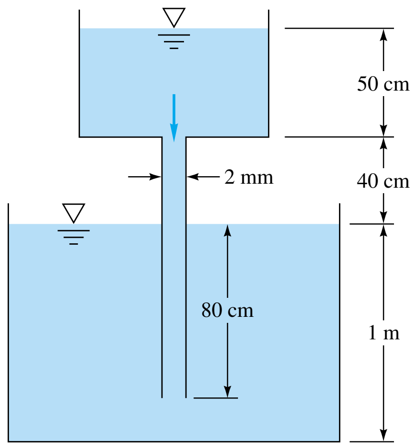

P6.33

P6.34 For the system in Fig. P6.33, if the fluid has density of 920 kg/m^3 and the flow rate is unknown, for what value of viscosity will the capillary Reynolds number exactly equal the critical value of 2300?

***P6.35** Let us attack Prob. 6.33 in symbolic fashion, using Fig. P6.35. All parameters are constant except the upper tank depth $Z(t)$. Find an expression for the flow rate $Q(t)$ as a function of $Z(t)$. Set up a differential equation, and solve for the time t_0 to drain the upper tank completely. Assume quasi-steady laminar flow.

P6.36 For straightening and smoothing an airflow in a 50-cm-diameter duct, the duct is packed with a "honeycomb" of thin straws of length 30 cm and diameter 4 mm, as in Fig.

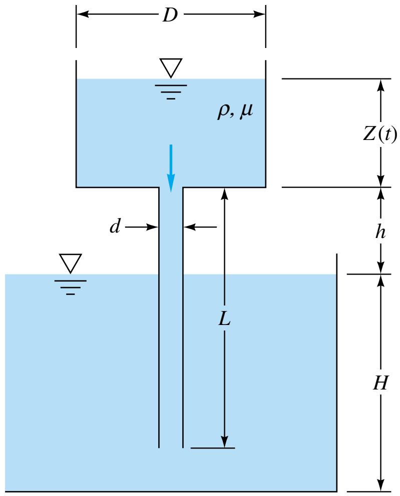

P6.35

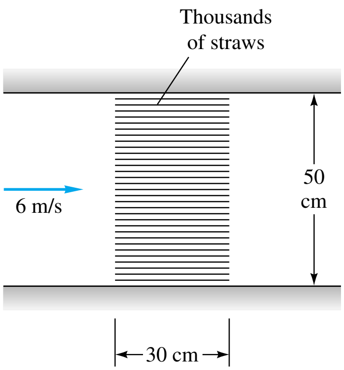

P6.36

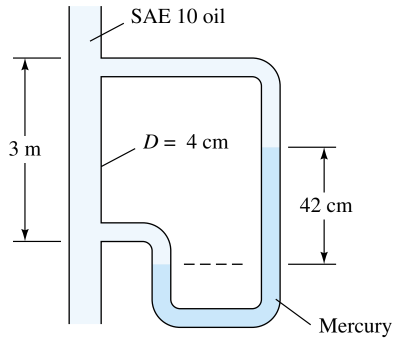

P6.38

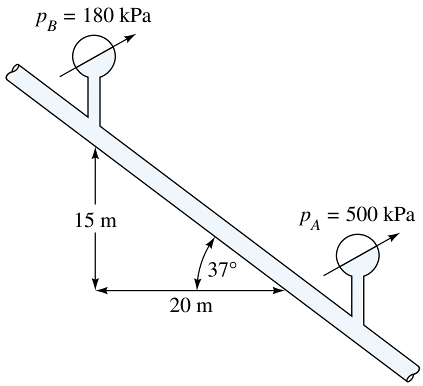

P6.40

P6.36. The inlet flow is air at 110 kPa and 20°C, moving at an average velocity of 6 m/s. Estimate the pressure drop across the honeycomb.

P6.37 Oil, with $\rho = 880$ kg/m^3 and $\mu = 0.08$ kg/(m · s), flows through a pipe with $d = 2$ cm and $L = 12$ m. The wall shear stress is 30 Pa. Estimate (*a*) the Reynolds number, (*b*) the total pressure drop, and (*c*) the power required to drive the fluid.

P6.38 SAE 10 oil at 20°C flows through the 4-cm-diameter vertical pipe of Fig. P6.38. For the mercury manometer reading $h = 42$ cm shown, (*a*) calculate the volume flow rate in m^3/h and (*b*) state the direction of flow.

P6.39 Light oil, $\rho = 880$ kg/m^3 and $\mu = 0.015$ kg/(m · s), flows down a vertical 6-mm-diameter tube due to gravity only. Estimate the volume flow rate in m^3/h if (*a*) $L = 1$ m and (*b*) $L = 2$ m. (*c*) Verify that the flow is laminar.

P6.40 SAE 30 oil at 20°C flows in the 3-cm-diameter pipe in Fig. P6.40, which slopes at 37°. For the pressure measurements shown, determine (*a*) whether the flow is up or down and (*b*) the flow rate in m^3/h.

P6.41 In Prob. 6.40 suppose it is desired to add a pump between *A* and *B* to drive the oil upward from *A* to *B* at a rate of 3 kg/s. At 100 percent efficiency, what pump power is required?

***P6.42** It is clear by comparing Figs. 6.12*b* and 6.13 that the effects of sand roughness and commercial (manufactured) roughness are not quite the same. Take the special case of commercial roughness ratio $\epsilon/d = 0.001$ in Fig. 6.13, and replot in the form of the wall-law shift ΔB (Fig. 6.12*a*) versus the logarithm of $\epsilon^+ = \epsilon u^*/\nu$. Compare your plot with Eq. (6.61).

P6.43 Water at 20°C flows for 1 mi through a 3-in-diameter horizontal wrought-iron pipe at 250 gal/min. Estimate the head loss and the pressure drop in this length of pipe.

P6.44 Mercury at 20°C flows through 4 m of 7-mm-diameter glass tubing at an average velocity of 5 m/s. Estimate the head loss in m and the pressure drop in kPa.

P6.45 EES Oil, SG = 0.88 and $\nu = 4$ E-5 m^2/s, flows at 400 gal/min through a 6-in asphalted cast-iron pipe. The pipe is 0.5 mi long and slopes upward at 8° in the flow direction. Compute the head loss in ft and the pressure change.

P6.46 Kerosine at 20°C is pumped at 0.15 m^3/s through 20 km of 16-cm-diameter cast-iron horizontal pipe. Compute the input power in kW required if the pumps are 85 percent efficient.

P6.47 Derive Eq. (6.59), showing all steps. The constant 1.33 dates back to Prandtl's work in 1935 and may change slightly to 1.29 in your analysis.

P6.48 Show that if Eq. (6.49) is accurate, the position in a turbulent pipe flow where local velocity u equals average velocity V occurs exactly at $r = 0.777R$, independent of the Reynolds number.

P6.49 The tank-pipe system of Fig. P6.49 is to deliver at least 11 m^3/h of water at 20°C to the reservoir. What is the maximum roughness height ϵ allowable for the pipe?

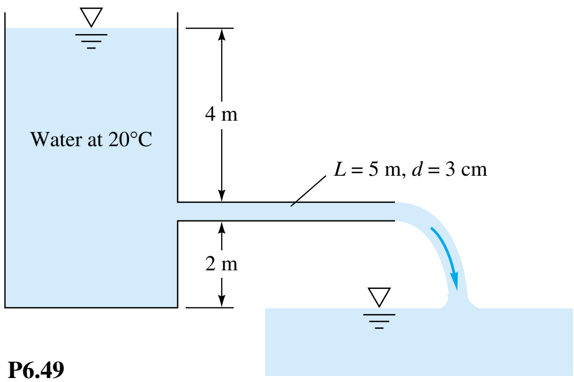

P6.49

P6.50 Ethanol at 20°C flows at 125 U.S. gal/min through a horizontal cast-iron pipe with $L = 12$ m and $d = 5$ cm. Neglecting entrance effects, estimate (*a*) the pressure gradient dp/dx, (*b*) the wall shear stress τ_w, and (*c*) the percent reduction in friction factor if the pipe walls are polished to a smooth surface.

P6.51 The viscous sublayer (Fig. 6.9) is normally less than 1 percent of the pipe diameter and therefore very difficult to probe with a finite-sized instrument. In an effort to generate a thick sublayer for probing, Pennsylvania State University in 1964 built a pipe with a flow of glycerin. Assume a smooth 12-in-diameter pipe with $V = 60$ ft/s and glycerin at 20°C. Compute the sublayer thickness in inches and the pumping horsepower required at 75 percent efficiency if $L = 40$ ft.

P6.52 The pipe flow in Fig. P6.52 is driven by pressurized air in the tank. What gage pressure p_1 is needed to provide a 20°C water flow rate $Q = 60$ m^3/h?

***P6.53** In Fig. P6.52 suppose $P_1 = 700$ kPa and the fluid specific gravity is 0.68. If the flow rate is 27 m^3/h, estimate the viscosity of the fluid. What fluid in Table A.5 is the likely suspect?

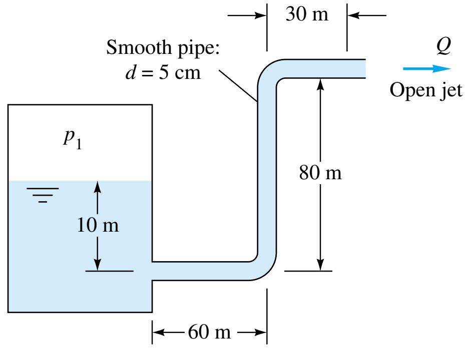

P6.52

P6.54 In Fig. P6.52 suppose that the fluid is carbon tetrachloride at 20°C and $p_1 = 1100$ kPa gage. What pipe diameter, in cm, is required to deliver a flow rate of 25 m^3/h?

P6.55 EES The reservoirs in Fig. P6.55 contain water at 20°C. If the pipe is smooth with $L = 4500$ m and $d = 4$ cm, what will the flow rate in m^3/h be for $\Delta z = 100$ m?

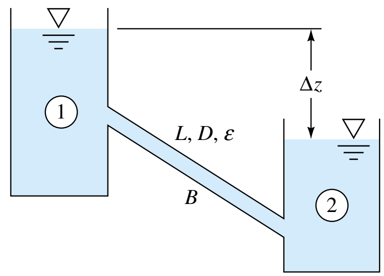

P6.55

P6.56 Consider a horizontal 4-ft-diameter galvanized-iron pipe simulating the Alaskan pipeline. The oil flow is 70 million U.S. gallons per day, at a density of 910 kg/m^3 and viscosity of 0.01 kg/(m · s) (see Fig. A.1 for SAE 30 oil at 100°C). Each pump along the line raises the oil pressure to 8 MPa, which then drops, due to head loss, to 400-kPa at the entrance to the next pump. Estimate (*a*) the appropriate distance between pumping stations and (*b*) the power required if the pumps are 88 percent efficient.

P6.57 John Laufer (*NACA Tech. Rep.* 1174, 1954) gave velocity data for 20°C airflow in a smooth 24.7-cm-diameter pipe at Re ≈ 5 E5:

u/u_{CL}	1.0	0.997	0.988	0.959	0.908	0.847	0.818	0.771	0.690
r/R	0.0	0.102	0.206	0.412	0.617	0.784	0.846	0.907	0.963

The centerline velocity u_{CL} was 30.5 m/s. Determine (*a*) the average velocity by numerical integration and (*b*) the wall shear stress from the log-law approximation. Compare with the Moody chart and with Eq. (6.59).

P6.58 In Fig. P6.55 assume that the pipe is cast iron with $L = 550$ m, $d = 7$ cm, and $\Delta Z = 100$ m. If an 80 percent efficient pump is placed at point B, what input power is required to deliver 160 m^3/h of water upward from reservoir 2 to 1?

P6.59 The following data were obtained for flow of 20°C water at 20 m^3/h through a badly corroded 5-cm-diameter pipe which slopes downward at an angle of 8°: $p_1 = 420$ kPa, $z_1 = 12$ m, $p_2 = 250$ kPa, $z_2 = 3$ m. Estimate (*a*) the roughness ratio of the pipe and (*b*) the percent change in head loss if the pipe were smooth and the flow rate the same.

P6.60 J. Nikuradse in 1932 suggested that smooth-wall turbulent pipe flow could be approximated by a power-law profile

$$\frac{u}{u_{CL}} \approx \left(\frac{y}{R}\right)^{1/N}$$

where y is distance from the wall and $N \approx 6$ to 9. Find the best value of N which fits Laufer's data in Prob. 6.57. Then use your formula to estimate the pipe volume flow, and compare with the measured value of 45 ft^3/s.

P6.61 A straight 10-cm commercial-steel pipe is 1 km long and is laid on a constant slope of 5°. Water at 20°C flows downward, due to gravity only. Estimate the flow rate in m^3/h. What happens if the pipe length is 2 km?

P6.62 The Moody chart, Fig. 6.13, is best for finding head loss (or Δp) when Q, V, d, and L are known. It is awkward for the second type of problem, finding Q when h_f or Δp is known (see Example 6.9). Prepare a modified Moody chart whose abscissa is independent of Q and V, using ϵ/d as a parameter, from which one can immediately read the ordinate to find (dimensionless) Q or V. Use your chart to solve Example 6.9.

P6.63 A tank contains 1 m^3 of water at 20°C and has a drawn-capillary outlet tube at the bottom, as in Fig. P6.63. Find the outlet volume flux Q in m^3/h at this instant.

P6.64 For the system in Fig. P6.63, solve for the flow rate in m^3/h if the fluid is SAE 10 oil at 20°C. Is the flow laminar or turbulent?

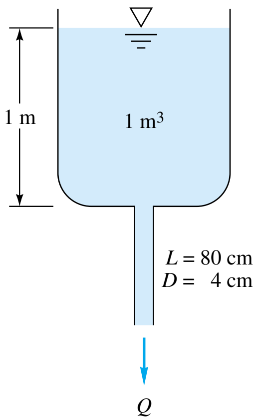

P6.63

P6.65 In Prob. 6.63 the initial flow is turbulent. As the water drains out of the tank, will the flow revert to laminar motion as the tank becomes nearly empty? If so, at what tank depth? Estimate the time, in h, to drain the tank completely.

P6.66 Ethyl alcohol at 20°C flows through a 10-cm horizontal drawn tube 100 m long. The fully developed wall shear stress is 14 Pa. Estimate (*a*) the pressure drop, (*b*) the volume flow rate, and (*c*) the velocity u at $r = 1$ cm.

P6.67 What level h must be maintained in Fig. P6.67 to deliver a flow rate of 0.015 ft^3/s through the $\frac{1}{2}$-in commercial-steel pipe?

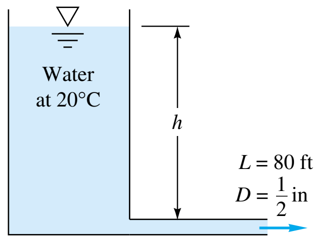

P6.67

P6.68 Water at 20°C is to be pumped through 2000 ft of pipe from reservoir 1 to 2 at a rate of 3 ft^3/s, as shown in Fig. P6.68. If the pipe is cast iron of diameter 6 in and the pump is 75 percent efficient, what horsepower pump is needed?

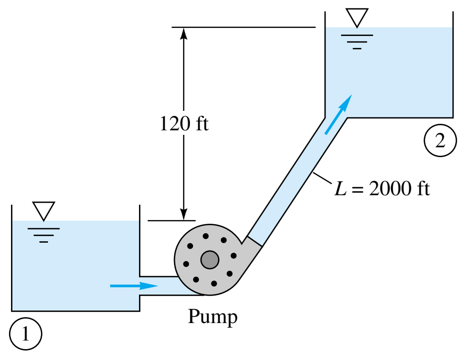

P6.68

P6.69 For Prob. 6.68 suppose the only pump available can deliver 80 hp to the fluid. What is the proper pipe size in inches to maintain the 3 ft^3/s flow rate?

P6.70 In Fig. P6.68 suppose the pipe is 6-in-diameter cast iron and the pump delivers 75 hp to the flow. What flow rate Q ft^3/s results?

P6.71 It is desired to solve Prob. 6.68 for the most economical pump and cast-iron pipe system. If the pump costs \$125 per horsepower delivered to the fluid and the pipe costs \$7000 per inch of diameter, what are the minimum cost and the pipe and pump size to maintain the 3 ft^3/s flow rate? Make some simplifying assumptions.

P6.72 The 5-m-long pipe in Fig. P6.72 may be oriented at any angle θ. If entrance losses are negligible for any θ (pure Moody friction loss), what is the optimum value of θ for which the jet height loss Δh is minimum?

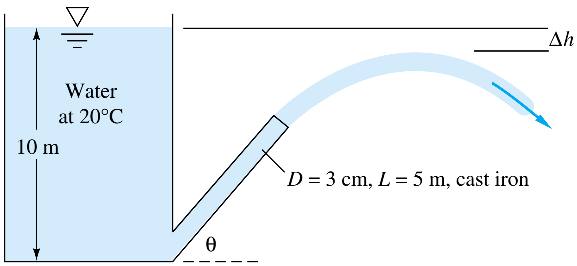

P6.72

P6.73 The Moody chart, Fig. 6.13, is best for finding head loss (or Δp) when Q, V, d, and L are known. It is awkward for the third type of problem, finding d when h_f (or Δp) and Q are known (see Example 6.11). Prepare a modified Moody chart whose abscissa is independent of d, using as a parameter ϵ nondimensionalized without d, from which one can immediately read the (dimensionless) ordinate to find d. Use your chart to solve Example 6.11.

P6.74 In Fig. P6.67 suppose the fluid is gasoline at 20°C and h = 90 ft. What commercial-steel pipe diameter is required for the flow rate to be 0.015 ft^3/s?

P6.75 You wish to water your garden with 100 ft of $\frac{5}{8}$-in-diameter hose whose roughness is 0.011 in. What will be the delivery, in ft^3/s, if the gage pressure at the faucet is 60 lbf/in^2? If there is no nozzle (just an open hose exit), what is the maximum horizontal distance the exit jet will carry?

P6.76 The small turbine in Fig. P6.76 extracts 400 W of power from the water flow. Both pipes are wrought iron. Compute the flow rate Q m^3/h. Sketch the EGL and HGL accurately.

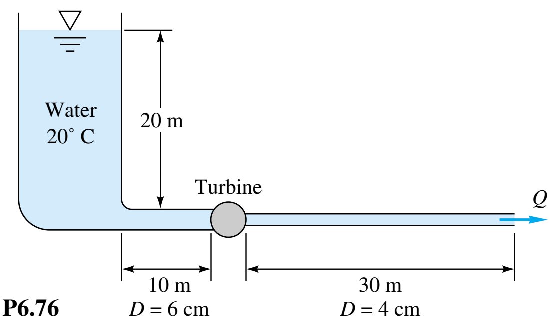

P6.76

P6.77 Modify Prob. 6.76 into an economic analysis, as follows. Let the 40 m of wrought-iron pipe have a uniform diameter d. Let the steady water flow available be Q = 30 m^3/h. The cost of the turbine is \$4 per watt developed, and the cost of the piping is \$75 per centimeter of diameter. The power generated may be sold for \$0.08 per kilowatthour. Find the proper pipe diameter for minimum *payback time*, i.e., minimum time for which the power sales will equal the initial cost of the system.

P6.78 In Fig. P6.78 the connecting pipe is commercial steel 6 cm in diameter. Estimate the flow rate, in m^3/h, if the fluid is water at 20°C. Which way is the flow?

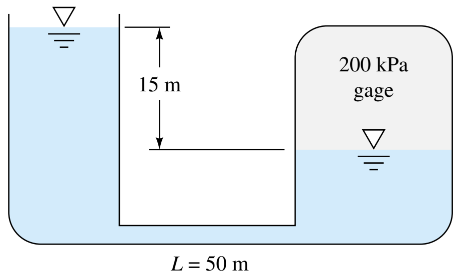

P6.78

P6.79 A garden hose is to be used as the return line in a waterfall display at a mall. In order to select the proper pump, you need to know the roughness height inside the garden hose. Unfortunately, roughness information is not something supplied by the hose manufacturer. So you devise a simple experiment to measure the roughness. The hose is attached to the drain of an aboveground swimming pool, the surface of which is 3.0 m above the hose outlet. You estimate the minor loss coefficient of the entrance region as 0.5, and the drain valve has a minor loss equivalent length of 200 diameters when fully open. Using a bucket and stopwatch, you open the valve and measure the flow rate to be 2.0×10^{-4} m^3/s for a hose that is 10.0 m long and has an inside diameter of 1.50 cm. Estimate the roughness height in mm inside the hose.

P6.80 The head-versus-flow-rate characteristics of a centrifugal pump are shown in Fig. P6.80. If this pump drives water at 20°C through 120 m of 30-cm-diameter cast-iron pipe, what will be the resulting flow rate, in m^3/s?

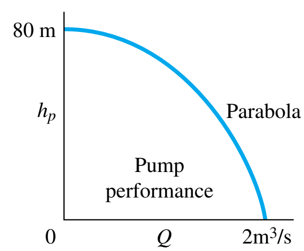

P6.80

P6.81 The pump in Fig. P6.80 is used to deliver gasoline at 20°C through 350 m of 30-cm-diameter galvanized iron pipe.

Estimate the resulting flow rate, in m^3/s. (Note that the pump head is now in meters of gasoline.)

P6.82 The pump in Fig. P6.80 has its maximum efficiency at a head of 45 m. If it is used to pump ethanol at 20°C through 200 m of commercial-steel pipe, what is the proper pipe diameter for maximum pump efficiency?

P6.83 For the system of Fig. P6.55, let $\Delta z = 80$ m and $L = 185$ m of cast-iron pipe. What is the pipe diameter for which the flow rate will be 7 m^3/h?

P6.84 It is desired to deliver 60 m^3/h of water at 20°C through a horizontal asphalted cast-iron pipe. Estimate the pipe diameter which will cause the pressure drop to be exactly 40 kPa per 100 m of pipe length.

P6.85 EES The pump of Fig. P6.80 is used to deliver 0.7 m^3/s of methanol at 20°C through 95 m of cast-iron pipe. What is the proper pipe diameter?

P6.86 SAE 10 oil at 20°C flows at an average velocity of 2 m/s between two smooth parallel horizontal plates 3 cm apart. Estimate (*a*) the centerline velocity, (*b*) the head loss per meter, and (*c*) the pressure drop per meter.

P6.87 A commercial-steel annulus 40 ft long, with $a = 1$ in and $b = \frac{1}{2}$ in, connects two reservoirs which differ in surface height by 20 ft. Compute the flow rate in ft^3/s through the annulus if the fluid is water at 20°C.

P6.88 Show that for laminar flow through an annulus of very small clearance the flow rate Q is approximately proportional to the cube of the clearance $a - b$.

P6.89 An annulus of narrow clearance causes a very large pressure drop and is useful as an accurate measurement of viscosity. If a smooth annulus 1 m long with $a = 50$ mm and $b = 49$ mm carries an oil flow at 0.001 m^3/s, what is the oil viscosity if the pressure drop is 250 kPa?

P6.90 A 90-ft-long sheet-steel duct carries air at approximately 20°C and 1 atm. The duct cross section is an equilateral triangle whose side measures 9 in. If a blower can supply 1 hp to the flow, what flow rate, in ft^3/s, will result?

P6.91 Heat exchangers often consist of many triangular passages. Typical is Fig. P6.91, with $L = 60$ cm and an isosceles-triangle cross section of side length $a = 2$ cm and included angle $\beta = 80°$. If the average velocity is $V = 2$ m/s and the fluid is SAE 10 oil at 20°C, estimate the pressure drop.

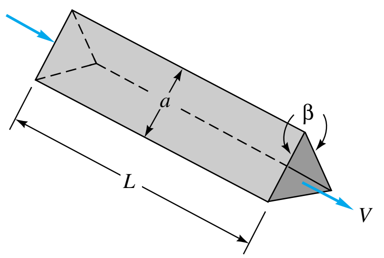

P6.91

P6.92 A large room uses a fan to draw in atmospheric air at 20°C through a 30-cm by 30-cm commercial-steel duct 12 m long, as in Fig. P6.92. Estimate (*a*) the air flow rate in m^3/h if the room pressure is 10 Pa vacuum and (*b*) the room pressure if the flow rate is 1200 m^3/h. Neglect minor losses.

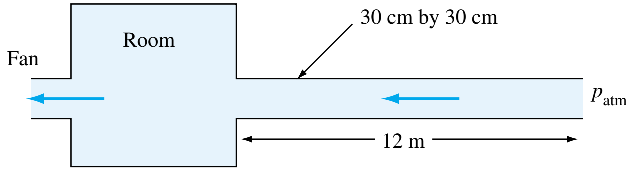

P6.92

P6.93 Modify Prob. 6.91 so that the angle β is unknown. For SAE 10 oil at 20°C, if the pressure drop is 120 kPa and the flow rate is 4 m^3/h, what is the proper value of the angle β, in degrees?

P6.94 As shown in Fig. P6.94, a multiduct cross section consists of seven 2-cm-diameter smooth thin tubes packed tightly in a hexagonal "bundle" within a single 6-cm-diameter tube. Air, at about 20°C and 1 atm, flows through this system at 150 m^3/h. Estimate the pressure drop per meter.

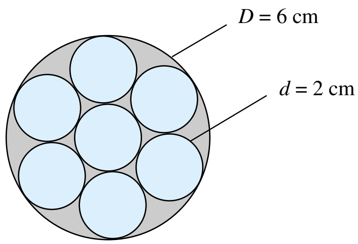

P6.94

P6.95 Modify Prob. 6.94 as follows. Let the seven 2-cm tubes be solid rods, so that the air can only pass through the curved triangular cusped passages. Compute the pressure drop per meter of duct length.

P6.96 Hydrogen, at 20°C and approximately 1 atm, is to be pumped through a smooth rectangular duct 85 m long of aspect ratio 5:1. If the flow rate is 0.7 m^3/s and the pressure drop is 80 Pa, what should the width and height of the duct cross section be?

P6.97 A wind tunnel has a wooden rectangular section 45 cm by 95 cm by 26 m long. It uses sea-level standard air at 31-m/s average velocity. Estimate the pressure drop and the power required if the fan efficiency is 75 percent.

P6.98 A rectangular heat exchanger is to be divided into smaller sections using sheets of commercial steel 0.4 mm thick, as sketched in Fig. P6.98. The flow rate is 20 kg/s of water at 20°C. Basic dimensions are $L = 1$ m, $W = 20$ cm, and $H = 10$ cm. What is the proper number of *square* sections if the overall pressure drop is to be no more than 1600 Pa?

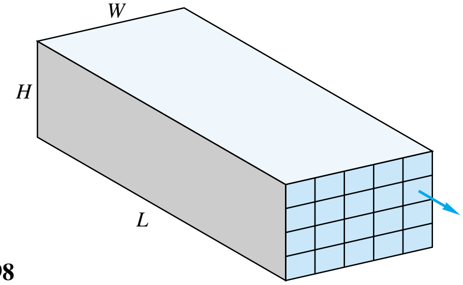

P6.98

P6.99 Air, approximately at sea-level standard conditions, is to be delivered at 3 m^3/s through a horizontal square commercial-steel duct. What are the appropriate duct dimensions if the pressure drop is not to exceed 90 Pa over a 100-m length?

***P6.100** Repeat Prob. 6.92 by including minor losses due to a sharp-edged entrance, the exit into the room, and an open gate valve. If the room pressure is 10 Pa vacuum, by what percentage is the air flow rate decreased from part (*a*) of Prob. 6.92?

P6.101 Repeat Prob. 6.67 by including losses due to a sharp entrance and a fully open screwed swing-check valve. By what percentage is the required tank level h increased?

***P6.102** A 70 percent efficient pump delivers water at 20°C from one reservoir to another 20 ft higher, as in Fig. P6.102. The piping system consists of 60 ft of galvanized-iron 2-in pipe, a reentrant entrance, two screwed 90° long-radius elbows, a screwed-open gate valve, and a sharp exit. What is the input power required in horsepower with and without a 6° well-designed conical expansion added to the exit? The flow rate is 0.4 ft^3/s.

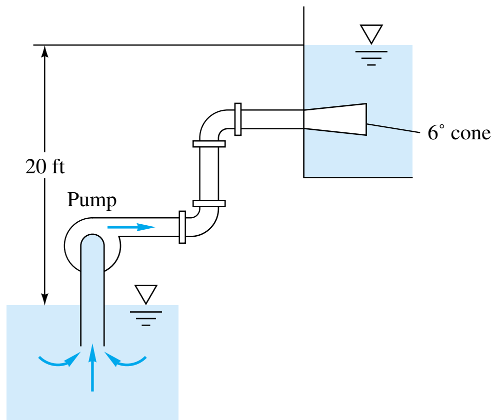

P6.102

P6.103 The reservoirs in Fig. P6.103 are connected by cast-iron pipes joined abruptly, with sharp-edged entrance and exit. Including minor losses, estimate the flow of water at 20°C if the surface of reservoir 1 is 45 ft higher than that of reservoir 2.

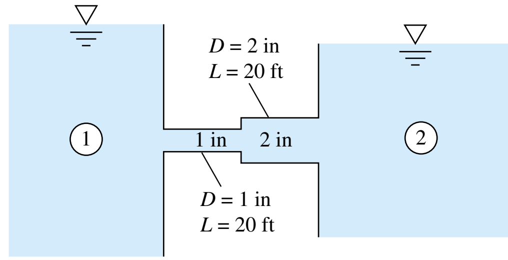

P6.103

***P6.104** Reconsider the air hockey table of Prob. 3.162 but with inclusion of minor losses. The table is 3.0 × 6.0 ft in area, with $\frac{1}{16}$-in-diameter holes spaced every inch in a rectangular grid pattern (2592 holes total). The required jet speed from each hole is estimated to be V_{jet} = 50 ft/s. Your job is to select an appropriate blower which will meet the requirements. *Hint:* Assume that the air is stagnant in the large volume of the manifold under the table surface, and assume sharp edge inlets at each hole. (*a*) Estimate the pressure rise (in lb/in^2) required of the blower. (*b*) Compare your answer to the previous calculation in which minor losses were ignored. Are minor losses significant in this application?

P6.105 The system in Fig. P6.105 consists of 1200 m of 5 cm cast-iron pipe, two 45° and four 90° flanged long-radius elbows, a fully open flanged globe valve, and a sharp exit into a reservoir. If the elevation at point 1 is 400 m, what gage pressure is required at point 1 to deliver 0.005 m^3/s of water at 20°C into the reservoir?

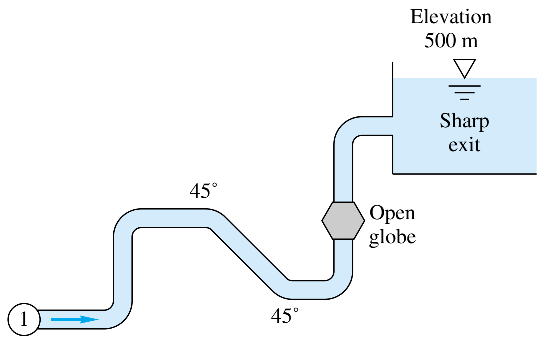

P6.105

P6.106 The water pipe in Fig. P6.106 slopes upward at 30°. The pipe has a 1-in diameter and is smooth. The flanged globe valve is fully open. If the mercury manometer shows a 7-in deflection, what is the flow rate in ft^3/s?

P6.107 In Fig. P6.107 the pipe is galvanized iron. Estimate the percentage increase in the flow rate (*a*) if the pipe entrance

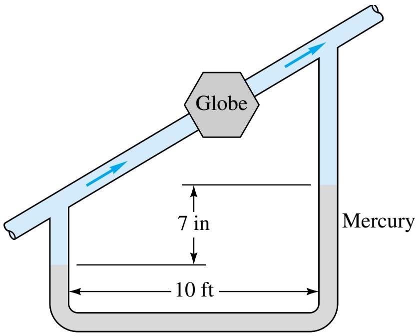

P6.106

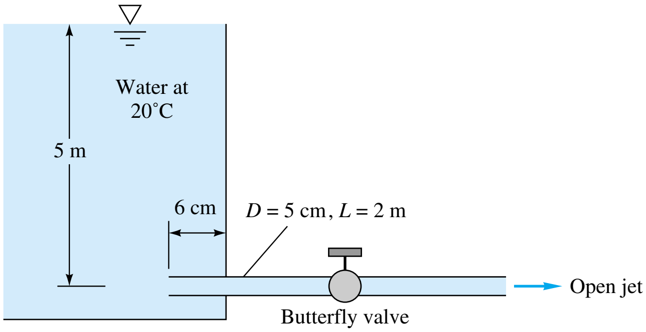

P6.107

is cut off flush with the wall and (*b*) if the butterfly valve is opened wide.

P6.108 Consider the flow system of Fig. P6.102, including the 6° cone diffuser. Suppose the pump head versus flow rate is approximated by

$$h_p \approx 45 - 125Q^2$$

with h_p in ft and Q in ft^3/s. Estimate the resulting flow rate, in ft^3/s.

P6.109 In Fig. P6.109 there are 125 ft of 2-in pipe, 75 ft of 6-in pipe, and 150 ft of 3-in pipe, all cast iron. There are three 90° elbows and an open globe valve, all flanged. If the exit elevation is zero, what horsepower is extracted by the turbine when the flow rate is 0.16 ft^3/s of water at 20°C?

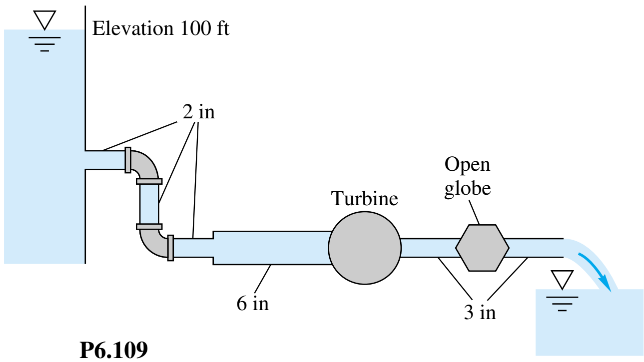

P6.109

P6.110 In Fig. P6.110 the pipe entrance is sharp-edged. If the flow rate is 0.004 m^3/s, what power, in W, is extracted by the turbine?

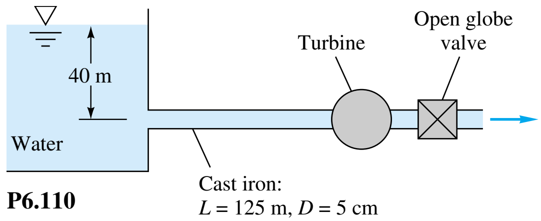

P6.110

P6.111 For the parallel-pipe system of Fig. P6.111, each pipe is cast iron, and the pressure drop $p_1 - p_2 = 3$ lbf/in^2. Compute the total flow rate between 1 and 2 if the fluid is SAE 10 oil at 20°C.

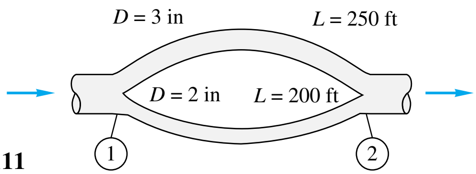

P6.111

P6.112 If the two pipes in Fig. P6.111 are instead laid in series with the same total pressure drop of 3 lbf/in^2, what will the flow rate be? The fluid is SAE 10 oil at 20°C.

P6.113 The parallel galvanized-iron pipe system of Fig. P6.113 delivers gasoline at 20°C with a total flow rate of 0.036 m^3/s. If the pump is wide open and not running, with a loss coefficient $K = 1.5$, determine (*a*) the flow rate in each pipe and (*b*) the overall pressure drop.

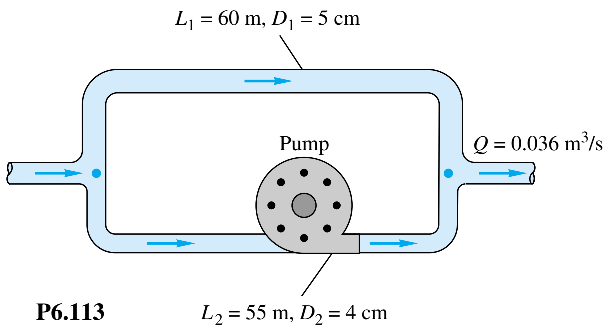

P6.113

P6.114 Modify Prob. 6.113 as follows. Let the pump be running and delivering 45 kW to the flow in pipe 2. The fluid is gasoline at 20°C. Determine (*a*) the flow rate in each pipe and (*b*) the overall pressure drop.

EES

P6.115 In Fig. P6.115 all pipes are 8-cm-diameter cast iron. Determine the flow rate from reservoir 1 if valve *C* is (*a*) closed and (*b*) open, $K = 0.5$.

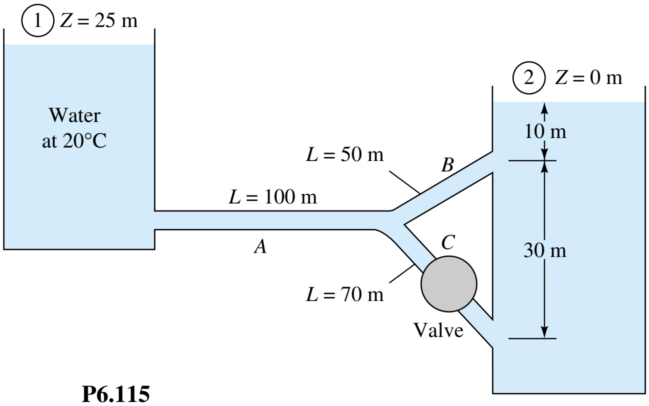

P6.115

P6.116 For the series-parallel system of Fig. P6.116, all pipes are 8-cm-diameter asphalted cast iron. If the total pressure drop $p_1 - p_2 = 750$ kPa, find the resulting flow rate Q m^3/h for water at 20°C. Neglect minor losses.

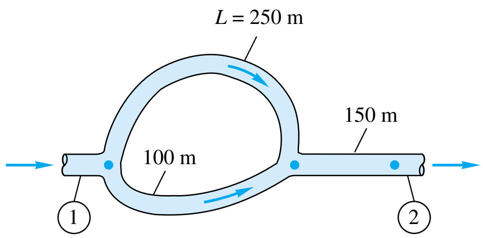

P6.116

P6.117 Modify Prob. 6.116 as follows. Let the flow rate be 45 m^3/h of water at 20°C. Determine the overall pressure drop $p_1 - p_2$ in kPa. Neglect minor losses.

P6.118 For the piping system of Fig. P6.118, all pipes are concrete with a roughness of 0.04 in. Neglecting minor losses, compute the overall pressure drop $p_1 - p_2$ in lbf/in^2 if $Q = 20\ ft^3/s$. The fluid is water at 20°C.

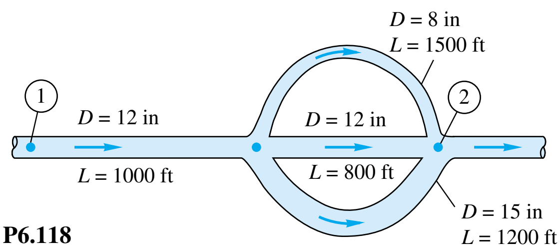

P6.118

P6.119 Modify Prob. 6.118 as follows. Let the pressure drop $p_1 - p_2$ be 98 lbf/in^2. Neglecting minor losses, determine the flow rate in m^3/h.

P6.120 Three cast-iron pipes are laid in parallel with these dimensions:

Pipe	Length, m	Diameter, cm
1	800	12
2	600	8
3	900	10

The total flow rate is 200 m^3/h of water at 20°C. Determine (*a*) the flow rate in each pipe and (*b*) the pressure drop across the system.

P6.121 Consider the three-reservoir system of Fig. P6.121 with the following data:

$$L_1 = 95 \text{ m} \quad L_2 = 125 \text{ m} \quad L_3 = 160 \text{ m}$$

$$z_1 = 25 \text{ m} \quad z_2 = 115 \text{ m} \quad z_3 = 85 \text{ m}$$

All pipes are 28-cm-diameter unfinished concrete ($\epsilon = 1$ mm). Compute the steady flow rate in all pipes for water at 20°C.

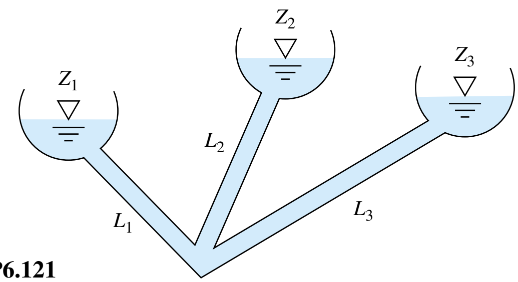

P6.121

P6.122 Modify Prob. 6.121 as follows. Reduce the diameter to 15 cm (with $\epsilon = 1$ mm), and compute the flow rates for water at 20°C. These flow rates distribute in nearly the same manner as in Prob. 6.121 but are about 5.2 times lower. Can you explain this difference?

EES

P6.123 Modify Prob. 6.121 as follows. All data are the same except that z_3 is unknown. Find the value of z_3 for which the flow rate in pipe 3 is 0.2 m^3/s toward the junction. (This problem requires iteration and is best suited to a digital computer.)

P6.124 The three-reservoir system in Fig. P6.124 delivers water at 20°C. The system data are as follows:

$$D_1 = 8 \text{ in} \quad D_2 = 6 \text{ in} \quad D_3 = 9 \text{ in}$$

$$L_1 = 1800 \text{ ft} \quad L_2 = 1200 \text{ ft} \quad L_3 = 1600 \text{ ft}$$

All pipes are galvanized iron. Compute the flow rate in all pipes.

P6.125 Modify Prob. 6.124 as follows. Let all data be the same except z_3, which is unknown. What value of z_3 will cause the flow rate through pipe 3 to be 1.0 ft^3/s toward the junction?

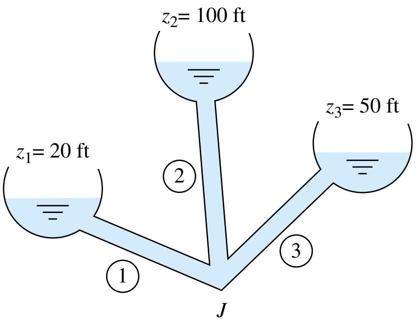

P6.124

P6.126 Modify Prob. 6.124 as follows. Let all data be the same except that pipe 1 is fitted with a butterfly valve (Fig. 6.19*b*). Estimate the proper valve opening angle (in degrees) for the flow rate through pipe 1 to be reduced to 1.5 ft^3/s toward reservoir 1. (This problem requires iteration and is best suited to a digital computer.)

P6.127 In the five-pipe horizontal network of Fig. P6.127, assume that all pipes have a friction factor f = 0.025. For the given inlet and exit flow rate of 2 ft^3/s of water at 20°C, determine the flow rate and direction in all pipes. If p_A = 120 lbf/in^2 gage, determine the pressures at points B, C, and D.

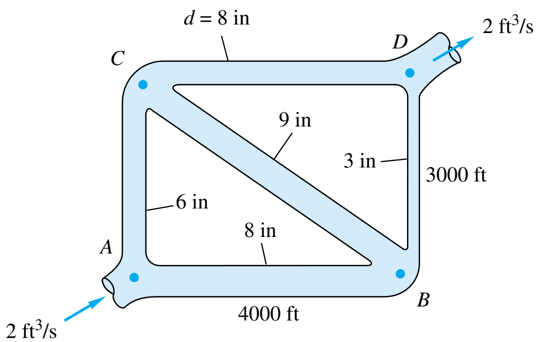

P6.127

P6.128 Modify Prob. 6.127 as follows. Let the inlet flow rate at A and the exit flow at D be unknown. Let $p_A - p_B$ = 100 lbf/in^2. Compute the flow rate in all five pipes.

P6.129 In Fig. P6.129 all four horizontal cast-iron pipes are 45 m long and 8 cm in diameter and meet at junction a, delivering water at 20°C. The pressures are known at four points as shown:

$$p_1 = 950 \text{ kPa} \qquad p_2 = 350 \text{ kPa}$$

$$p_3 = 675 \text{ kPa} \qquad p_4 = 100 \text{ kPa}$$

Neglecting minor losses, determine the flow rate in each pipe.

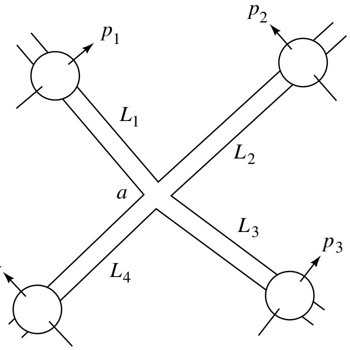

P6.129

P6.130 In Fig. P6.130 lengths AB and BD are 2000 and 1500 ft, respectively. The friction factor is 0.022 everywhere, and p_A = 90 lbf/in^2 gage. All pipes have a diameter of 6 in. For water at 20°C, determine the flow rate in all pipes and the pressures at points B, C, and D.

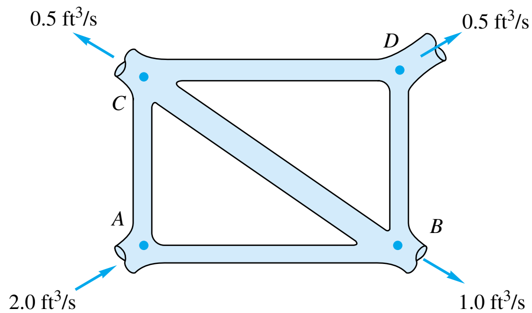

P6.130

P6.131 A water-tunnel test section has a 1-m diameter and flow properties V = 20 m/s, p = 100 kPa, and T = 20°C. The boundary-layer blockage at the end of the section is 9 percent. If a conical diffuser is to be added at the end of the section to achieve maximum pressure recovery, what should its angle, length, exit diameter, and exit pressure be?

P6.132 For Prob. 6.131 suppose we are limited by space to a total diffuser length of 10 m. What should the diffuser angle, exit diameter, and exit pressure be for maximum recovery?

P6.133 A wind-tunnel test section is 3 ft square with flow properties V = 150 ft/s, p = 15 lbf/in^2 absolute, and T = 68°F. Boundary-layer blockage at the end of the test section is 8 percent. Find the angle, length, exit height, and exit pressure of a flat-walled diffuser added onto the section to achieve maximum pressure recovery.

P6.134 For Prob. 6.133 suppose we are limited by space to a total diffuser length of 30 ft. What should the diffuser angle, exit height, and exit pressure be for maximum recovery?

P6.135 A small airplane flying at 5000-m altitude uses a pitot stagnation probe without static holes. The measured stagnation pressure is 56.5 kPa. Estimate the airplane's speed in mi/h and its uncertainty. Is a compressibility correction needed?

P6.136 For the pitot-static pressure arrangement of Fig. P6.136, the manometer fluid is (colored) water at 20°C. Estimate (*a*) the centerline velocity, (*b*) the pipe volume flow, and (*c*) the (smooth) wall shear stress.

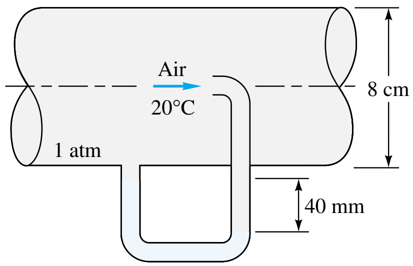

P6.136

P6.137 For the 20°C water flow of Fig. P6.137, use the pitot-static arrangement to estimate (*a*) the centerline velocity and (*b*) the volume flow in the 5-in-diameter smooth pipe. (*c*) What error in flow rate is caused by neglecting the 1-ft elevation difference?

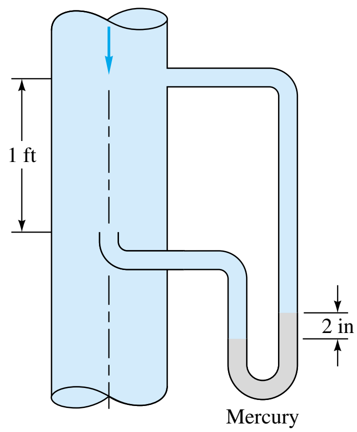

P6.137

P6.138 An engineer who took college fluid mechanics on a pass-fail basis has placed the static pressure hole far upstream of the stagnation probe, as in Fig. P6.138, thus contaminating the pitot measurement ridiculously with pipe friction losses. If the pipe flow is air at 20°C and 1 atm and the manometer fluid is Meriam red oil (SG = 0.827), estimate the air centerline velocity for the given manometer reading of 16 cm. Assume a smooth-walled tube.

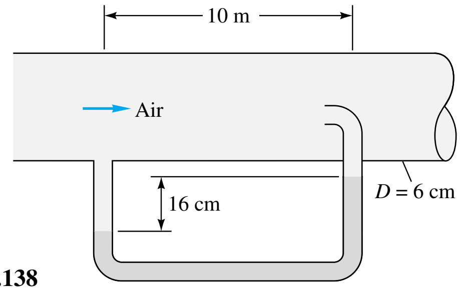

P6.138

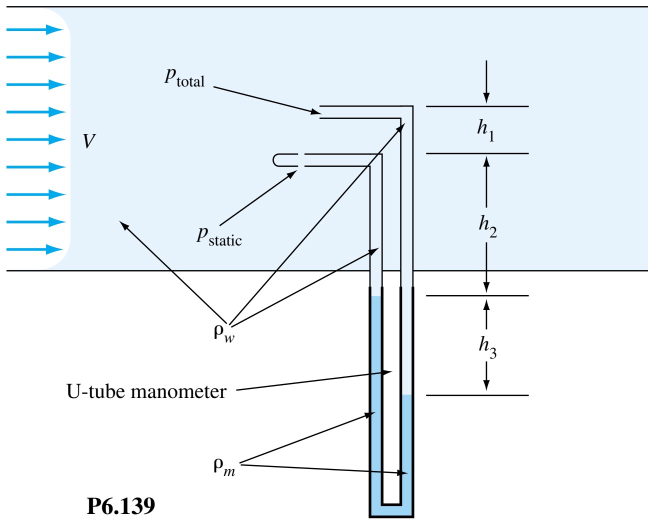

P6.139

P6.139 Professor Walter Tunnel needs to measure the flow velocity in a water tunnel. Due to budgetary restrictions, he cannot afford a pitot-static probe, but instead inserts a total head probe and a static pressure probe, as shown in Fig. P6.139, a distance h_1 apart from each other. Both probes are in the main free stream of the water tunnel, unaffected by the thin boundary layers on the sidewalls. The two probes are connected as shown to a U-tube manometer. The densities and vertical distances are shown in Fig. P6.139. (*a*) Write an expression for velocity *V* in terms of the parameters in the problem. (*b*) Is it critical that distance h_1 be measured accurately? (*c*) How does the expression for velocity *V* differ from that which would be obtained if a pitot-static probe had been available and used with the same U-tube manometer?

P6.140 Kerosine at 20°C flows at 18 m^3/h in a 5-cm-diameter pipe. If a 2-cm-diameter thin-plate orifice with corner taps is installed, what will the measured pressure drop be, in Pa?

P6.141 EES Gasoline at 20°C flows at 105 m^3/h in a 10-cm-diameter pipe. We wish to meter the flow with a thin-plate orifice and a differential pressure transducer which reads best at about 55 kPa. What is the proper β ratio for the orifice?

P6.142 The shower head in Fig. P6.142 delivers water at 50°C. An orifice-type flow reducer is to be installed. The upstream pressure is constant at 400 kPa. What flow rate, in

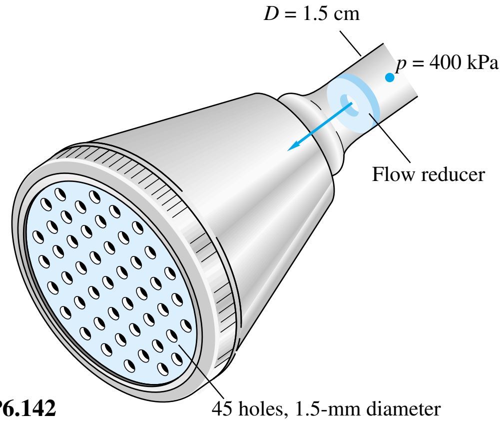

P6.142

gal/min, results without the reducer? What reducer orifice diameter would decrease the flow by 40 percent?

P6.143 A 10-cm-diameter smooth pipe contains an orifice plate with D: $\frac{1}{2}D$ taps and $\beta = 0.5$. The measured orifice pressure drop is 75 kPa for water flow at 20°C. Estimate the flow rate, in m^3/h. What is the nonrecoverable head loss?

P6.144 Accurate solution of Prob. 6.143, using Fig. 6.40, requires iteration because both the ordinate and the abscissa of this figure contain the unknown flow rate Q. In the spirit of Example 5.8, rescale the variables and construct a new plot in which Q may be read directly from the ordinate. Solve Prob. 6.143 with your new chart.

P6.145 The 1-m-diameter tank in Fig. P6.145 is initially filled with gasoline at 20°C. There is a 2-cm-diameter orifice in the bottom. If the orifice is suddenly opened, estimate the time for the fluid level $h(t)$ to drop from 2.0 to 1.6 m.

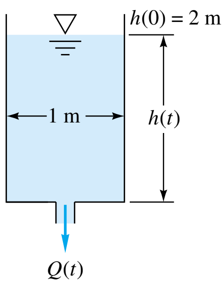

P6.145

P6.146 A pipe connecting two reservoirs, as in Fig. P6.146, contains a thin-plate orifice. For water flow at 20°C, estimate (*a*) the volume flow through the pipe and (*b*) the pressure drop across the orifice plate.

P6.147 Air flows through a 6-cm-diameter smooth pipe which has a 2-m-long perforated section containing 500 holes (diameter 1 mm), as in Fig. P6.147. Pressure outside the pipe is sea-level standard air. If p_1 = 105 kPa and Q_1 = 110 m^3/h, estimate p_2 and Q_2, assuming that the holes are approximated by thin-plate orifices. *Hint:* A momentum control volume may be very useful.

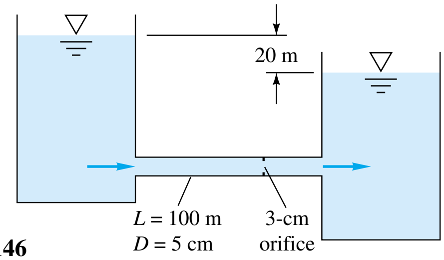

P6.146

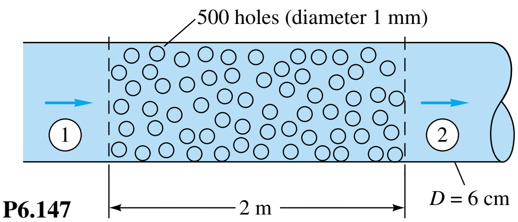

P6.147

P6.148 A smooth pipe containing ethanol at 20°C flows at 7 m^3/h through a Bernoulli obstruction, as in Fig. P6.148. Three piezometer tubes are installed, as shown. If the obstruction is a thin-plate orifice, estimate the piezometer levels (*a*) h_2 and (*b*) h_3.

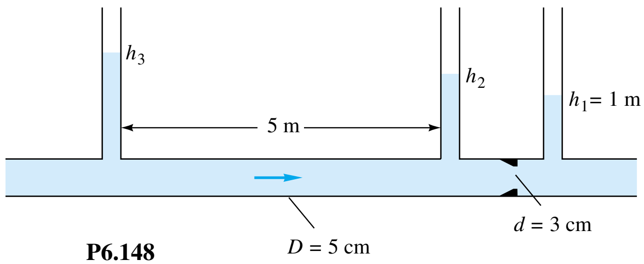

P6.148

P6.149 Repeat Prob. 6.148 if the obstruction is a long-radius flow nozzle.

P6.150 Gasoline at 20°C flows at 0.06 m^3/s through a 15-cm pipe and is metered by a 9-cm long-radius flow nozzle (Fig. 6.39*a*). What is the expected pressure drop across the nozzle?

P6.151 Ethyl alcohol at 20°C flowing in a 6-cm-diameter pipe is metered through a 3-cm long-radius flow nozzle. If the measured pressure drop is 45 kPa, what is the estimated volume flow, in m^3/h?

P6.152 Kerosine at 20°C flows at 20 m^3/h in an 8-cm-diameter pipe. The flow is to be metered by an ISA 1932 flow nozzle so that the pressure drop is 7000 Pa. What is the proper nozzle diameter?

P6.153 Two water tanks, each with base area of 1 ft^2, are connected by a 0.5-in-diameter long-radius nozzle as in Fig. P6.153. If $h = 1$ ft as shown for $t = 0$, estimate the time for $h(t)$ to drop to 0.25 ft.

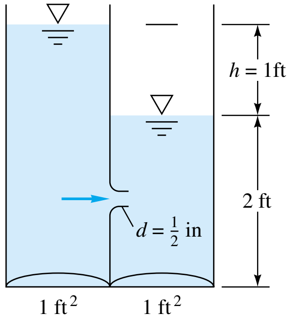

P6.153

***P6.154** Water at 20°C flows through the orifice in Fig. P6.154, which is monitored by a mercury manometer. If $d = 3$ cm, (*a*) what is h when the flow rate is 20 m^3/h and (*b*) what is Q in m^3/h when $h = 58$ cm?

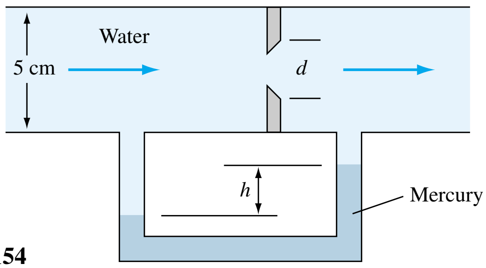

P6.154

P6.155 It is desired to meter a flow of 20°C gasoline in a 12-cm-diameter pipe, using a modern venturi nozzle. In order for international standards to be valid (Fig. 6.42), what is the permissible range of (*a*) flow rates, (*b*) nozzle diameters, and (*c*) pressure drops? (*d*) For the highest pressure-drop condition, would compressibility be a problem?

P6.156 Ethanol at 20°C flows down through a modern venturi nozzle as in Fig. P6.156. If the mercury manometer reading is 4 in, as shown, estimate the flow rate, in gal/min.

P6.157 Modify Prob. 6.156 if the fluid is air at 20°C, entering the venturi at a pressure of 18 lbf/in^2. Should a compressibility correction be used?

P6.158 Water at 20°C flows in a long horizontal commercial-steel 6-cm-diameter pipe which contains a classical Herschel venturi with a 4-cm throat. The venturi is connected to a mercury manometer whose reading is $h = 40$ cm. Estimate (*a*) the flow rate, in m^3/h, and (*b*) the total pressure difference between points 50 cm upstream and 50 cm downstream of the venturi.

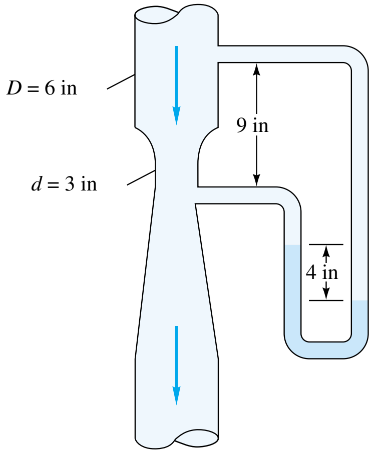

P6.156

P6.159 A modern venturi nozzle is tested in a laboratory flow with water at 20°C. The pipe diameter is 5.5 cm, and the venturi throat diameter is 3.5 cm. The flow rate is measured by a weigh tank and the pressure drop by a water-mercury manometer. The mass flow rate and manometer readings are as follows:

$\dot{m}$, kg/s	0.95	1.98	2.99	5.06	8.15
h, mm	3.7	15.9	36.2	102.4	264.4

Use these data to plot a calibration curve of venturi discharge coefficient versus Reynolds number. Compare with the accepted correlation, Eq. (6.134).

***P6.160** The butterfly-valve losses in Fig. 6.19*b* may be viewed as a type of Bernoulli obstruction device, as in Fig. 6.38. The "throat area" A_t in Eq. (6.125) can be interpreted as the two slivers of opening around the butterfly disk when viewed from upstream. First fit the average loss K_{mean} versus the opening angle in Fig. 6.19*b* to an exponential curve. Then use your curve fit to compute the "discharge coefficient" of a butterfly valve as a function of the opening angle. Plot the results and compare them to those for a typical flowmeter.

Word Problems

W6.1 In fully developed straight-duct flow, the velocity profiles do not change (why?), but the pressure drops along the pipe axis. Thus there is pressure work done on the fluid. If, say, the pipe is insulated from heat loss, where does this energy go? Make a thermodynamic analysis of the pipe flow.

W6.2 From the Moody chart (Fig. 6.13), rough surfaces, such as sand grains or ragged machining, do not affect laminar flow. Can you explain why? They *do* affect turbulent flow. Can you develop, or suggest, an analytical-physical model of turbulent flow near a rough surface which might be used to predict the known increase in pressure drop?

W6.3 Differentiation of the laminar pipe-flow solution, Eq. (6.40), shows that the fluid shear stress $\tau(r)$ varies linearly from zero at the axis to τ_w at the wall. It is claimed that this is also true, at least in the time mean, for fully developed *turbulent* flow. Can you verify this claim analytically?

W6.4 A porous medium consists of many tiny tortuous passages, and Reynolds numbers based on pore size are usually very low, of order unity. In 1856 H. Darcy proposed that the pressure gradient in a porous medium was directly proportional to the volume-averaged velocity **V** of the fluid:

$$\nabla p = -\frac{\mu}{K}\mathbf{V}$$

where K is termed the *permeability* of the medium. This is now called *Darcy's law* of porous flow. Can you make a Poiseuille flow model of porous-media flow which verifies Darcy's law? Meanwhile, as the Reynolds number increases, so that $VK^{1/2}/\nu > 1$, the pressure drop becomes nonlinear, as was shown experimentally by P. H. Forscheimer as early as 1782. The flow is still decidedly laminar, yet the pressure gradient is quadratic:

$$\nabla p = -\frac{\mu}{K}\mathbf{V} - C\left|V\right|\mathbf{V} \quad \text{Darcy-Forscheimer law}$$

where C is an empirical constant. Can you explain the reason for this nonlinear behavior?

W6.5 One flowmeter device, in wide use in the water supply and gasoline distribution industries, is the *nutating disk*. Look this up in the library, and explain in a brief report how it works and the advantages and disadvantages of typical designs.

Fundamentals of Engineering Exam Problems

FE6.1 In flow through a straight, smooth pipe, the diameter Reynolds number for transition to turbulence is generally taken to be
(*a*) 1500, (*b*) 2100, (*c*) 4000, (*d*) 250,000, (*e*) 500,000

FE6.2 For flow of water at 20°C through a straight, smooth pipe at 0.06 m^3/h, the pipe diameter for which transition to turbulence occurs is approximately
(*a*) 1.0 cm, (*b*) 1.5 cm, (*c*) 2.0 cm, (*d*) 2.5 cm, (*e*) 3.0 cm

FE6.3 For flow of oil [μ = 0.1 kg/(m · s), SG = 0.9] through a long, straight, smooth 5-cm-diameter pipe at 14 m^3/h, the pressure drop per meter is approximately
(*a*) 2200 Pa, (*b*) 2500 Pa, (*c*) 10,000 Pa, (*d*) 160 Pa, (*e*) 2800 Pa

FE6.4 For flow of water at a Reynolds number of 1.03 E6 through a 5-cm-diameter pipe of roughness height 0.5 mm, the approximate Moody friction factor is
(*a*) 0.012, (*b*) 0.018, (*c*) 0.038, (*d*) 0.049, (*e*) 0.102

FE6.5 Minor losses through valves, fittings, bends, contractions, etc., are commonly modeled as proportional to
(*a*) total head, (*b*) static head, (*c*) velocity head, (*d*) pressure drop, (*e*) velocity

FE6.6 A smooth 8-cm-diameter pipe, 200 m long, connects two reservoirs, containing water at 20°C, one of which has a surface elevation of 700 m and the other with its surface elevation at 560 m. If minor losses are neglected, the expected flow rate through the pipe is
(*a*) 0.048 m^3/h, (*b*) 2.87 m^3/h, (*c*) 134 m^3/h, (*d*) 172 m^3/h, (*e*) 385 m^3/h

FE6.7 If, in Prob. FE6.6 the pipe is rough and the actual flow rate is 90 m^3/h, then the expected average roughness height of the pipe is approximately
(*a*) 1.0 mm, (*b*) 1.25 mm, (*c*) 1.5 mm, (*d*) 1.75 mm, (*e*) 2.0 mm

FE6.8 Suppose in Prob. FE6.6 the two reservoirs are connected, not by a pipe, but by a sharp-edged orifice of diameter 8 cm. Then the expected flow rate is approximately
(*a*) 90 m^3/h, (*b*) 579 m^3/h, (*c*) 748 m^3/h, (*d*) 949 m^3/h, (*e*) 1048 m^3/h

FE6.9 Oil [μ = 0.1 kg/(m · s), SG = 0.9] flows through a 50-m-long smooth 8-cm-diameter pipe. The maximum pressure drop for which laminar flow is expected is approximately
(*a*) 30 kPa, (*b*) 40 kPa, (*c*) 50 kPa, (*d*) 60 kPa, (*e*) 70 kPa

FE6.10 Air at 20°C and approximately 1 atm flows through a smooth 30-cm-square duct at 1500 ft^3/min. The expected pressure drop per meter of duct length is
(*a*) 1.0 Pa, (*b*) 2.0 Pa, (*c*) 3.0 Pa, (*d*) 4.0 Pa, (*e*) 5.0 Pa

FE6.11 Water at 20°C flows at 3 m^3/h through a sharp-edged 3-cm-diameter orifice in a 6-cm-diameter pipe. Estimate the expected pressure drop across the orifice.
(*a*) 440 Pa, (*b*) 680 Pa, (*c*) 875 Pa, (*d*) 1750 Pa, (*e*) 1870 Pa

FE6.12 Water flows through a straight 10-cm-diameter pipe at a diameter Reynolds number of 250,000. If the pipe roughness is 0.06 mm, what is the approximate Moody friction factor?
(*a*) 0.015, (*b*) 0.017, (*c*) 0.019, (*d*) 0.026, (*e*) 0.032

FE6.13 What is the hydraulic diameter of a rectangular air-ventilation duct whose cross section is 1 m by 25 cm?
(*a*) 25 cm, (*b*) 40 cm, (*c*) 50 cm, (*d*) 75 cm, (*e*) 100 cm

FE6.14 Water at 20°C flows through a pipe at 300 gal/min with a friction head loss of 45 ft. What is the power required to drive this flow?
(*a*) 0.16 kW, (*b*) 1.88 kW, (*c*) 2.54 kW, (*d*) 3.41 kW, (*e*) 4.24 kW

FE6.15 Water at 20°C flows at 200 gal/min through a pipe 150 m long and 8 cm in diameter. If the friction head loss is 12 m, what is the Moody friction factor?
(*a*) 0.010, (*b*) 0.015, (*c*) 0.020, (*d*) 0.025, (*e*) 0.030

Comprehensive Problems

C6.1 A pitot-static probe will be used to measure the velocity distribution in a water tunnel at 20°C. The two pressure lines from the probe will be connected to a U-tube manometer which uses a liquid of specific gravity 1.7. The maximum velocity expected in the water tunnel is 2.3 m/s. Your job is to select an appropriate U-tube from a manufacturer which supplies manometers of heights 8, 12, 16, 24, and 36 in. The cost increases significantly with manometer height. Which of these should you purchase?

***C6.2** A pump delivers a steady flow of water (ρ, μ) from a large tank to two other higher-elevation tanks, as shown in Fig. C6.2. The same pipe of diameter d and roughness ϵ is used throughout. All minor losses *except through the valve* are neglected, and the partially closed valve has a loss coefficient K_{valve}. Turbulent flow may be assumed with all kinetic energy flux correction coefficients equal to 1.06. The pump net head H is a known function of Q_A and hence also of $V_A = Q_A/A_{pipe}$; for example, $H = a - bV_A^2$, where a and b are constants. Subscript J refers to the junction point at the tee where branch A splits into B and C. Pipe length L_C is much longer than L_B. It is desired to predict the pressure at J, the three pipe velocities and friction factors, and the pump head. Thus there are eight variables: H, V_A, V_B, V_C, f_A, f_B, f_C, p_J. Write down the eight equations needed to resolve this problem, but *do not solve,* since an elaborate iteration procedure, or an equation solver such as EES, would be required.

C6.3 A small water slide is to be installed inside a swimming pool. See Fig. C6.3. The slide manufacturer recommends a continuous water flow rate Q of 1.39×10^{-3} m^3/s (about 22 gal/min) down the slide, to ensure that the customers do not burn their bottoms. A pump is to be installed under the slide, with a 5.00-m-long, 4.00-cm-diameter hose supplying swimming pool water for the slide. The pump is 80 percent efficient and will rest fully submerged 1.00 m below the water surface. The roughness inside the hose is about 0.0080 cm. The hose discharges the water at the top of the slide as a free jet open to the atmosphere. The hose outlet is 4.00 m above the water surface. For fully developed turbulent pipe flow, the kinetic energy flux correction factor is about 1.06. Ignore any minor losses here. Assume that $\rho = 998$ kg/m^3 and $\nu = 1.00 \times 10^{-6}$ m^2/s for this water. Find the brake horsepower (i.e., the actual shaft power in watts) required to drive the pump.

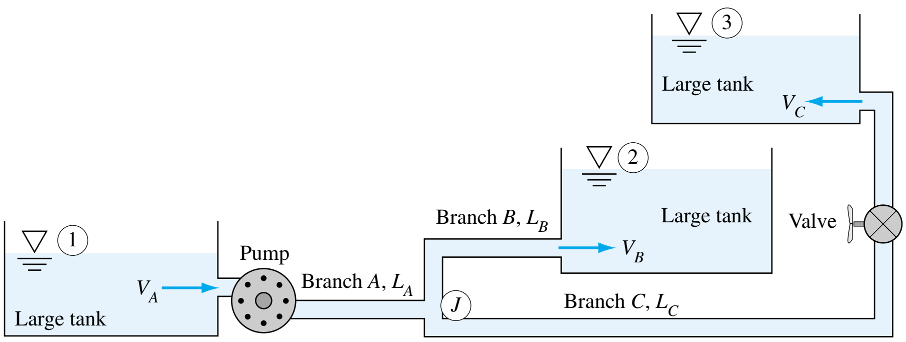

C6.2

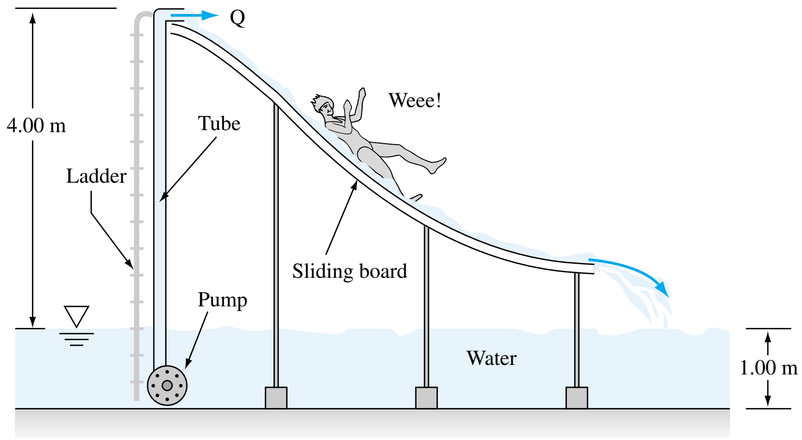

C6.3

***C6.4** Suppose you build a house out in the "boonies" where you need to run a pipe to the nearest water supply, which is fortunately at an elevation of about 1000 m above that of your house. The pipe will be 6.0 km long (the distance to the water supply), and the gage pressure at the water supply is 1000 kPa. You require a minimum of 3.0 gal/min of water when the end of your pipe is open to the atmosphere. To minimize cost, you want to buy the smallest-diameter pipe possible. The pipe you will use is extremely smooth. (*a*) Find the total head loss from the pipe inlet to its exit. Neglect any minor losses due to valves, elbows, entrance lengths, etc., since the length is so long here and major losses dominate. Assume the outlet of the pipe is open to the atmosphere. (*b*) Which is more important in this problem, the head loss due to elevation difference or the head loss due to pressure drop in the pipe? (*c*) Find the minimum required pipe diameter.

C6.5 Water at room temperature flows at the *same* volume flow rate, $Q = 9.4 \times 10^{-4}$ m^3/s, through two ducts, one a round pipe and one an annulus. The cross-sectional area A of the two ducts is identical, and all walls are made of commercial steel. Both ducts are the same length. In the cross sections shown in Fig. C6.5 R = 15.0 mm and a = 25.0 mm. (*a*) What is the radius b such that the cross-sectional areas of the two ducts are identical? (*b*) Compare the frictional head loss h_f per unit length of pipe for the two cases, assuming fully developed flow. For the annulus, do both a quick estimate (using the hydraulic diameter) and a more accurate estimate (using the effective diameter correction), and compare. (*c*) If the losses are different for the two cases, explain why. Which duct, if any, is more "efficient"?

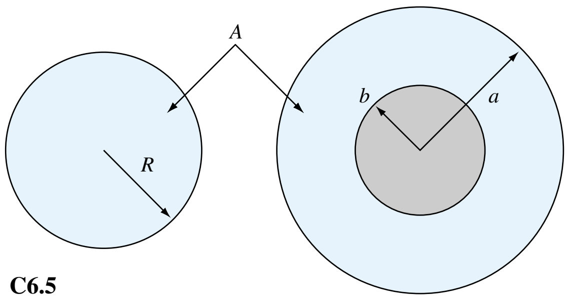

C6.5

Design Projects

D6.1 A hydroponic garden uses the 10-m-long perforated-pipe system in Fig. D6.1 to deliver water at 20°C. The pipe is 5 cm in diameter and contains a circular hole every 20 cm. A pump delivers water at 75 kPa (gage) at the entrance, while the other end of the pipe is closed. If you attempted, e.g., Prob. 3.125, you know that the pressure near the closed end of a perforated "manifold" is surprisingly high, and there will be too much flow through the holes near that end. One remedy is to vary the hole size along the pipe axis. Make a design analysis, perhaps using a personal computer, to pick the optimum hole-size distribution that will make the discharge flow rate as uniform as possible along the pipe axis. You are constrained to pick hole sizes that correspond only to commercial (numbered) metric drill-bit sizes available to the typical machine shop.

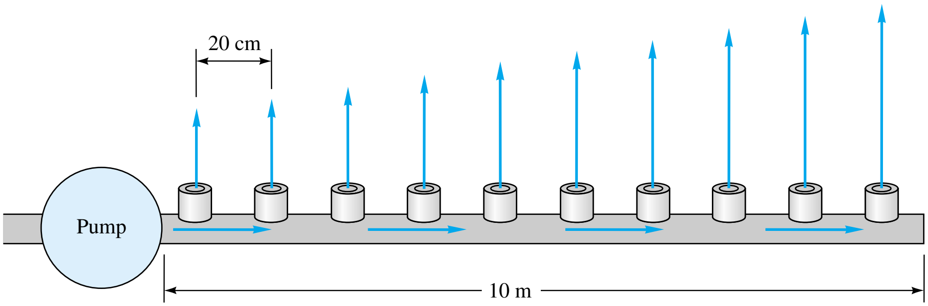

D6.1

D6.2 It is desired to design a pump-piping system to keep a 1-million-gallon capacity water tank filled. The plan is to use a modified (in size and speed) version of the model 1206 centrifugal pump manufactured by Taco Inc., Cranston, Rhode Island. Test data have been provided to us by Taco Inc. for a small model of this pump: D = 5.45 in, Ω = 1760 r/min, tested with water at 20°C:

Q, gal/min	0	5	10	15	20	25	30	35	40	45	50	55	60
H, ft	28	28	29	29	28	28	27	26	25	23	21	18	15
Efficiency, %	0	13	25	35	44	48	51	53	54	55	53	50	45

The tank is to be filled daily with rather chilly (10°C) groundwater from an aquifer, which is 0.8 mi from the tank and 150 ft lower than the tank. Estimated daily water use is 1.5 million gal/day. Filling time should not exceed 8 h per day. The piping system should have four "butterfly" valves with variable openings (see Fig. 6.19), 10 elbows of various angles, and galvanized-iron pipe of a size to be selected in the design. The design should be economical—both in capital costs and operating expense. Taco Inc. has provided the following cost estimates for system components:

Pump and motor	\$3500 plus \$1500 per inch of impeller size
Pump speed	Between 900 and 1800 r/min
Valves	\$300 + \$200 per inch of pipe size
Elbows	\$50 plus \$50 per inch of pipe size
Pipes	\$1 per inch of diameter per foot of length
Electricity cost	10¢ per kilowatthour

Your design task is to select an economical pipe size and pump impeller size and speed for this task, using the pump-test data in nondimensional form (see Prob. 5.61) as design data. Write a brief report (5 to 6 pages) showing your calculations and graphs.

References

1. J. O. Hinze, *Turbulence,* 2d ed., McGraw-Hill, New York, 1975.
2. H. Schlichting, *Boundary Layer Theory,* 7th ed., McGraw-Hill, New York, 1979.
3. F. M. White, *Viscous Fluid Flow,* 2d ed., McGraw-Hill, New York, 1991.
4. O. Reynolds, "An Experimental Investigation of the Circumstances which Determine Whether the Motion of Water Shall Be Direct or Sinuous and of the Law of Resistance in Parallel Channels," *Phil. Trans. R. Soc.,* vol. 174, 1883, pp. 935–982.
5. P. G. Drazin and W. H. Reid, *Hydrodynamic Stability,* Cambridge University Press, London, 1981.
6. H. Rouse and S. Ince, *History of Hydraulics,* Iowa Institute of Hydraulic Research, State University of Iowa, Iowa City, 1957.
7. J. Nikuradse, "Strömungsgesetze in Rauhen Rohren," *VDI Forschungsh.* 361, 1933; English trans., *NACA Tech. Mem.* 1292.
8. L. F. Moody, "Friction Factors for Pipe Flow," *ASME Trans.,* vol. 66, pp. 671–684, 1944.
9. C. F. Colebrook, "Turbulent Flow in Pipes, with Particular Reference to the Transition between the Smooth and Rough Pipe Laws," *J. Inst. Civ. Eng. Lond.,* vol. 11, 1938–1939, pp. 133–156.
10. O. C. Jones, Jr., "An Improvement in the Calculations of Tur-

bulent Friction in Rectangular Ducts," *J. Fluids Eng.,* June 1976, pp. 173–181.
11. R. Berker, *Handbuch der Physik,* vol. 7, no. 2, pp. 1–384, Springer-Verlag, Berlin, 1963.
12. R. M. Olson and S. J. Wright, *Essentials of Engineering Fluid Mechanics,* 5th ed., Harper & Row, New York, 1990.
13. D. Alciatore and W. S. Janna, "Modified Pipe Friction Diagrams that Eliminate Trial-and-Error Solutions," *Proc. 1st Natl. Fluid Dynamics Congress,* pt. 2, pp. 911–916, AIAA, Washington, DC, 1988.
14. P. W. Runstadler, Jr., et al., "Diffuser Data Book," *Creare Inc. Tech. Note* 186, Hanover, NH, 1975.
15. "Flow of Fluids through Valves, Fittings, and Pipe," *Crane Co. Tech. Pap.* 410, Chicago, 1957.
16. *Pipe Friction Manual,* 3d ed., The Hydraulic Institute, New York, 1961.
17. Hardy Cross, "Analysis of Flow in Networks of Conduits or Conductors," *Univ. Ill. Bull.* 286, November 1936.
18. R. W. Jepson, *Analysis of Flow in Pipe Networks,* Ann Arbor Pub., Ann Arbor, MI, 1976.
19. L. E. Ormsbee and D. J. Wood, "Explicit Pipeline Network Calibration," *J. Water Resources Planning and Management,* vol. 112, no. 2, April 1986, pp. 166–182.
20. J. Bardina et al,. "A Prediction Method for Planar Diffuser Flows," *J. Fluids Eng.,* vol. 103, 1981, pp. 315–321.
21. R. W. Fox and S. J. Kline, "Flow Regime Data and Design Methods for Curved Subsonic Diffusers," *J. Basic Eng*., vol. 84, 1962, pp. 303–312.
22. J. P. Holman, *Experimental Methods for Engineers,* 6th ed., McGraw-Hill, New York, 1993.
23. T. G. Beckwith and R. D. Marangoni, *Mechanical Measurements,* 4th ed., Addison-Wesley, Reading, MA, 1990.
24. B. Warren and C. Wunsch (eds.), *Evolution of Physical Oceanography,* M.I.T. Press, Cambridge, MA, 1981.
25. U.S. Department of Commerce, *Tidal Current Tables,* National Oceanographic and Atmospheric Administration, Washington, DC, 1971.
26. J. A. Shercliff, *Electromagnetic Flow Measurement,* Cambridge University Press, New York, 1962.
27. J. A. Miller, "A Simple Linearized Hot-Wire Anemometer," *J. Fluids Eng.,* December 1976, pp. 749–752.
28. R. J. Goldstein (ed.), *Fluid Mechanics Measurements,* 2d ed., Hemisphere, New York, 1996.
29. D. Eckardt, "Detailed Flow Investigations within a High Speed Centrifugal Compressor Impeller," *J. Fluids Eng.,* September 1976, pp. 390–402.
30. H. S. Bean (ed.), *Fluid Meters: Their Theory and Application,* 6th ed., American Society of Mechanical Engineers, New York, 1971.
31. "Measurement of Fluid Flow by Means of Orifice Plates, Nozzles, and Venturi Tubes Inserted in Circular Cross Section Conduits Running Full," *Int. Organ. Stand. Rep*. DIS-5167, Geneva, April 1976.
32. P. Moin and P. R. Spalart, in *Advances in Turbulence,* W. K. George and R. Arndt (eds.), Hemisphere, New York, 1989, pp. 11–38.
33. S. E. Haaland, "Simple and Explicit Formulas for the Friction Factor in Turbulent Pipe Flow," *J. Fluids Eng.,* March 1983, pp. 89–90.
34. R. K. Shah and A. L. London, *Laminar Flow Forced Convection in Ducts,* Academic, New York, 1979.
35. J. L. Lyons, *Lyons' Valve Designers Handbook,* Van Nostrand Reinhold, New York, 1982.
36. A. O. Demuren and W. Rodi, "Calculations of Turbulence-Driven Secondary Motion in Non-circular Ducts," *J. Fluid Mech.,* vol. 140, 1984, pp. 189– 222.
37. *ASHRAE Handbook of Fundamentals,* chap. 33, ASHRAE, Atlanta, 1981.
38. F. Durst, A. Melling, and J. H. Whitelaw, *Principles and Practice of Laser-Doppler Anemometry,* 2d ed., Academic, New York, 1981.
39. A. Dybbs and B. Ghorashi, *Laser Anemometry: Advances and Applications,* American Society of Mechanical Engineers, New York, 1991.
40. J. G. Kopp, "Vortex Flowmeters," *Meas. Control,* June 1983, pp. 280–284.
41. J. C. Graber, Jr., "Ultrasonic Flow," *Meas. Control,* October 1983, pp. 258–266.
42. ASME Fluid Meters Research Committee, "The ISO-ASME Orifice Coefficient Equation," *Mech. Eng.* July 1981, pp. 44–45.
43. R. D. Blevins, *Applied Fluid Dynamics Handbook,* Van Nostrand Reinhold, New York, 1984.
44. O. C. Jones, Jr., and J. C. M. Leung, "An Improvement in the Calculation of Turbulent Friction in Smooth Concentric Annuli," *J. Fluids Eng.,* December 1981, pp. 615–623.
45. P. R. Bandyopadhyay, "Aspects of the Equilibrium Puff in Transitional Pipe Flow, *J. Fluid Mech.,* vol. 163, 1986, pp. 439–458.
46. I. E. Idelchik, *Handbook of Hydraulic Resistance,* 3d ed., CRC Press, Boca Raton, FL, 1993.
47. Sanford Klein and William Beckman, *Engineering Equation Solver (EES),* University of Wisconsin, Madison, WI, 1997.
48. R. D. Coffield, P. T. McKeown, and R. B. Hammond, "Irrecoverable Pressure Loss Coefficients for Two Elbows in Series with Various Orientation Angles and Separation Distances," *Report WAPD-T-3117,* Bettis Atomic Power Laboratory, West Mifflin, PA, 1997.